Chapter 9

Model Risk of Exotic Derivatives

In Chapter 2, we have seen that options and derivative instruments present non-linear risks that are more difficult to assess and measure than for a long-only portfolio of stocks or bonds. Moreover, those financial instruments are traded in OTC markets, meaning that their market value is not known with certainty. These issues imply that the current value is a mark-to-model price and the risk factors depend on the pricing model and the underlying assumptions. The pricing problem is then at the core of the risk management of derivative instruments. However, risk management of such financial products cannot be reduced to a pricing problem. Indeed, the main difficulty lies in managing dynamically the hedging of the option in order to ensure that the replication cost is equal to the option price. In this case, the real challenge is the model risk and concerns three levels: the model risk of pricing the option, the model risk of hedging the option and the discrepancy risk between the pricing model and the hedging model. Therefore, this chapter cannot be just a catalogue of pricing models, but focuses more on pricing errors and hedging uncertainties.

9.1 Basics of option pricing

In this section, we present the basic models that are used for pricing derivatives instruments: the Black-Scholes model, the Vasicek model and the HJM model. While the first one is general and valid for all asset classes, the last two models concern interest rate derivatives.

9.1.1 The Black-Scholes model

9.1.1.1 The general framework

Black and Scholes (1973) assume that the dynamics of the asset price $S(t)$ is given by a geometric Brownian motion:

$$\left\{ \begin{array}{l} \mathrm{d}S(t) = \mu S(t)\,\mathrm{d}t + \sigma S(t)\,\mathrm{d}W(t) \\ S(t_0) = S_0 \end{array} \right. \tag{9.1}$$

where S_0 is the current price, μ is the drift, σ is the volatility of the diffusion and $W(t)$ is a standard Brownian motion. We consider a contingent claim that pays $f(S(T))$ at the maturity T of the derivative contract. For example, if we consider an European option with strike K, we have $f(S(T)) = (S(T) - K)^+$.

Under some conditions, we can show that this contingent claim may be replicated by a hedging portfolio, which is composed of the asset and a risk-free asset, whose instantaneous return is equal to $r(t)$. The price V of the contingent claim is then equal to the cost of the hedging portfolio. In this case, Black and Scholes show that it is the solution of the following backward equation:

$$\begin{cases} \frac{1}{2}\sigma^2 S^2 \partial_S^2 V(t,S) + (\mu - \lambda(t)\sigma) S \partial_S V(t,S) + \partial_t V(t,S) - r(t) V(t,S) = 0 \\ V(T, S(T)) = f(S(T)) \end{cases}$$

This equation is called the fundamental pricing equation. The function $\lambda(t)$ is interpreted as the risk price of the Wiener process $W(t)$. For an asset whose cost-of-carry is equal to $b(t)$, we have:

$$\lambda(t) = \frac{\mu - b(t)}{\sigma}$$

The previous equation then becomes:

$$\begin{cases} \frac{1}{2}\sigma^2 S^2 \partial_S^2 V(t,S) + b(t) S \partial_S V(t,S) + \partial_t V(t,S) - r(t) V(t,S) = 0 \\ V(T, S(T)) = f(S(T)) \end{cases} \tag{9.2}$$

The current price of the derivatives contract is obtained by solving this partial differential equation (PDE) and to take $V(t_0, S_0)$.

A way to obtain the solution is to apply the Girsanov theorem[1] to the SDE (9.1) with $g(t) = -\lambda(t)$. It follows that:

$$\begin{cases} \mathrm{d}S(t) = b(t) S(t)\,\mathrm{d}t + \sigma S(t)\,\mathrm{d}W^{\mathbb{Q}}(t) \\ S(t_0) = S_0 \end{cases} \tag{9.3}$$

where $W^{\mathbb{Q}}(t)$ is a Brownian motion under the probability $\mathbb{Q}$ defined by:

$$\frac{\mathrm{d}\mathbb{Q}}{\mathrm{d}\mathbb{P}} = \exp\left(-\int_0^t \lambda(s)\,\mathrm{d}W(s) - \frac{1}{2}\int_0^t \lambda^2(s)\,\mathrm{d}s\right)$$

We may then apply the Feynman-Kac formula[2] with $h(t,x) = r(t)$ and $g(t,x) = 0$ to obtain the martingale solution[3]:

$$V_0 = \mathbb{E}^{\mathbb{Q}}\left[e^{-\int_0^T r(t)\,\mathrm{d}t} f(S(T)) \middle| \mathcal{F}_0 \right] \tag{9.4}$$

Remark 96 *$\mathbb{Q}$ is called the risk-neutral probability (or martingale) measure, because the option price V_0 is the expected discounted value of the payoff[4].*

9.1.1.2 Application to European options

We consider an European call option whose payoff at maturity is equal to:

$$\mathcal{C}(T) = (S(T) - K)^+$$

We assume that the interest rate $r(t)$ and the cost-of-carry parameter $b(t)$ are constant. Then we obtain:

$$\begin{aligned} \mathcal{C}_0 &= \mathbb{E}^{\mathbb{Q}}\left[e^{-\int_0^T r\,\mathrm{d}t} (S(T) - K)^+ \middle| \mathcal{F}_0 \right] \\ &= e^{-rT}\mathbb{E}\left[\left(S_0 e^{\left(b - \frac{1}{2}\sigma^2\right)T + \sigma W^{\mathbb{Q}}(T)} - K \right)^+ \right] \\ &= e^{-rT}\int_{-d_2}^{\infty} \left(S_0 e^{\left(b - \frac{1}{2}\sigma^2\right)T + \sigma\sqrt{T}x} - K \right) \phi(x)\,\mathrm{d}x \\ &= S_0 e^{(b-r)T}\Phi(d_1) - K e^{-rT}\Phi(d_2) \end{aligned} \tag{9.5}$$

[1]See Appendix A.3.5 on page 1072.
[2]See Appendix A.3.4 on page 1070.
[3]We assume that the current date t_0 is equal to 0.
[4]See Exercise 9.4.1 on page 593 for more details.

where:

$$\begin{aligned} d_1 &= \frac{1}{\sigma\sqrt{T}}\left(\ln\frac{S_0}{K}+bT\right)+\frac{1}{2}\sigma\sqrt{T} \\ d_2 &= d_1-\sigma\sqrt{T} \end{aligned}$$

Let us now consider an European put option with the following payoff:

$$\boldsymbol{\mathcal{P}}(T)=(K-S(T))^+$$

We have:

$$\begin{aligned} \boldsymbol{\mathcal{C}}(T)-\boldsymbol{\mathcal{P}}(T) &= (S(T)-K)^+-(K-S(T))^+ \\ &= S(T)-K \end{aligned}$$

We deduce that:

$$\begin{aligned} \boldsymbol{\mathcal{C}}_0-\boldsymbol{\mathcal{P}}_0 &= \mathbb{E}^{\mathbb{Q}}\left[e^{-\int_0^T r\,\mathrm{d}t}(S(T)-K)\Big|\,\mathcal{F}_0\right] \\ &= \mathbb{E}^{\mathbb{Q}}\left[e^{-rT}S(T)\big|\,\mathcal{F}_0\right]-Ke^{-rT} \\ &= S_0e^{(b-r)T}-Ke^{-rT} \end{aligned}$$

This equation is known as the put-call parity. It follows that:

$$\begin{aligned} \boldsymbol{\mathcal{P}}_0 &= \boldsymbol{\mathcal{C}}_0-S_0e^{(b-r)T}+Ke^{-rT} \\ &= -S_0e^{(b-r)T}\Phi(-d_1)+Ke^{-rT}\Phi(-d_2) \end{aligned} \tag{9.6}$$

Remark 97 *Equations (9.5) and (9.6) are the famous Black-Scholes formulas. Generally, they are presented with $b=r$, that is for physical assets not paying dividends. The cost-of-carry concept is explained in the next paragraphs.*

We consider a call option on an asset, whose cost-of-carry is equal to 5%. We also assume that the interest rate is equal to 5%. Figure 9.1 represents the option premium with respect to the current value S_0 of the asset. We notice that the price of the call option increases with the current price S_0, the volatility σ and the maturity T. In Figure 9.2, we report the option premium of the put option. In both cases, it may be interesting to decompose the option premium into two components:

- The intrinsic value is the value of exercising the option now:

$$\mathrm{IV}(t)=f(S_0)$$

  For instance, the intrinsic value of the call option is equal to $(S_0-K)^+$. If the intrinsic value is positive, the option is said in-the-money (ITM). If the intrinsic value is equal to zero, the option is at-the-money (ATM) or out-of-the-money (OTM).

- The time value is the difference between the option premium and the intrinsic value:

$$\mathrm{TV}(t)=V(t_0,S_0)-\mathrm{IV}(t)$$

  This quantity is always positive and is related to the risk that the intrinsic value will increase with the time-to-maturity.

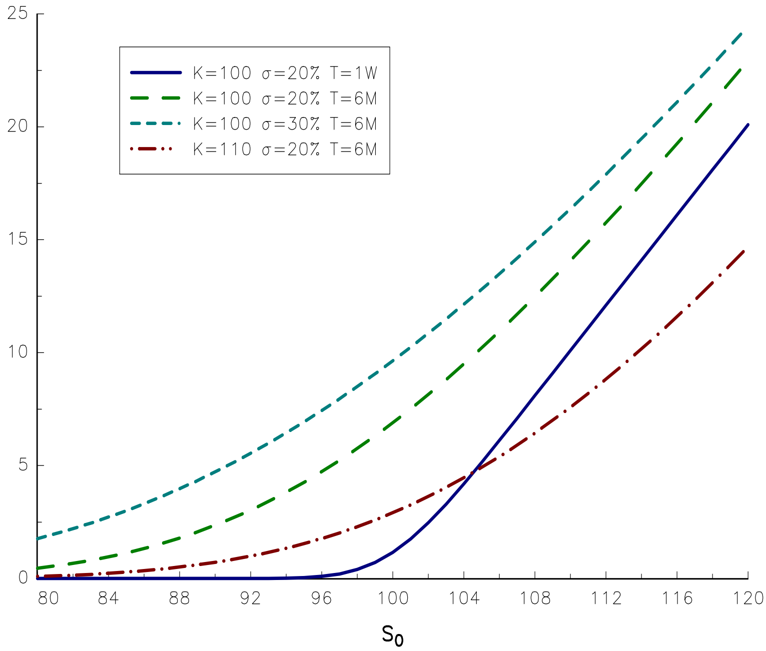

FIGURE 9.1: Price of the call option

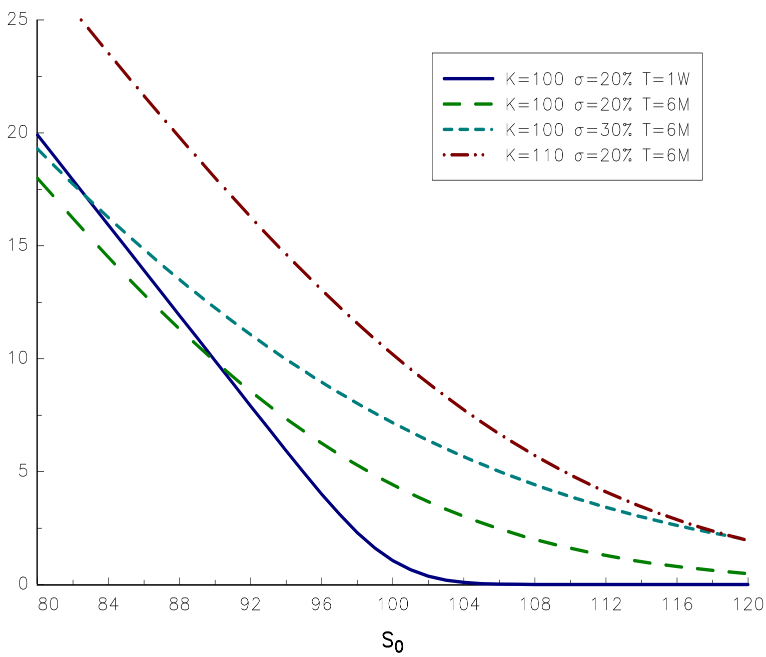

FIGURE 9.2: Price of the put option

9.1.1.3 Principle of dynamic hedging

Self-financing strategy We consider n assets that do not pay dividends or coupons during the period $[0, T]$ and we assume that the price vector $S(t)$ follows a diffusion process. For asset i, we have then:

$$S_i(t) = S_i(0) + \int_0^t \mu_i(u)\,\mathrm{d}u + \int_0^t \sigma_i(u)\,\mathrm{d}W_i(u)$$

We set up a trading portfolio $(\phi_1(t), \ldots, \phi_n(t))$ invested in the assets $(S_1(t), \ldots, S_n(t))$. We note $X(t)$ the value of this portfolio:

$$X(t) = \sum_{i=1}^n \phi_i(t) S_i(t)$$

We say that the portfolio is self-financing if the following conditions hold:

$$\begin{cases} \mathrm{d}X(t) - \sum_{i=1}^n \phi_i(t)\,\mathrm{d}S_i(t) = 0 \\ X(0) = 0 \end{cases}$$

The first condition means that all trades are financed by selling or buying assets in the portfolio, whereas the second condition implies that we don't need money to set up the initial portfolio. This implies that:

$$\begin{aligned} X(t) &= X_0 + \sum_{i=1}^n \int_0^t \phi_i(u)\,\mathrm{d}S_i(u) \\ &= \sum_{i=1}^n \phi_i(0) S_i(0) + \sum_{i=1}^n \int_0^t \phi_i(u)\,\mathrm{d}S_i(u) \end{aligned}$$

In the Black-Scholes model, we consider a stock that does not pay dividends or coupons during the period $[0, T]$ and we assume that its price process $S(t)$ follows a geometric Brownian motion:

$$\mathrm{d}S(t) = \mu S(t)\,\mathrm{d}t + \sigma S(t)\,\mathrm{d}W(t)$$

We also assume the existence of a risk-free asset $B(t)$ that satisfies:

$$\mathrm{d}B(t) = rB(t)\,\mathrm{d}t$$

We set up a trading portfolio $(\phi(t), \psi(t))$ invested in the stock $S(t)$ and the risk-free asset $B(t)$. We note $V(t)$ the value of this portfolio:

$$V(t) = \phi(t) S(t) + \psi(t) B(t)$$

We now form a strategy $X(t)$ in which we are long the call option $\boldsymbol{\mathcal{C}}(t, S(t))$ and short the trading portfolio $V(t)$:

$$\begin{aligned} X(t) &= \boldsymbol{\mathcal{C}}(t, S(t)) - V(t) \\ &= \boldsymbol{\mathcal{C}}(t, S(t)) - \phi(t) S(t) - \psi(t) B(t) \end{aligned}$$

Using Itô's lemma, we have:

$$\begin{aligned} \mathrm{d}X(t) = {} & \partial_S \boldsymbol{\mathcal{C}}(t, S(t))\,\mathrm{d}S(t) + {} \\ & \left(\partial_t \boldsymbol{\mathcal{C}}(t, S(t)) + \frac{1}{2}\sigma^2 S^2(t)\,\partial_S^2 \boldsymbol{\mathcal{C}}(t, S(t))\right)\mathrm{d}t - {} \\ & \phi(t)\,\mathrm{d}S(t) - \psi(t)\,\mathrm{d}B(t) \end{aligned}$$

By assuming that $\phi(t) = \partial_S \boldsymbol{\mathcal{C}}(t, S(t))$, we obtain:

$$\mathrm{d}X(t) = \left(\partial_t \boldsymbol{\mathcal{C}}(t, S(t)) + \frac{1}{2}\sigma^2 S^2(t)\, \partial_S^2 \boldsymbol{\mathcal{C}}(t, S(t)) - r\psi(t) B(t)\right) \mathrm{d}t$$

$X(t)$ is self-financing if $\mathrm{d}X(t) = 0$ or:

$$\psi(t) = \frac{\partial_t \boldsymbol{\mathcal{C}}(t, S(t)) + \frac{1}{2}\sigma^2 S^2(t)\, \partial_S^2 \boldsymbol{\mathcal{C}}(t, S(t))}{rB(t)}$$

We deduce that:

$$\begin{aligned}
\boldsymbol{\mathcal{C}}(t, S(t)) &= \phi(t) S(t) + \psi(t) B(t) \\
&= \partial_S \boldsymbol{\mathcal{C}}(t, S(t)) S(t) + \\
&\quad \frac{\partial_t \boldsymbol{\mathcal{C}}(t, S(t)) + \frac{1}{2}\sigma^2 S^2(t)\, \partial_S^2 \boldsymbol{\mathcal{C}}(t, S(t))}{rB(t)} B(t)
\end{aligned}$$

This implies that $\boldsymbol{\mathcal{C}}(t, S(t))$ satisfies the following PDE:

$$\frac{1}{2}\sigma^2 S^2 \partial_S^2 \boldsymbol{\mathcal{C}}(t, S) + rS\partial_S \boldsymbol{\mathcal{C}}(t, S) + \partial_t \boldsymbol{\mathcal{C}}(t, S) - r\boldsymbol{\mathcal{C}}(t, S) = 0$$

Since $X(t)$ is self-financing ($X(t) = 0$), we also deduce that the trading portfolio $V(t)$ is the replicating portfolio of the call option:

$$\begin{aligned}
V(t) &= \phi(t) S(t) + \psi(t) B(t) \\
&= \boldsymbol{\mathcal{C}}(t, S(t)) - X(t) \\
&= \boldsymbol{\mathcal{C}}(t, S(t))
\end{aligned}$$

If we define the replicating cost as follows:

$$\begin{aligned}
C(t) &= \int_0^t \phi(u)\, \mathrm{d}S(u) + \int_0^t \psi(u)\, \mathrm{d}B(u) \\
&= \int_0^t (\mu S(u) \phi(u) + rB(u) \psi(u))\, \mathrm{d}u + \int_0^T \sigma S(u) \phi(u)\, \mathrm{d}W(u)
\end{aligned}$$

we have:

$$\begin{aligned}
C(t) &= \int_0^t \mu S(u) \partial_S \boldsymbol{\mathcal{C}}(u, S(u))\, \mathrm{d}u + \int_0^T \sigma S(u) \partial_S \boldsymbol{\mathcal{C}}(u, S(u))\, \mathrm{d}W(u) \\
&\quad \int_0^t \left(\partial_t \boldsymbol{\mathcal{C}}(u, S(u)) + \frac{1}{2}\sigma^2 S^2(u)\, \partial_S^2 \boldsymbol{\mathcal{C}}(u, S(u))\right) \mathrm{d}u \\
&= \int_0^t \mathrm{d}\boldsymbol{\mathcal{C}}(u, S(u)) \\
&= \boldsymbol{\mathcal{C}}(t, S(t)) - \boldsymbol{\mathcal{C}}(0, S_0)
\end{aligned}$$

We verify that the replicating cost is exactly equal to the P&L of the long exposure on the call option.

Cost-of-carry When the stock does not pay dividends, the cost-of-carry parameter b is equal to the interest rate r. Let us now consider a stock that pays a continuous dividend yield δ, the self-financing portfolio is:

$$X(t) = \boldsymbol{\mathcal{C}}(t, S(t)) - \phi(t) S(t) - \psi(t) B(t)$$

We deduce that the change in the value of this portfolio is:

$$\mathrm{d}X(t) = \mathrm{d}\boldsymbol{\mathcal{C}}(t, S(t)) - \phi(t)\,\mathrm{d}S(t) - \psi(t)\,\mathrm{d}B(t) - \phi(t) \cdot \underbrace{\delta \cdot S(t)\,\mathrm{d}t}_{\text{dividend}}$$

Using the same rationale than previously, we obtain $\phi(t) = \partial_S \boldsymbol{\mathcal{C}}(t, S(t))$ and:

$$\psi(t) = \frac{\partial_t \boldsymbol{\mathcal{C}}(t, S(t)) + \frac{1}{2}\sigma^2 S^2(t)\,\partial_S^2 \boldsymbol{\mathcal{C}}(t, S(t)) - \delta S(t)\,\partial_S \boldsymbol{\mathcal{C}}(t, S(t))}{rB(t)}$$

Finally, we obtain the following PDE:

$$\frac{1}{2}\sigma^2 S^2 \partial_S^2 \boldsymbol{\mathcal{C}}(t, S) + (r - \delta) S \partial_S \boldsymbol{\mathcal{C}}(t, S) + \partial_t \boldsymbol{\mathcal{C}}(t, S) - r\boldsymbol{\mathcal{C}}(t, S) = 0$$

The cost-of-carry parameter b is now equal to $r - \delta$. It is the percentage cost required to carry the asset. Generally, the cost is equal to the interest rate r, but a continuous dividend reduces this cost. In the case of futures or forward contracts, the cost-of-carry is equal to zero. Indeed, the price of such contracts already incorporates the cost-of-carry of the underlying asset. For currency options, the cost-of-carry is the difference between the domestic interest rate r and the foreign interest rate $r^\star$.

TABLE 9.1: Impact of the dividend on the option premium

	Put option				Call option			
S_0 / δ	0.00	0.02	0.05	0.07	0.00	0.02	0.05	0.07
90	1.28	1.44	1.73	1.94	13.50	12.67	11.48	10.72
100	4.42	4.83	5.50	5.97	6.89	6.31	5.50	5.00
110	10.19	10.87	11.91	12.63	2.91	2.59	2.16	1.90

In order to illustrate the impact of the cost-of-carry, we have calculated the option premium in Table 9.1 with the following parameters: $K = 100$, $r = 5\%$ and a six-month maturity. In the case of the put option, the price increases with the dividend yield δ whereas it decreases in the case of the call option. In order to understand these figures, we have to come back to the definition of the replicating portfolio. A call option is replicated using a portfolio that is long on the asset. This implies that the replicating portfolio benefits from the dividends paid by the asset. The self-financing property of the strategy induces that we have to borrow less money. This is why the premium of the call option is lower when the asset pays a dividend. For the put option, this is the contrary. The replicating portfolio is short on the asset. Therefore, it does not receive the dividends, but pays them.

Remark 98 *The value of dividends is an example of model risk. Indeed, future dividends are uncertain, meaning that there is a risk of undervaluation of the option premium. In the case of a call option, the risk is to use expected dividends that are higher than realized values. In the case of put option, the risk is to use low dividends.*

Delta hedging The Black-Scholes model assumes that the replicating portfolio is rebalanced continuously. In practice, it is rebalanced at some fixed dates t_i:

$$0 = t_0 < t_1 < \cdots < t_n = T$$

At the initial date, we have:

$$X(t_0) = \boldsymbol{\mathcal{C}}(t_0, S(t_0)) - V(t_0) = 0$$

where:

$$V(t_0) = \phi(t_0) \cdot S(t_0) + \psi(t_0) \cdot B(t_0)$$

Because we have $\phi(t_0) = \boldsymbol{\Delta}(t_0)$ and $X(t_0) = 0$, we deduce that[5]:

$$\psi(t_0) = \boldsymbol{\mathcal{C}}(t_0, S(t_0)) - \boldsymbol{\Delta}(t_0) S(t_0)$$

At time t_1, the value of the replicating portfolio is then equal to:

$$V(t_1) = \boldsymbol{\Delta}(t_0) S(t_1) + (\boldsymbol{\mathcal{C}}(t_0, S(t_0)) - \boldsymbol{\Delta}(t_0) S(t_0)) \cdot (1 + r(t_0)(t_1 - t_0)) \tag{9.7}$$

It follows that:

$$X(t_1) = \boldsymbol{\mathcal{C}}(t_1, S(t_1)) - V(t_1)$$

Therefore, we are note sure that $X(t_1) = 0$ because it is not possible to hedge the jump $S(t_1) - S(t_0)$. We rebalance the portfolio and we have:

$$V(t_1) = \phi(t_1) \cdot S(t_1) + \psi(t_1) \cdot B(t_1)$$

We deduce that:

$$\phi(t_1) = \boldsymbol{\Delta}(t_1)$$

and:

$$\psi(t_1) = V(t_1) - \boldsymbol{\Delta}(t_1) S(t_1)$$

At time t_2, the value of the replicating portfolio is equal to:

$$V(t_2) = \boldsymbol{\Delta}(t_1) S(t_2) + (V(t_1) - \boldsymbol{\Delta}(t_1) S(t_1)) \cdot (1 + r(t_1)(t_2 - t_1)) \tag{9.8}$$

Equation (9.8) differs from Equation (9.7) because we don't have $V(t_1) = C(t_1, S(t_1))$. More generally, we have:

$$X(t_i) = \boldsymbol{\mathcal{C}}(t_i, S(t_i)) - V(t_i)$$

and:

$$V(t_i) = \underbrace{\boldsymbol{\Delta}(t_{i-1}) S(t_i)}_{V_S(t_i)} + \underbrace{(V(t_{i-1}) - \boldsymbol{\Delta}(t_{i-1}) S(t_{i-1})) \cdot (1 + r(t_{i-1})(t_i - t_{i-1}))}_{V_B(t_i)}$$

where $V_S(t_i)$ is the component due to the delta exposure on the asset and $V_B(t_i)$ is the component due to the cash exposure on the risk-free bond. We notice that:

$$\begin{aligned} V_S(t_i) &= \boldsymbol{\Delta}(t_{i-1}) \cdot S(t_i) \\ &= \boldsymbol{\Delta}(t_{i-1}) \cdot S(t_{i-1}) \cdot (1 + R_S(t_{i-1}; t_i)) \end{aligned}$$

[5]Without any loss of generality, we take the convention that $B(t_i) = 1$.

and:

$$\begin{aligned} V_B(t_i) &= (V(t_{i-1}) - \boldsymbol{\Delta}(t_{i-1}) \cdot S(t_{i-1})) \cdot (1 + r(t_{i-1}) \cdot (t_i - t_{i-1})) \\ &= (V(t_{i-1}) - \boldsymbol{\Delta}(t_{i-1}) \cdot S(t_{i-1})) \cdot (1 + R_B(t_{i-1}; t_i)) \end{aligned}$$

where $R_S(t_{i-1}; t_i)$ and $R_B(t_{i-1}; t_i)$ are the asset and bond returns between t_{i-1} and t_i. At the maturity, we obtain:

$$\begin{aligned} X(T) &= X(t_n) \\ &= (S(T) - K)^+ - V(t_n) \end{aligned}$$

$\Pi(T) = -X(T)$ is the P&L of the delta hedging strategy. To measure its efficiency, we consider the ratio π defined as follows:

$$\pi = \frac{\Pi(T)}{\boldsymbol{\mathcal{C}}(t_0, S(t_0))}$$

Example 78 *We consider the replication of 100 ATM call options. The current price of the asset is* 100 *and the maturity of the option is 20 weeks. We consider the following parameter:* $b = r = 5\%$ *and* $\sigma = 20\%$. *We rebalance the replicating portfolio every week.*

Since the maturity T is equal to $20/52$ and the strike K is equal to 100, the current value $\boldsymbol{\mathcal{C}}(t_0, S(t_0))$ of the call option is equal to \$5.90. The replicating portfolio is rebalanced at times t_i:

$$t_i = \frac{i}{52}$$

In Table 9.2, we have reported a simulated path of the underlying asset. We have $S(t_0) = 100$, $S(t_1) = 95.63$, $S(t_2) = 95.67$, etc. At the maturity date, the price of the underlying asset is equal to 101.83. In the Black-Scholes model, the delta is equal to:

$$\boldsymbol{\Delta}(t) = e^{(b-r)(T-t)} \Phi(d_1)$$

where:

$$d_1 = \frac{1}{\sigma\sqrt{T-t}} \left(\ln \frac{S(t)}{K} + b(T-t) \right) + \sigma\sqrt{T-t}$$

At each rebalancing date t_{i-1}, we compute the delta $\boldsymbol{\Delta}(t_{i-1})$ with respect to the price $S(t_{i-1})$ and the remaining maturity $T - t_{i-1}$. We can then deduce the values of $V_S(t_i)$, $V_B(t_i)$ and $V(t_i)$. We can also calculate the new value $\boldsymbol{\mathcal{C}}(t_i, S(t_i))$ of the call option and compare it with $V(t_i)$ in order to define $X(t_i)$ and $\Pi(t_i) = -X(t_i)$. We obtain $\Pi(T) = -29.76$, implying that:

$$\pi = \frac{-29.76}{100 \times 5.90} = -5.04\%$$

In this case, the delta hedging strategy has produced a negative P&L. If we consider another path of the underlying asset, we can also obtain a positive P&L (see Table 9.3).

We now assume that $S(t)$ is generated by the risk-neutral SDE:

$$\mathrm{d}S(t) = rS(t)\,\mathrm{d}t + \sigma S(t)\,\mathrm{d}W^{\mathbb{Q}}(t)$$

We estimate the probability density function of π by simulating 10 000 trajectories of the asset price and calculating the final P&L of the delta hedging strategy. We consider the

TABLE 9.2: An example of delta hedging strategy (negative P&L)

i	t_i	$S(t_i)$	$\boldsymbol{\Delta}(t_{i-1})$	$V_S(t_i)$	$V_B(t_i)$	$V(t_i)$	$\mathcal{C}(t_i, S(t_i))$	$X(t_i)$	$\Pi(t_i)$
0	0.00	100.00	0.00	0.00	590.90	590.90	590.90	0.00	0.00
1	0.02	95.63	58.59	5603.15	−5273.36	329.79	350.22	20.43	−20.43
2	0.04	95.67	43.72	4182.80	−3854.96	327.84	336.15	8.31	−8.31
3	0.06	94.18	43.24	4072.36	−3812.62	259.75	260.57	0.82	−0.82
4	0.08	92.73	37.29	3457.72	−3255.16	202.55	196.22	−6.33	6.33
5	0.10	96.59	31.34	3027.23	−2706.31	320.93	326.47	5.54	−5.54
6	0.12	101.68	44.63	4537.99	−3993.73	544.26	582.71	38.45	−38.45
7	0.13	101.41	63.39	6428.19	−5906.72	521.47	545.64	24.17	−24.17
8	0.15	100.22	62.36	6249.97	−5808.29	441.68	453.62	11.94	−11.94
9	0.17	99.32	57.57	5718.25	−5333.51	384.74	382.58	−2.16	2.16
10	0.19	101.64	53.46	5433.52	−4929.49	504.03	495.99	−8.04	8.04
11	0.21	101.81	63.27	6441.30	−5932.22	509.08	483.87	−25.21	25.21
12	0.23	102.62	64.10	6578.19	−6022.97	555.22	513.53	−41.69	41.69
13	0.25	107.56	67.97	7311.26	−6426.42	884.84	876.68	−8.16	8.16
14	0.27	102.05	86.90	8867.94	−8470.05	397.89	424.07	26.18	−26.18
15	0.29	100.88	66.19	6677.01	−6362.67	314.34	321.76	7.41	−7.41
16	0.31	106.90	59.86	6399.37	−5730.15	669.21	756.02	86.80	−86.80
17	0.33	107.66	90.32	9723.75	−8994.54	729.22	806.47	77.25	−77.25
18	0.35	101.79	94.74	9643.97	−9480.00	163.96	276.24	112.27	−112.27
19	0.37	101.76	69.88	7111.04	−6955.85	155.19	228.08	72.89	−72.89
20	0.38	101.83	75.10	7647.28	−7494.04	153.24	183.00	29.76	−29.76

TABLE 9.3: An example of delta hedging strategy (positive P&L)

i	t_i	$S(t_i)$	$\boldsymbol{\Delta}(t_{i-1})$	$V_S(t_i)$	$V_B(t_i)$	$V(t_i)$	$\mathcal{C}(t_i, S(t_i))$	$X(t_i)$	$\Pi(t_i)$
0	0.00	100.00	0.00	0.00	590.90	590.90	590.90	0.00	0.00
1	0.02	98.50	58.59	5771.31	−5273.36	497.95	489.70	−8.25	8.25
2	0.04	97.00	53.45	5184.51	−4771.31	413.19	396.75	−16.44	16.44
3	0.06	95.47	47.89	4571.99	−4236.14	335.85	311.62	−24.24	24.24
4	0.08	98.17	41.87	4110.19	−3664.81	445.38	419.94	−25.44	25.44
5	0.10	100.48	51.10	5134.88	−4575.85	559.03	528.68	−30.35	30.35
6	0.12	102.92	59.19	6092.33	−5394.04	698.28	664.00	−34.29	34.29
7	0.13	105.50	67.69	7140.94	−6274.05	866.89	829.99	−36.90	36.90
8	0.15	101.81	76.13	7750.53	−7171.44	579.09	550.21	−28.88	28.88
9	0.17	100.65	63.86	6427.97	−5928.66	499.31	457.48	−41.83	41.83
10	0.19	98.86	59.15	5847.59	−5459.40	388.19	337.04	−51.15	51.15
11	0.21	99.26	50.91	5053.11	−4649.03	404.09	335.31	−68.78	68.78
12	0.23	101.78	52.25	5317.65	−4786.50	531.15	458.03	−73.12	73.12
13	0.25	99.28	64.14	6367.78	−6002.74	365.03	288.19	−76.84	76.84
14	0.27	99.19	51.19	5077.96	−4722.07	355.89	257.52	−98.36	98.36
15	0.29	95.53	49.97	4773.36	−4604.77	168.59	92.40	−76.18	76.18
16	0.31	98.02	26.47	2594.85	−2362.61	232.23	148.05	−84.19	84.19
17	0.33	97.03	39.61	3843.35	−3653.84	189.51	83.97	−105.54	105.54
18	0.35	96.64	29.34	2835.17	−2659.65	175.51	44.51	−131.01	131.01
19	0.37	95.01	21.11	2005.37	−1866.05	139.32	3.75	−135.56	135.56
20	0.38	93.67	3.62	338.73	−204.45	134.27	0.00	−134.27	134.27

previous example, but the maturity is now fixed at 130 trading days[6]. Figure 9.3 represents the density function for different fixed rebalancing frequencies[7]. We notice that π is approximately a Gaussian random variable, which is centered around 0. However, the variance depends on the rebalancing frequency. In Figure 9.4, we have reported the relationship between the hedging efficiency $\sigma(\pi)$ and the rebalancing frequency. We confirm that we can perfectly replicate the option with a continuous rebalancing.

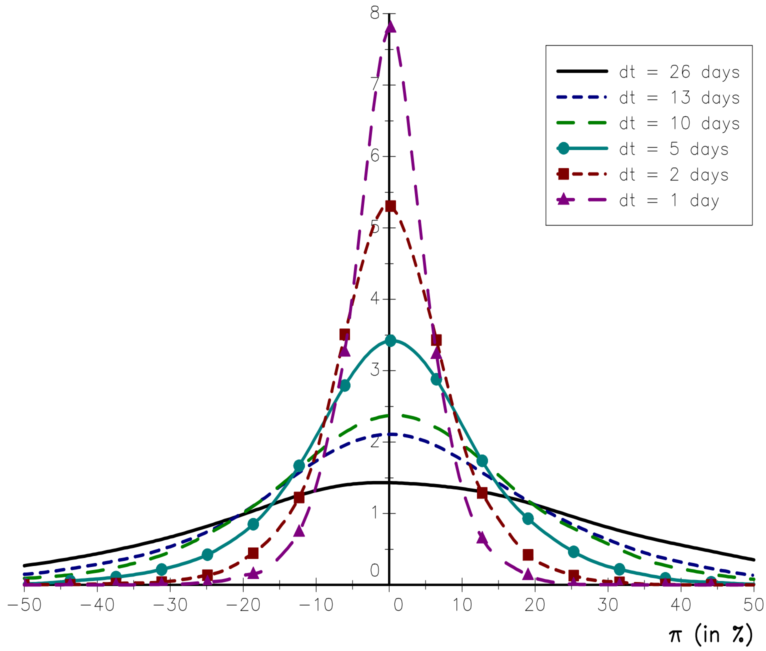

FIGURE 9.3: Probability density function of the hedging ratio π

Let us now understand how the hedging ratio is impacted by the dynamics of the underlying asset. We consider again the previous example and simulate one trajectory (see the first panel in Figure 9.5). We hedge the call option every half an hour. At the maturity, the hedging ratio is equal to 1.8%. The maximum is reached at time $t = 0.466$ and is equal to 3.5%. We now introduce a jump at time $t = 0.25$. This jump induces a large negative P&L for the trader, whatever the sign of the jump (see the second and third panels in Figure 9.5). If we introduce a jump later at time $t = 0.40$, the cost depends on the magnitude and the sign of the jump (Figure 9.6). A positive jump has no impact on the cost of the replicating portfolio, whereas a negative jump has an impact only if the jump is very large. To understand these results, we have to analyze the delta coefficient. At time $t = 0.40$, the option is in-the-money and the delta is close to 1. This implies that a positive jump has low impact on the delta hedging, because the delta is bounded by one. If there is a negative jump, the impact is also limited because the delta is lowly reduced. However, in the case of a high negative jump, the impact may be important because the delta can be dramatically reduced. We also observe the same results when the option is highly out-of-the-money and the delta is close to zero. In this case, a negative jump has no impact, because it decreases

[6]We assume that a year corresponds to 260 trading days. This implies that the maturity of the option is exactly one-half year.

[7]We note $t_i - t_{i-1} = \mathrm{d}t$.

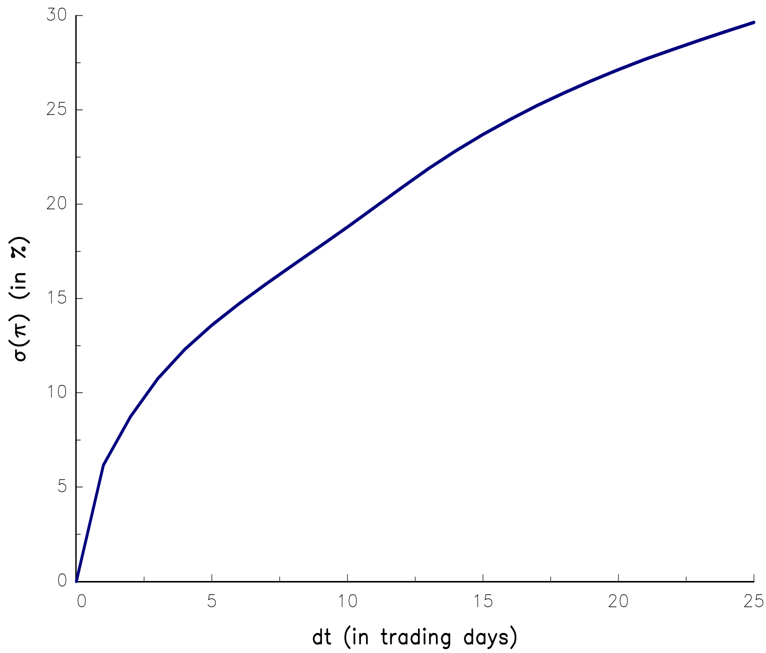

FIGURE 9.4: Relationship between the hedging efficiency $\sigma(\pi)$ and the hedging frequency

the delta but the delta is bounded by zero. Conversely, a positive jump may have an impact if the magnitude is enough sufficiently large to increase the delta.

In the case of liquid markets with low transaction costs, a delta neutral hedging may be efficiently implemented in a high frequency basis (daily or intra-day rebalancing). This is not the case of less liquid markets. Moreover, we observe an asymmetry between call and put options. The delta of call options is positive, implying that the replicating portfolio is long on the asset. For put option, the delta is negative and the replicating portfolio is short on the asset. We know that it is easier to implement a long position than a short position. Sometimes, it is even impossible to be short. For instance, this explains that there exist call options on mutual funds, but not put options on mutual funds. We understand that model risk of derivatives does not only concern the right values of model parameters. In fact, model risk also concerns the hedging management of the option including the feasibility and efficiency of the delta hedging strategy. A famous example is the difference between a put option on S&P 500 index and Eurostoxx 50 index. We know that the returns of the Eurostoxx 50 index present more discontinuous patterns than those of the S&P 500 index. The reason is that European markets react more strongly to American markets than the opposite. This explains that the difference between the closing price and the opening price is more higher in European markets than in American markets. Therefore, a put option on the Eurostoxx 50 index contains an additional premium compared to a put option on the S&P 500 index in order to take into account these stylized facts.

Greek sensitivities We have seen that the delta of the call option is defined by:

$$\boldsymbol{\Delta}(t) = \frac{\partial \boldsymbol{\mathcal{C}}(t, S(t))}{\partial S(t)}$$

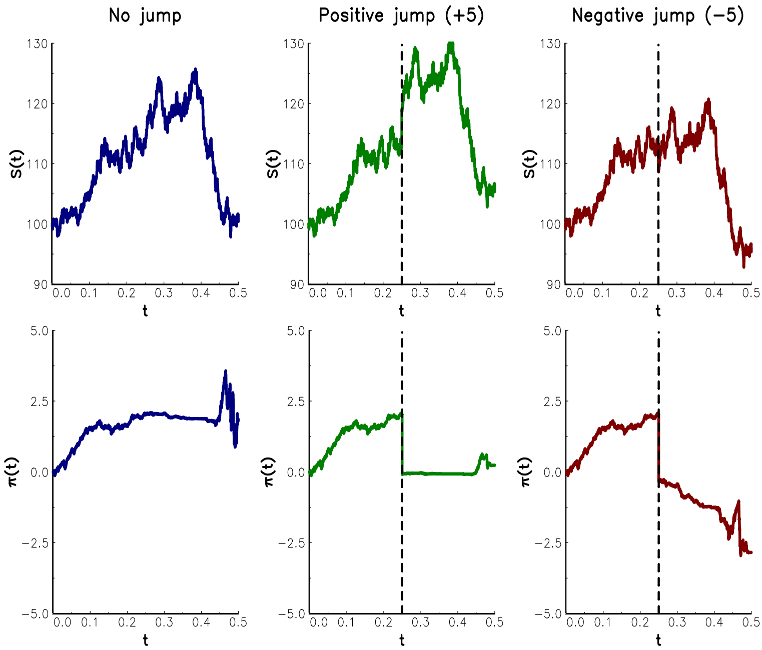

FIGURE 9.5: Impact of a jump on the hedging ratio $\pi(t)$

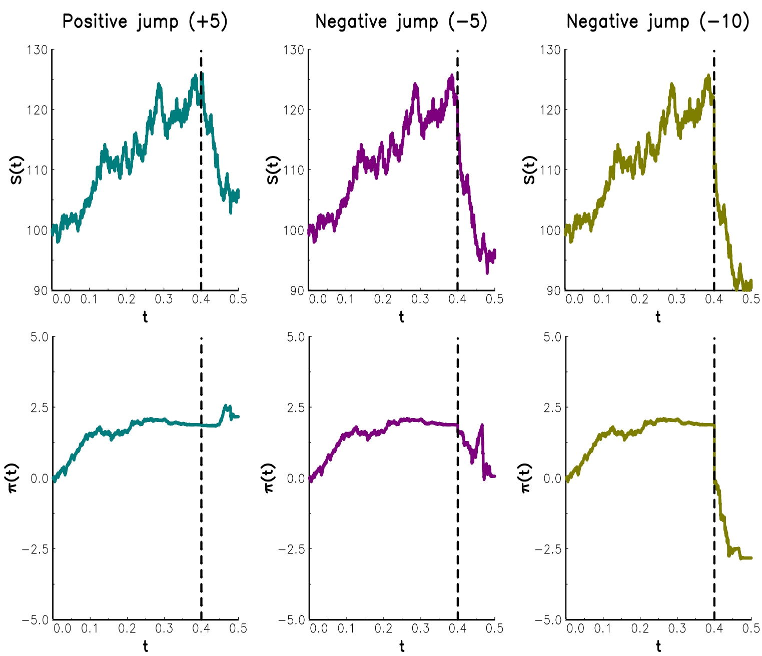

FIGURE 9.6: Impact of a jump on the hedging ratio $\pi(t)$

We have then:

$$\boldsymbol{\mathcal{C}}\left(t+\mathrm{d}t,S\left(t+h\right)\right)-\boldsymbol{\mathcal{C}}\left(t,S\left(t\right)\right)\approx\boldsymbol{\Delta}\left(t\right)\cdot\left(S\left(t+\mathrm{d}t\right)-S\left(t\right)\right)$$

This Taylor expansion can be extended to other orders and other parameters. For instance, the delta-gamma-theta approximation is:

$$\begin{aligned}\boldsymbol{\mathcal{C}}\left(t+\mathrm{d}t,S\left(t+h\right)\right)-\boldsymbol{\mathcal{C}}\left(t,S\left(t\right)\right) \quad\approx\quad & \boldsymbol{\Delta}\left(t\right)\cdot\left(S\left(t+\mathrm{d}t\right)-S\left(t\right)\right)+\\ & \frac{1}{2}\boldsymbol{\Gamma}\left(t\right)\cdot\left(S\left(t+\mathrm{d}t\right)-S\left(t\right)\right)^{2}+\\ & \boldsymbol{\Theta}\left(t\right)\cdot\left(\left(t+\mathrm{d}t\right)-t\right)\end{aligned}$$

where the gamma is the second-order derivative of the call option price with respect to the underlying asset price:

$$\boldsymbol{\Gamma}\left(t\right)=\frac{\partial^{2}\boldsymbol{\mathcal{C}}\left(t,S\left(t\right)\right)}{\partial\,S\left(t\right)^{2}}=\frac{\partial\,\boldsymbol{\Delta}\left(t\right)}{\partial\,S\left(t\right)}$$

and the theta is the derivative of the call option price with respect to the time:

$$\boldsymbol{\Theta}\left(t\right)=\frac{\partial\,\boldsymbol{\mathcal{C}}\left(t,S\left(t\right)\right)}{\partial\,t}=-\frac{\partial\,\boldsymbol{\mathcal{C}}\left(t,S\left(t\right)\right)}{\partial\,T}$$

A positive theta coefficient implies that the option value increases if nothing changes, in particular the price of the underlying asset. By construction, the theta is related to the time value of the option. This is why the theta is generally low for options with a short maturity. In fact, understanding theta effects is complicated, because the theta coefficient is not monotonic in any of the parameters (underlying price, volatility and maturity). We recall that the option price satisfies the PDE:

$$\frac{1}{2}\sigma^{2}S^{2}\boldsymbol{\Gamma}+bS\boldsymbol{\Delta}+\boldsymbol{\Theta}-r\boldsymbol{\mathcal{C}}=0$$

We deduce that the theta of the option can be calculated as follows:

$$\boldsymbol{\Theta}=r\boldsymbol{\mathcal{C}}-\frac{1}{2}\sigma^{2}S^{2}\boldsymbol{\Gamma}-bS\boldsymbol{\Delta}$$

This equation shows that the different coefficients are highly related.

Example 79 *We consider a call option, whose strike K is equal to 100. The risk-free rate and the cost-of-carry parameter are equal to 5%. For the volatility coefficient, we consider two cases: (a) $\sigma = 20\%$ and (b) $\sigma = 50\%$.*

In Figure 9.7, we have reported the option delta for different values of the asset price S_0 and different values of the maturity T. We have $\boldsymbol{\Delta}(t)\in[0,1]$. The delta is close to zero when the asset price is far below the option strike, whereas it is close to one when the option is highly in-the-money. We also notice that the coefficient $\boldsymbol{\Delta}$ is an increasing function of the price of the underlying asset. The relationship between the option delta and the maturity parameter is not monotonous and depends whether the option is in-the-money or out-of-the-money. In a similar way, the impact of the volatility is not obvious, and may be different if the option maturity is long or short.

Figure 9.8 represents the option gamma[8]. It is close to zero when the current price of the underlying asset is far from the option strike. In this case, the option trader does not

[8] See Exercise 2.4.7 on page 121 for the analytical expression of the different sensitivity coefficients of the call option.

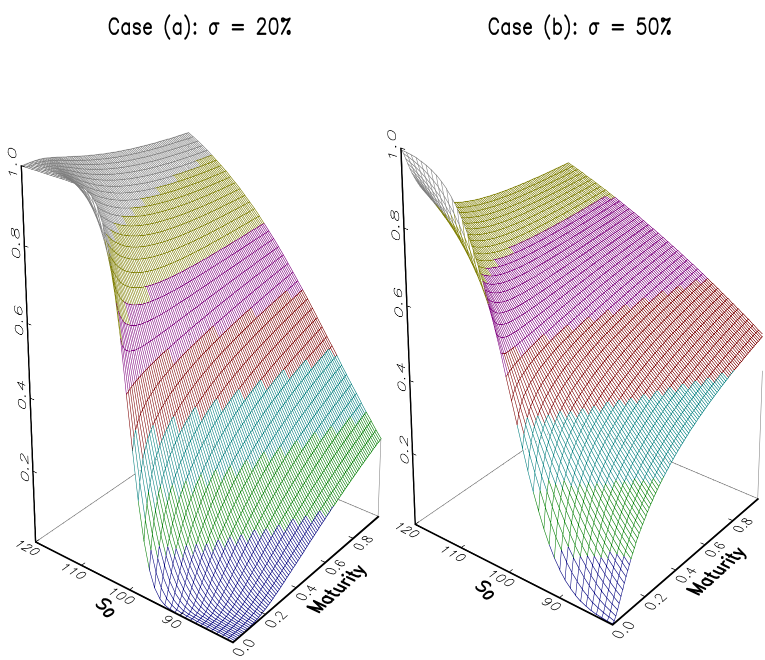

FIGURE 9.7: Delta coefficient of the call option

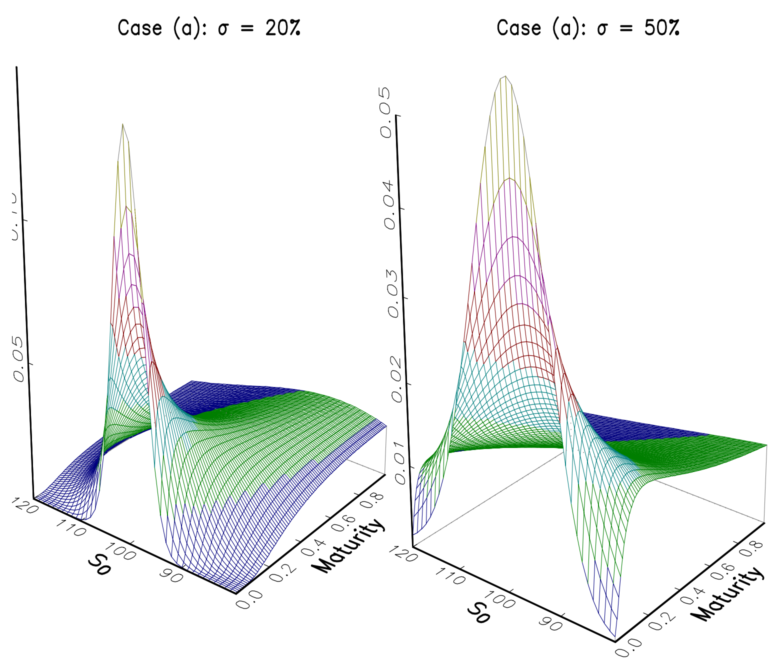

FIGURE 9.8: Gamma coefficient of the call option

need to revise its delta exposure frequently. The gamma coefficient is maximum in the at-the-money region or when the delta is close to 50%. In this situation, the delta can highly vary and the trader must rebalance the replicating portfolio more frequently in order to reduce the residual risk.

Let us assume a delta neutral hedging portfolio. The trader can face four configurations of residual risk given by the following table:

		$\boldsymbol{\Gamma}$ $-$	$\boldsymbol{\Gamma}$ $+$
$\boldsymbol{\Theta}$	$-$		✓
$\boldsymbol{\Theta}$	$+$	✓	

The configuration $(\boldsymbol{\Gamma} < 0, \boldsymbol{\Theta} < 0)$ is not realistic, because the trader will not accept to build a portfolio, whose P&L is almost surely negative. The configuration $(\boldsymbol{\Gamma} > 0, \boldsymbol{\Theta} > 0)$ is also not realistic, because it would mean that the P&L is always positive whatever the market. Therefore, two main configurations are interesting:

(a) a negative gamma exposure with a positive theta;

(b) a positive gamma exposure with a negative theta.

We have represented these two cases in Figure 9.9, and we notice that they lead to different P&L profiles[9]:

(a) If the gamma is negative, the best situation is obtained when the asset price does not move. Any changes in the asset price reduce the P&L, which can be negative if the gamma effect is more important than the theta effect. We also notice that the gain is bounded and the loss is unbounded in this configuration.

(b) If the theta is negative, the loss is bounded and maximum when the asset price does not move. Any changes in the asset price increase the P&L because the gamma is positive. In this configuration, the gain is unbounded.

In order to understand these P&L profiles, we have represented the gamma and theta effects in Figure 9.10 for the case (b). The portfolio is long on a call option and short on the delta neutral hedging strategy. The parameters are the following: $S_0 = 98$, $K = 100$, $\sigma = 10\%$, $b = 5\%$, $r = 5\%$ and $T = 0.25$. The value of the option is equal to 1.601 and we have $\boldsymbol{\Delta}(t_0) = 44.87\%$. In the first panel in Figure 9.10, we have reported the option price (solid curve) and the delta hedging strategy (dashed line) at the current date t_0 when the asset price moves. The area between the two curves represents the gamma effect. We notice that it is positive. For instance, we have $\boldsymbol{\Gamma}(t_0) = 11.55\%$. We do not rebalance the portfolio until time $t = t_0 + \mathrm{d}t$ where $\mathrm{d}t = 0.15$. The dashed curve indicates the value of the option price[10] at the date t. The area between $\boldsymbol{\mathcal{C}}(t, S(t))$ (dashed curve) and $\boldsymbol{\mathcal{C}}(t_0, S(t))$ (solid curve) represents the theta effect. We notice that it is negative[11]. In the second panel, we have reported the resulting P&L. This is the difference between the first area (positive gamma effect) and the second area (negative theta effect). We retrieve the results given in the second panel in Figure 9.9.

[9] We have also indicated the case (a') where the gamma is equal to zero. In this case, we obtain a gamma neutral hedging portfolio and it is not necessary to adjust frequently the hedging portfolio.

[10] We use the same parameters, except that the maturity is now equal to 0.10.

[11] We have $\boldsymbol{\Theta}(t_0, S_0) = -7.09$.

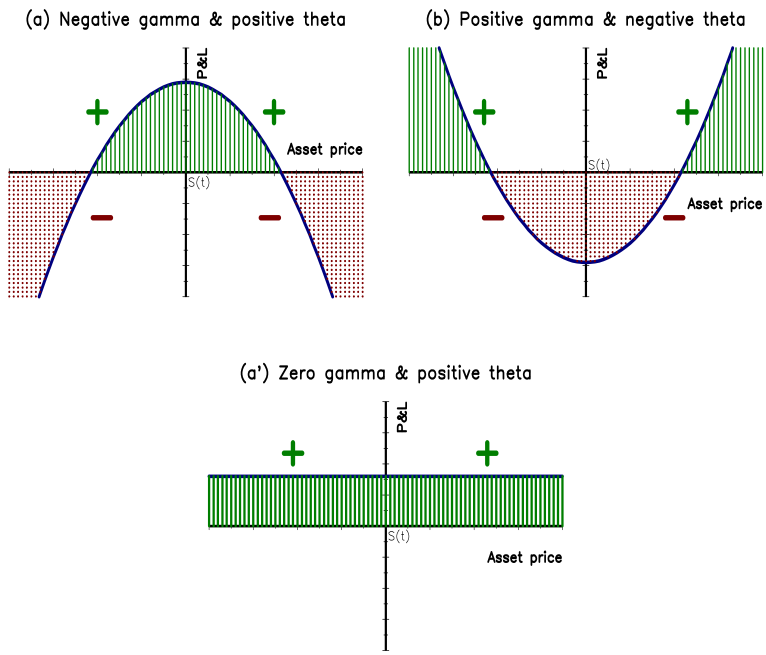

FIGURE 9.9: P&L of the delta neutral hedging portfolio

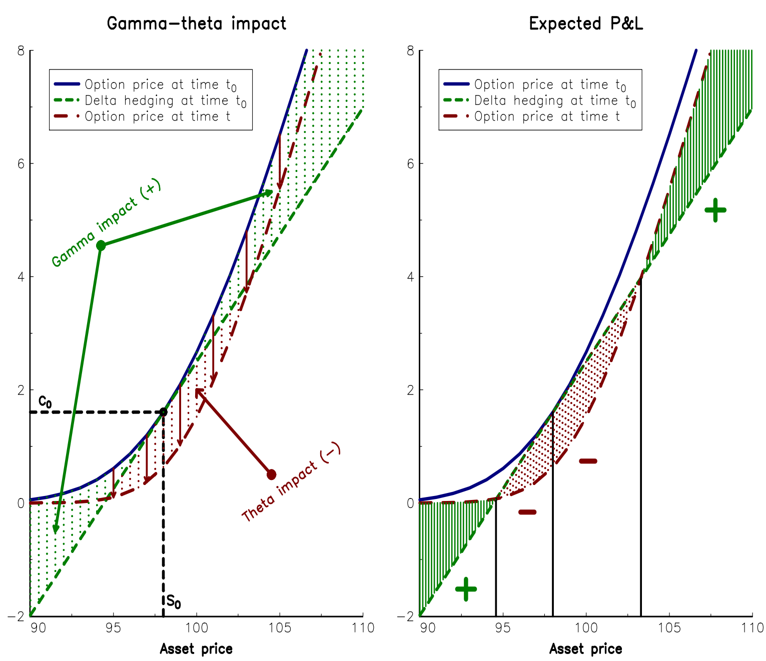

FIGURE 9.10: Illustration of the configuration ($\mathbf{\Gamma} > 0, \mathbf{\Theta} < 0$)

9.1.1.4 The implied volatility

Definition In the Black-Scholes formula, all the parameters are objective except the volatility σ. To calibrate this parameter, we can use a historical estimate $\hat{\sigma}$. However, the option prices computed with the historical volatility $\hat{\sigma}$ do not fit the option prices observed in the market. In practice, we use the Black-Scholes formula to deduce the implied volatility that gives the market prices:

$$f_{\mathrm{BS}}\left(S_0, K, \sigma_{\mathrm{implied}}, T, b, r\right) = V\left(T, K\right)$$

where f_{BS} is the Black-scholes formula and $V\left(T, K\right)$ is the market price of the option, whose maturity date is T and whose strike is K. By convention, the implied volatility is denoted by Σ, and is a function of the parameters[12] T and K:

$$\sigma_{\mathrm{implied}} = \Sigma\left(T, K\right)$$

Example 80 *We consider a call option, whose maturity is one year. The current price of the underlying asset is normalized and is equal to* 100. *Moreover, the risk-free rate and the cost-of-carry parameter are equal to* 5%. *Below, we report the market price of European call options of three assets for several strikes:*

K	90	95	98	100	101	102	105	110
$\mathcal{C}_1\left(T, K\right)$	16.70	13.35	11.55	10.45	9.93	9.42	8.02	6.04
$\mathcal{C}_2\left(T, K\right)$	18.50	14.50	12.00	10.45	9.60	9.00	7.50	5.70
$\mathcal{C}_3\left(T, K\right)$	18.00	14.00	11.80	10.45	9.90	9.50	8.40	7.40

TABLE 9.4: Implied volatility $\Sigma\left(T, K\right)$

K	90	95	98	100	101	102	105	110
$\Sigma_1\left(T, K\right)$	20.00	20.01	19.99	20.0	20.01	19.99	20.00	20.00
$\Sigma_2\left(T, K\right)$	26.18	23.41	21.24	20.0	19.14	18.90	18.69	19.14
$\Sigma_3\left(T, K\right)$	24.53	21.95	20.68	20.0	19.93	20.20	20.95	23.43

For each asset and each strike, we calculate $\Sigma\left(T, K\right)$ and report the results in Table 9.4 and Figure 9.11. For the first set $\mathcal{C}_1$ of options, the implied volatility is constant. In the case of the options $\mathcal{C}_2$, the implied volatility is decreasing with respect to the strike K. In the third case, the implied volatility is decreasing for in-the-money options and increasing for out-of-the-money options.

Remark 99 *When the curve of implied volatility is decreasing and increasing, the curve is called a volatility smile. When the curve of implied volatility is just decreasing, it is called a volatility skew. If we consider the maturity dimension, the term structure of implied volatility is known as the volatility surface.*

Relationship between the implied volatility and the risk-neutral density Breeden and Litzenberger (1978) showed that volatility smile and risk-neutral density are related. Let $\mathcal{C}_t\left(T, K, \right)$ be the market price of the European call option at time t, whose maturity is

[12] $\Sigma\left(T, K\right)$ also depends on the other parameters S_0, b and r, but they are fixed values at the current date t_0.

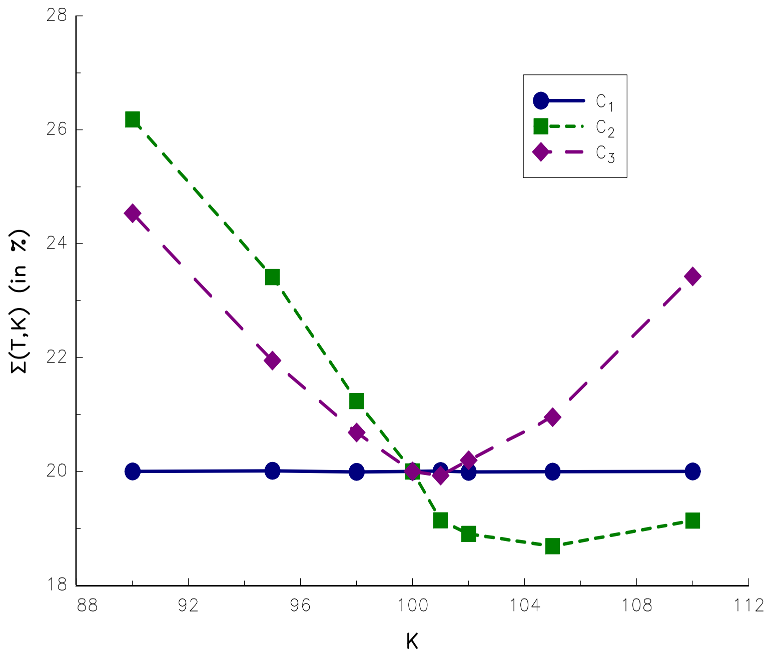

FIGURE 9.11: Volatility smile

T and strike is K. We have:

$$\begin{aligned}
\boldsymbol{\mathcal{C}}_t(T,K) &= \mathbb{E}^{\mathbb{Q}}\left[e^{-\int_t^T r\,\mathrm{d}s}\,(S(T)-K)^+ \,\middle|\, \mathcal{F}_t \right] \\
&= e^{-r(T-t)} \int_{-\infty}^{\infty} (S-K)^+\, q_t(T,S)\,\mathrm{d}S \\
&= e^{-r(T-t)} \int_{K}^{\infty} (S-K)\, q_t(T,S)\,\mathrm{d}S
\end{aligned}$$

where $q_t(T,S)$ is the risk-neutral probability density function of $S(T)$ at time t. By definition, the risk-neutral cumulative distribution function $\mathbb{Q}_t(T,S)$ is equal to[13]:

$$\mathbb{Q}_t(T,S) = \int_{-\infty}^{S} q_t(T,x)\,\mathrm{d}x$$

We deduce that:

$$\begin{aligned}
\frac{\partial\,\boldsymbol{\mathcal{C}}_t(T,K)}{\partial\,K} &= -e^{-r(T-t)} \int_K^{\infty} q_t(T,S)\,\mathrm{d}S \\
&= -e^{-r(T-t)}\left(1-\mathbb{Q}_t(T,K)\right)
\end{aligned}$$

and:

$$\frac{\partial^2\,\boldsymbol{\mathcal{C}}_t(T,K)}{\partial\,K^2} = e^{-r(T-t)} q_t(T,K)$$

[13]We use the notations $\mathbb{Q}_t(T,S)$ and $q_t(T,S)$ instead of $\mathbb{Q}(S)$ and $q(S)$ because they will be convenient when considering the local volatility model.

It follows that the risk-neutral cumulative distribution function is related to the first derivative of the call option price:

$$\begin{aligned}\mathbb{Q}_t(T,K) &= \Pr\{S(T) \le K \mid \mathcal{F}_t\} \\ &= 1 + e^{r(T-t)} \cdot \partial_K \boldsymbol{\mathcal{C}}_t(T,K)\end{aligned}$$

We note $\Sigma_t(T,K)$ the volatility surface and $\boldsymbol{\mathcal{C}}_t^\star(T,K,\Sigma)$ the Black-Scholes formula. It follows that:

$$\begin{aligned}\mathbb{Q}_t(T,K) &= 1 + e^{r(T-t)} \cdot \partial_K \boldsymbol{\mathcal{C}}_t^\star(T,K,\Sigma_t(T,K)) + \\ & \quad e^{r(T-t)} \cdot \partial_\Sigma \boldsymbol{\mathcal{C}}_t^\star(T,K,\Sigma_t(T,K)) \cdot \partial_K \Sigma_t(T,K)\end{aligned}$$

where:

$$\partial_K \boldsymbol{\mathcal{C}}_t^\star(T,K,\Sigma) = -e^{-r(T-t)} \cdot \Phi(d_2)$$

and:

$$\partial_\Sigma \boldsymbol{\mathcal{C}}_t^\star(T,K,\Sigma) = S(t) \cdot e^{(b-r)(T-t)} \cdot \sqrt{T-t} \cdot \phi\left(d_2 + \Sigma\sqrt{T-t}\right)$$

If we are interested in the risk-neutral probability density function, we obtain:

$$\begin{aligned}q_t(T,K) &= \partial_K \mathbb{Q}_t(T,K) \\ &= e^{r(T-t)} \cdot \partial_K^2 \boldsymbol{\mathcal{C}}_t(T,K)\end{aligned}$$

where:

$$\begin{aligned}\partial_K^2 \boldsymbol{\mathcal{C}}_t(T,K) &= \partial_K^2 \boldsymbol{\mathcal{C}}_t^\star(T,K,\Sigma_t) + \\ & \quad 2 \cdot \partial_{K,\Sigma}^2 \boldsymbol{\mathcal{C}}_t^\star(T,K,\Sigma_t) \cdot \partial_K \Sigma_t(T,K) + \\ & \quad \partial_\Sigma \boldsymbol{\mathcal{C}}_t^\star(T,K,\Sigma_t) \cdot \partial_K^2 \Sigma_t(T,K) + \\ & \quad \partial_\Sigma^2 \boldsymbol{\mathcal{C}}_t^\star(T,K,\Sigma_t) \cdot (\partial_K \Sigma_t(T,K))^2\end{aligned}$$

and:

$$\begin{aligned}\partial_K^2 \boldsymbol{\mathcal{C}}_t^\star(T,K,\Sigma) &= e^{-r(T-t)} \frac{\phi(d_2)}{K\Sigma\sqrt{T-t}} \\ \partial_{K,\Sigma}^2 \boldsymbol{\mathcal{C}}_t^\star(T,K,\Sigma) &= e^{(b-r)(T-t)} \frac{S(t)\, d_1 \phi(d_1)}{\Sigma K} \\ \partial_\Sigma^2 \boldsymbol{\mathcal{C}}_t^\star(T,K,\Sigma) &= e^{(b-r)(T-t)} \frac{S(t)\, d_1 d_2 \sqrt{T-t}\phi(d_1)}{\Sigma}\end{aligned}$$

Example 81 *We assume that $S(t) = 100$, $T-t = 10$, $b = r = 5\%$ and:*

$$\Sigma_t(T,K) = 0.25 + \ln\left(1 + 10^{-6}(K-90)^2 + 10^{-6}(K-180)^2\right)$$

In Figure 9.12, we have represented the volatility surface and the associated risk-neutral probability density function. In fact, they both contain the same information, but professionals are more familiar with implied volatilities than risk-neutral probabilities. We have also reported the Black-Scholes risk-neutral distribution by considering the at-the-money implied volatility. We notice that the Black-Scholes model underestimates the probability of extreme events in this example.

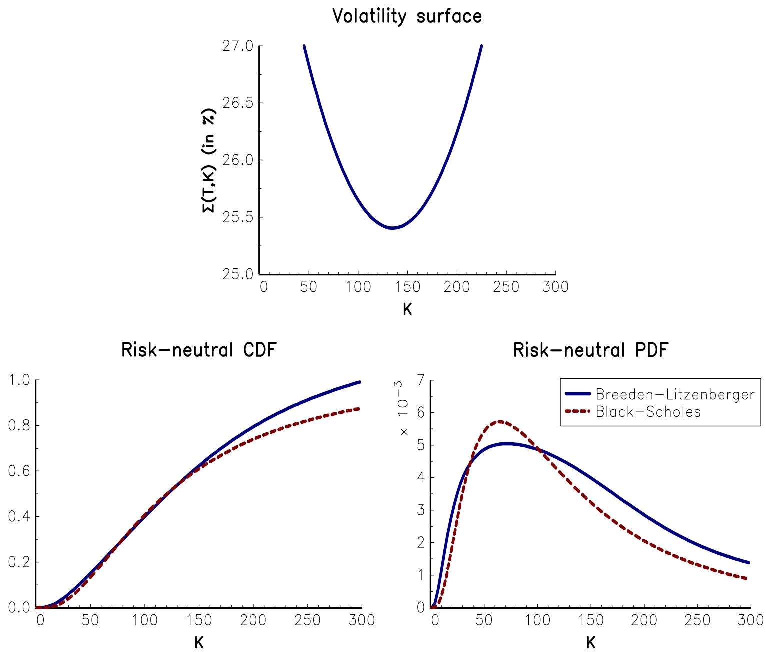

FIGURE 9.12: Risk-neutral probability density function

Robustness of the Black-Scholes formula El Karoui *et al.* (1998) assume that the underlying price process is given by:

$$\mathrm{d}S(t) = \mu(t) S(t) \,\mathrm{d}t + \sigma(t) S(t) \,\mathrm{d}W(t) \tag{9.9}$$

whereas the trader hedges the call option with the implied volatility $\Sigma(T, K)$, meaning that the risk-neutral process is:

$$\mathrm{d}S(t) = rS(t) \,\mathrm{d}t + \Sigma(T, K) S(t) \,\mathrm{d}W^{\mathbb{Q}}(t) \tag{9.10}$$

We reiterate that the dynamics of the replicating portfolio is:

$$\begin{aligned}
\mathrm{d}V(t) &= \phi(t) \,\mathrm{d}S(t) + \psi(t) \,\mathrm{d}B(t) \\
&= \phi(t) \,\mathrm{d}S(t) + \frac{(V(t) - \phi(t) S(t))}{B(t)} rB(t) \,\mathrm{d}t \\
&= \phi(t) \,\mathrm{d}S(t) + r(V(t) - \phi(t) S(t)) \,\mathrm{d}t \\
&= rV(t) \,\mathrm{d}t + \phi(t) (\mathrm{d}S(t) - rS(t) \,\mathrm{d}t)
\end{aligned}$$

Since $\boldsymbol{\mathcal{C}}(t) = \boldsymbol{\mathcal{C}}(t, S(t))$, we also have:

$$\begin{aligned}
\mathrm{d}\boldsymbol{\mathcal{C}}(t) &= \left(\partial_t \boldsymbol{\mathcal{C}}(t, S(t)) + \frac{1}{2}\sigma^2(t) S^2(t) \partial_S^2 \boldsymbol{\mathcal{C}}(t, S(t))\right) \mathrm{d}t + \\
&\quad \partial_S \boldsymbol{\mathcal{C}}(t, S(t)) \,\mathrm{d}S(t)
\end{aligned}$$

Using the PDE (9.2), we notice that:

$$\begin{aligned}
\partial_t \boldsymbol{\mathcal{C}}(t, S(t)) &= r\boldsymbol{\mathcal{C}}(t, S(t)) - rS(t) \partial_S \boldsymbol{\mathcal{C}}(t, S(t)) - \\
&\quad \frac{1}{2}\Sigma^2(T, K) S^2(t) \partial_S^2 \boldsymbol{\mathcal{C}}(t, S(t))
\end{aligned}$$

We deduce that:

$$\begin{aligned}\mathrm{d}\boldsymbol{\mathcal{C}}(t) &= r\boldsymbol{\mathcal{C}}(t,S(t))\,\mathrm{d}t + \\ &\quad \partial_S \boldsymbol{\mathcal{C}}(t,S(t))\,(\mathrm{d}S(t) - rS(t)\,\mathrm{d}t) + \\ &\quad \frac{1}{2}\left(\sigma^2(t) - \Sigma^2(T,K)\right) S^2(t)\,\partial_S^2 \boldsymbol{\mathcal{C}}(t,S(t))\,\mathrm{d}t\end{aligned}$$

We consider the hedging error defined by:

$$e(t) = V(t) - \boldsymbol{\mathcal{C}}(t)$$

Since $\phi(t) = \partial_S \boldsymbol{\mathcal{C}}(t,S(t))$, we have:

$$\begin{aligned}\mathrm{d}e(t) &= \mathrm{d}V(t) - \mathrm{d}\boldsymbol{\mathcal{C}}(t) \\ &= rV(t)\,\mathrm{d}t + \phi(t)\,(\mathrm{d}S(t) - rS(t)\,\mathrm{d}t) - r\boldsymbol{\mathcal{C}}(t,S(t))\,\mathrm{d}t - \\ &\quad \partial_S \boldsymbol{\mathcal{C}}(t,S(t))\,(\mathrm{d}S(t) - rS(t)\,\mathrm{d}t) + \\ &\quad \frac{1}{2}\left(\Sigma^2(T,K) - \sigma^2(t)\right) S^2(t)\,\partial_S^2 \boldsymbol{\mathcal{C}}(t,S(t))\,\mathrm{d}t \\ &= re(t)\,\mathrm{d}t + \frac{1}{2}\left(\Sigma^2(T,K) - \sigma^2(t)\right) S^2(t)\,\partial_S^2 \boldsymbol{\mathcal{C}}(t,S(t))\,\mathrm{d}t\end{aligned}$$

We deduce that[14]:

$$V(T) - \boldsymbol{\mathcal{C}}(T) = \frac{1}{2}\int_0^T e^{r(T-t)}\boldsymbol{\Gamma}(t)\left(\Sigma^2(T,K) - \sigma^2(t)\right) S^2(t)\,\mathrm{d}t \qquad (9.11)$$

This equation is know as the robustness formula of Black-Scholes hedging (El Karoui *et al.*, 1998). Formula (9.11) is one of the most important results of this chapter. Indeed, since the gamma coefficient of a call option is always positive, we can obtain an almost sure P&L if the implied volatility is larger than the realized volatility and if there is no jump. More generally, the previous result is valid for all types of European options:

$$V(T) - f(S(T)) = \frac{1}{2}\int_0^T e^{r(T-t)}\boldsymbol{\Gamma}(t)\left(\Sigma^2(T,K) - \sigma^2(t)\right) S^2(t)\,\mathrm{d}t \qquad (9.12)$$

where $f(S(T))$ is the payoff of the option. We obtain the following results:

- if $\boldsymbol{\Gamma}(t) \geq 0$, a positive P&L is achieved by overestimating the realized volatility:

$$\Sigma(T,K) \geq \sigma(t) \Longrightarrow V(T) \geq f(S(T))$$

- if $\boldsymbol{\Gamma}(t) \leq 0$, a positive P&L is achieved by underestimating the realized volatility:

$$\Sigma(T,K) \leq \sigma(t) \Longrightarrow V(T) \geq f(S(T))$$

- the variance of the hedging error is an increasing function of the absolute value of the gamma coefficient:

$$|\boldsymbol{\Gamma}(t)| \nearrow \Longrightarrow \operatorname{var}(V(T) - f(S(T))) \nearrow$$

In terms of model risk, the robustness formula highlights the role of the implied volatility, the realized volatility and the gamma coefficient. An important issue concerns the case when the gamma can be positive and negative and changes sign during the life of the option. We cannot then control the P&L by using a lower or an upper bound for the implied volatility[15].

[14] Because we have $e(0) = V(0) - \boldsymbol{\mathcal{C}}(0) = 0$.

[15] This issue is solved on page 530.

Example 82 *We consider the replication of 100 ATM call options. The current price of the asset is* 100 *and the maturity of the option is* 6 *months (or* 130 *trading days). We consider the following parameters:* $b = r = 5\%$. *We rebalance the delta hedging portfolio every trading day. Moreover, we assume that the option is priced and hedged with a* 20% *implied volatility.*

Figure 9.13 represents the density function of the hedging ratio π. In the case where the realized volatility $\sigma(t)$ is equal to the implied volatility, we retrieve the previous results: π is centered around zero. However, if the realized volatility $\sigma(t)$ is below (or above) the implied volatility, π is shifted to the right (or the left). If $\sigma(t) < \Sigma$, then there is a higher probability that the trader makes a profit. In our example, we obtain:

$$\Pr\{\pi > 0 \mid \Sigma = 20\%, \sigma = 15\%\} = 99.04\%$$

and:

$$\Pr\{\pi > 0 \mid \Sigma = 20\%, \sigma = 25\%\} = 0.09\%$$

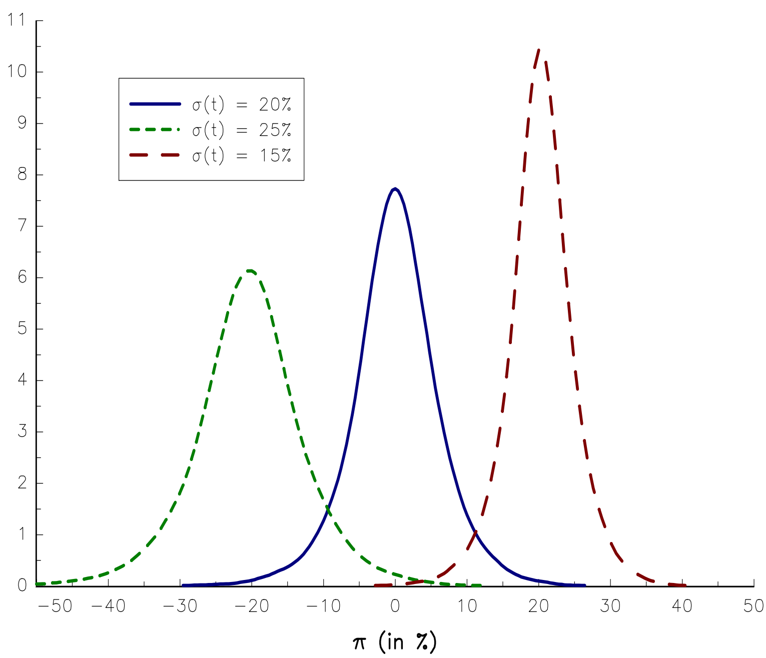

FIGURE 9.13: Hedging error when the implied volatility is 20%

9.1.2 Interest rate risk modeling

Even if the Vasicek model is not used today by practitioners, it is interesting to study it in order to understand the calibration challenge when considering fixed income derivatives. Indeed, in the Black-Scholes model, the calibration consists in estimating a few number of parameters and the main issue concerns the implied volatility. We will see that pricing exotic fixed income derivatives is a more difficult task, because the choice of the risk factors is not obvious and may depend on the tractability of the pricing model[16].

[16]We invite the reader to refer to the book of Brigo and Mercurio (2006) for a more comprehensive presentation on the pricing of fixed income derivatives.

9.1.2.1 Pricing zero-coupon bonds with the Vasicek model

Vasicek (1977) assumes that the state variable is the instantaneous interest rate and follows an Ornstein-Uhlenbeck process:

$$\begin{cases} \mathrm{d}r(t) = a(b - r(t))\,\mathrm{d}t + \sigma\,\mathrm{d}W(t) \\ r(t_0) = r_0 \end{cases}$$

We recall that a zero-coupon bond is a bond that pays \$1 at the maturity date T. Therefore, we have $V(T, r) = 1$ if we note $V(t, r)$ the price of the zero-coupon bond at time t when the interest rate $r(t)$ is equal to r. The corresponding partial differential equation becomes then:

$$\frac{1}{2}\sigma^2 \frac{\partial^2 V(t,r)}{\partial r^2} + (a(b - r(t)) - \lambda(t)\sigma)\frac{\partial V(t,r)}{\partial r} + \frac{\partial V(t,r)}{\partial t} - r(t)V(t,r) = 0$$

By applying the Feynman-Kac representation theorem, we deduce that:

$$V(0, r_0) = \mathbb{E}^{\mathbb{Q}}\left[e^{-\int_0^T r(t)\,\mathrm{d}t} \middle| \mathcal{F}_0 \right] \tag{9.13}$$

where the risk-neutral dynamic of $r(t)$ is:

$$\begin{cases} \mathrm{d}r(t) = (a(b - r(t)) - \lambda(t)\sigma)\,\mathrm{d}t + \sigma\,\mathrm{d}W^{\mathbb{Q}}(t) \\ r(t_0) = r_0 \end{cases}$$

Vasicek (1977) assumes that the risk price of the Wiener process is constant: $\lambda(t) = \lambda$. It follows that the risk-neutral dynamic of $r(t)$ is an Ornstein-Uhlenbeck process:

$$\begin{cases} \mathrm{d}r(t) = a(b' - r(t))\,\mathrm{d}t + \sigma\,\mathrm{d}W^{\mathbb{Q}}(t) \\ r(t_0) = r_0 \end{cases}$$

where:

$$b' = b - \frac{\lambda\sigma}{a}$$

We note $Z = \int_0^T r(t)\,\mathrm{d}t$. In Exercise 9.4.2 on page 593, we show that Z is a Gaussian random variable where:

$$\mathbb{E}[Z] = bT + (r_0 - b)\left(\frac{1 - e^{-aT}}{a}\right)$$

and:

$$\operatorname{var}(Z) = \frac{\sigma^2}{a^2}\left(T - \left(\frac{1 - e^{-aT}}{a}\right) - \frac{1}{2a}\left(1 - e^{-aT}\right)^2\right)$$

We deduce that:

$$\begin{aligned} V(0, r_0) &= \mathbb{E}^{\mathbb{Q}}\left[e^{-Z} \middle| \mathcal{F}_0 \right] \\ &= \exp\left(-\mathbb{E}^{\mathbb{Q}}[Z] + \frac{1}{2}\operatorname{var}^{\mathbb{Q}}(Z)\right) \\ &= \exp\left(-r_0\beta - \left(b' - \frac{\sigma^2}{2a^2}\right)(T - \beta) - \frac{\sigma^2\beta^2}{4a}\right) \end{aligned}$$

where:

$$\beta = \frac{1 - e^{-aT}}{a}$$

If we use the standard notation $B(t,T)$, we have $B(t,T) = V(T-t, r(t))$. We recall that the zero-coupon rate $R(t,T)$ is defined by:

$$B(t,T) = e^{-(T-t)R(t,T)}$$

We deduce that:

$$\begin{aligned} R(t,T) &= -\frac{1}{T-t}\ln B(t,T) \\ &= \frac{r_t\beta}{T-t} + \left(b' - \frac{\sigma^2}{2a^2}\right)\left(\frac{T-t-\beta}{T-t}\right) + \frac{\sigma^2\beta^2}{4a(T-t)} \\ &= \left(b' - \frac{\sigma^2}{2a^2}\right) + \left(r_t - b' + \frac{\sigma^2}{2a^2}\right)\frac{\beta}{T-t} + \frac{\sigma^2\beta^2}{4a(T-t)} \end{aligned}$$

Since we have:

$$R_\infty = \lim_{T\to\infty} R(t,T) = b' - \frac{\sigma^2}{2a^2}$$

the zero-coupon rate has the following expression:

$$R(t,T) = R_\infty + (r_t - R_\infty)\left(\frac{1-e^{-a(T-t)}}{a(T-t)}\right) + \frac{\sigma^2\left(1-e^{-a(T-t)}\right)^2}{4a^3(T-t)} \tag{9.14}$$

The yield curve can take three different forms (Figure 9.14). Vasicek (1977) shows that the curve is increasing if $r_t \leq R_\infty - \dfrac{\sigma^2}{4a^2}$ and decreasing if $r_t \geq R_\infty + \dfrac{\sigma^2}{2a^2}$. Otherwise, it is a bell curve.

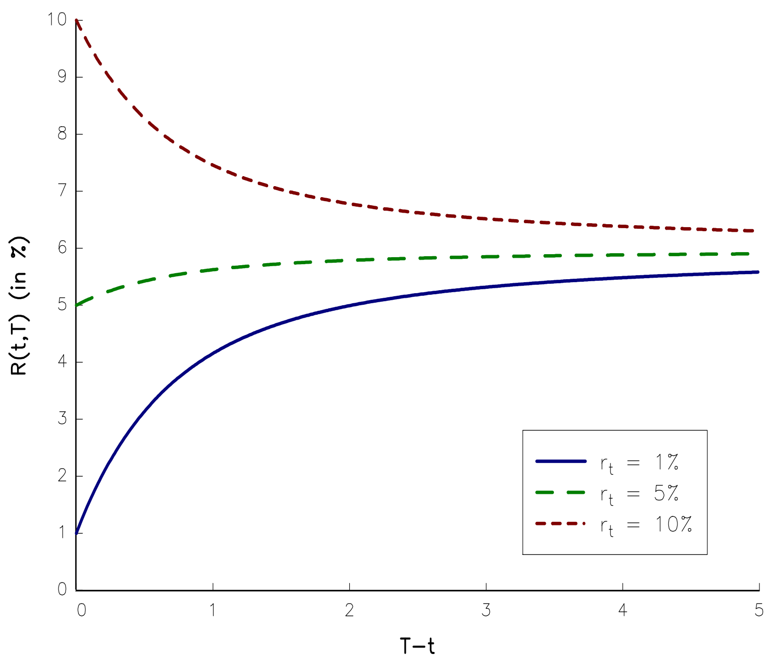

FIGURE 9.14: Vasicek model ($a = 2.5$, $b = 6\%$ and $\sigma = 5\%$)

Let $F(t, T_1, T_2)$ be the forward rate at time t for the period $[T_1, T_2]$. It verifies the following relationship:

$$B(t, T_2) = e^{-(T_2 - T_1)F(t, T_1, T_2)} B(t, T_1)$$

We deduce that the expression of $F(t, T_1, T_2)$ is:

$$F(t, T_1, T_2) = -\frac{1}{(T_2 - T_1)} \ln \frac{B(t, T_2)}{B(t, T_1)}$$

It follows that the instantaneous forward rate is given by this equation[17]:

$$f(t, T) = F(t, T, T) = -\frac{\partial \ln B(t, T)}{\partial T}$$

Using Equation (9.14), we deduce another expression of the price of the zero-coupon bond:

$$B(t, r_t) = \exp\left(-(T-t) R_\infty - (r_t - R_\infty)\left(\frac{1 - e^{-a(T-t)}}{a}\right) - \frac{\sigma^2 \left(1 - e^{-a(T-t)}\right)^2}{4a^3}\right)$$

Therefore, the instantaneous forward rate in the Vasicek model is:

$$f(t, T) = R_\infty + (r_t - R_\infty) e^{-a(T-t)} + \frac{\sigma^2 \left(1 - e^{-a(T-t)}\right) e^{-a(T-t)}}{2a^2}$$

Remark 100 *Forward rates are interest rates that are locked in forward rate agreements (FRA). It involves two dates: T_1 is the start of the period the rate will be fixed for, and T_2 is the maturity date of the FRA. $T_2 - T_1$ is the maturity of the locked interest rate. It is also called the tenor of the interest rate that is being fixed. Therefore, $F(t, T_1, T_2)$ is the forward value of the spot rate $R(t, T_2 - T_1)$.*

9.1.2.2 The calibration issue of the yield curve

Hull and White (1990) propose to extend the Vasicek model by considering that the three parameters a, b and σ are deterministic functions of time. Under the risk-neutral probability measure, the dynamics of the interest rate is then:

$$\mathrm{d}r(t) = a(t)(b(t) - r(t))\,\mathrm{d}t + \sigma(t)\,\mathrm{d}W^{\mathbb{Q}}(t)$$

The underlying idea is to fit the term structure of interest rates and other quantities, such as the term structure of spot volatilities. However, the generalized Vasicek model produces unrealistic volatility term structures. Therefore, Hull and White (1994) focused on this extension:

$$\begin{aligned}\mathrm{d}r(t) &= a(b(t) - r(t))\,\mathrm{d}t + \sigma\,\mathrm{d}W^{\mathbb{Q}}(t) \\ &= (\theta(t) - ar(t))\,\mathrm{d}t + \sigma\,\mathrm{d}W^{\mathbb{Q}}(t)\end{aligned}$$

[17] We also notice that $B(t, T)$ can be expressed in terms of instantaneous forward rates:

$$B(t, T) = e^{-\int_t^T f(t, u)\,\mathrm{d}u}$$

where $\theta(t) = a \cdot b(t)$. If we want to fit exactly the yield curve, we can consider arbitrary values for the parameters a and σ, because the calibration of the yield curve is done by the time-varying mean-reverting parameter:

$$\theta(t) = \frac{\partial f(0,t)}{\partial t} + af(0,t) + \frac{\sigma^2}{2a}\left(1 - e^{-2at}\right)$$

or:

$$b(t) = f(0,t) + \frac{1}{a}\partial_t f(0,t) + \frac{\sigma^2}{2a^2}\left(1 - e^{-2at}\right) \tag{9.15}$$

We notice that $b(t)$ depends on the instantaneous forward rate, which is the first derivative of the price of the zero-coupon bond.

Example 83 *We assume that the zero-coupon rates are given by the Nelson-Siegel model with $\theta_1 = 5.5\%$, $\theta_2 = 0.5\%$, $\theta_3 = -4.5\%$ and $\theta_4 = 1.8$.*

We reiterate that the spot rate $R(t,T)$ in the Nelson-Siegel model is equal to:

$$R(t,T) = \theta_1 + \theta_2\left(\frac{1 - e^{-(T-t)/\theta_4}}{(T-t)/\theta_4}\right) + \theta_3\left(\frac{1 - e^{-(T-t)/\theta_4}}{(T-t)/\theta_4} - e^{-(T-t)/\theta_4}\right)$$

We deduce that the instantaneous forward rate corresponds to the following expression:

$$\begin{aligned} f(t,T) &= \frac{\partial\,(T-t)\,R(t,T)}{\partial T} \\ &= \theta_1 + \theta_2 e^{-(T-t)/\theta_4} + \frac{\theta_3(T-t)}{\theta_4}e^{-(T-t)/\theta_4} \end{aligned}$$

For the slope, we have:

$$\frac{\partial f(t,T)}{\partial T} = \left(\frac{(\theta_3 - \theta_2)}{\theta_4} - \frac{\theta_3(T-t)}{\theta_4^2}\right)e^{-(T-t)/\theta_4}$$

Fitting exactly the Nelson-Siegel yield curve is then equivalent to define the time-varying mean-reverting parameter $b(t)$ of the extended Vasicek model as follows:

$$\begin{aligned} b(t) &= \theta_1 + \theta_2 e^{-t/\theta_4} + \frac{\theta_3 t}{\theta_4}e^{-t/\theta_4} + \frac{\sigma^2}{2a^2}\left(1 - e^{-2at}\right) + \\ &\quad \frac{1}{a}\left(\frac{(\theta_3 - \theta_2)}{\theta_4} - \frac{\theta_3 t}{\theta_4^2}\right)e^{-t/\theta_4} \\ &= \theta_1 + \left(\left(\theta_2 + \frac{\theta_3 t}{\theta_4}\right)\left(1 - \frac{1}{a\theta_4}\right) + \frac{\theta_3}{a\theta_4}\right)e^{-t/\theta_4} + \\ &\quad \frac{\sigma^2}{2a^2}\left(1 - e^{-2at}\right) \end{aligned}$$

In Figure 9.15, we have represented the yield curve obtained with the Nelson-Siegel model in the top/left panel. We have also reported the curve of instantaneous forward rates in the top/right panel. The bottom/left panel corresponds to the time-varying mean-reverting parameter $b(t)$. We have used three set of parameters (a,σ). Finally, we have recalculated the yield curve of the extended Vasicek model in the bottom/right panel. We retrieve the original yield curve. We can compare this solution with those obtained by minimizing the sum of the squared residuals:

$$\left(\hat{r}_0, \hat{a}, \hat{b}, \hat{\sigma}\right) = \arg\min \sum_i \left(R^{\mathrm{NS}}(t,T_i) - R(t,T_i;r_0,a,b,\sigma)\right)^2$$

where $R^{\text{NS}}(t,T_i)$ is the Nelson-Siegel spot rate, $R(t,T_i;r_0,a,b,\sigma)$ is the theoretical spot rate of the Vasicek model and i denotes the i^{th} observation. By considering all the maturities between zero and twenty years with a step of one month, we obtain $\hat{r}_0 = 6\%$, $\hat{a} = 16.88$, $\hat{b} = 7.47\%$ and $\hat{\sigma} = 3.91\%$. Unfortunately, the fitted Vasicek model (curve #2) does not reproduce the original yield curve contrary to the fitted extended Vasicek model (curve #1).

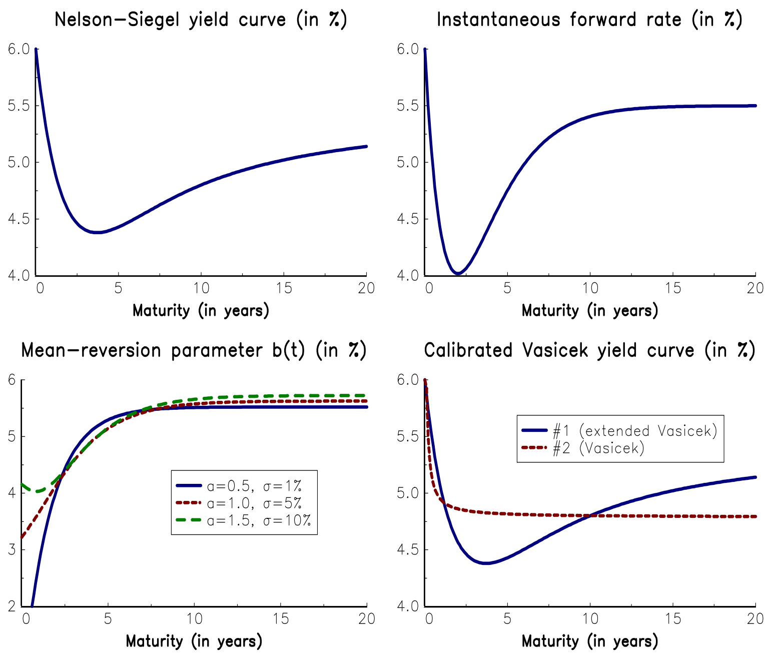

FIGURE 9.15: Calibration of the Vasicek model

The yield curve is not the only market information to calibrate. More generally, the calibration set of an interest rate model also includes caplets, floorlets and swaptions (Brigo and Mercurio, 2006). This explains that pricing interest rate exotic options is more difficult than pricing equity exotic options, and one-factor models based on the short rate are not sufficient, because it is not possible to calibrate caps, floors and swaptions.

9.1.2.3 Caps, floors and swaptions

We consider a number of future dates $T_0, T_1, \ldots, T_n$, and we assume that the period between two dates T_i and T_{i-1} is approximately constant (e.g. 3M or 6M). A caplet is the analog of a call option, whose underlying asset is a forward rate. It is defined by the payoff $(T_i - T_{i-1})\left(F(T_{i-1},T_{i-1},T_i) - K\right)^+$, where K is the strike of the caplet and $F(T_{i-1},T_{i-1},T_i)$ is the forward rate at the future date T_{i-1}. $\delta_{i-1} = T_i - T_{i-1}$ is then the tenor of the caplet, T_{i-1} is the resetting date (or the fixing date) of the forward rate whereas T_i is the maturity date of the caplet. A cap is a portfolio of successive caplets[18]:

$$\operatorname{Cap}(t) = \sum_{i=1}^{n} \operatorname{Caplet}(t,T_{i-1},T_i)$$

[18]We have $t \leq T_0$.

Similarly, a floor is a portfolio of successive floorlets:

$$\text{Floor}(t) = \sum_{i=1}^{n} \text{Floorlet}(t, T_{i-1}, T_i)$$

where the payoff of the floorlet is $(T_i - T_{i-1})(K - F(T_{i-1}, T_{i-1}, T_i))^+$.

A par swap rate is the fixed rate of an interest rate swap[19]:

$$\text{Sw}(t) = \frac{B(t, T_0) - B(t, T_n)}{\sum_{i=1}^{n} (T_i - T_{i-1}) \cdot B(t, T_i)}$$

Then, we define the payoff of a payer swaption as[20]:

$$(\text{Sw}(T_0) - K)^+ \sum_{i=1}^{n} (T_i - T_{i-1}) B(T_0, T_i)$$

where $\text{Sw}(T_0)$ is the forward swap rate.

Remark 101 *Generally, caps, floors and swaptions are written on the Libor rate, which is defined as a simple forward rate:*

$$L(t, T_{i-1}, T_i) = \frac{1}{T_i - T_{i-1}} \left(\frac{B(t, T_{i-1})}{B(t, T_i)} - 1 \right)$$

In order to price these interest rate products, we can use the risk-neutral probability measure $\mathbb{Q}$, and we have[21]:

$$\text{Caplet}(t, T_{i-1}, T_i) = \mathbb{E}^{\mathbb{Q}} \left[e^{-\int_t^{T_i} r(s)\,\mathrm{d}s} \delta_{i-1} (L(T_{i-1}, T_{i-1}, T_i) - K)^+ \middle| \mathcal{F}_t \right]$$

and:

$$\text{Swaption}(t) = \mathbb{E}^{\mathbb{Q}} \left[e^{-\int_t^{T_n} r(s)\,\mathrm{d}s} (\text{Sw}(T_0) - K)^+ \sum_{i=1}^{n} \delta_{i-1} B(T_0, T_i) \middle| \mathcal{F}_t \right]$$

We face here a problem because the discount factor is stochastic and is not independent from the forward rate $L(T_{i-1}, T_{i-1}, T_i)$ or the forward swap rate $\text{Sw}(T_0)$. Therefore, the risk-neutral transform does not help to price interest rate derivatives.

9.1.2.4 Change of numéraire and equivalent martingale measure

We recall that the price of the contingent claim, whose payoff is $V(T) = f(S(T))$ at time T, is given by:

$$V(0) = \mathbb{E}^{\mathbb{Q}} \left[e^{-\int_0^T r(s)\,\mathrm{d}s} \cdot V(T) \middle| \mathcal{F}_0 \right]$$

where $\mathbb{Q}$ is the risk-neutral probability measure. We can rewrite this equation as follows:

$$\frac{V(0)}{M(0)} = \mathbb{E}^{\mathbb{Q}} \left[\frac{V(T)}{M(T)} \middle| \mathcal{F}_0 \right] \tag{9.16}$$

[19] $T_0 = t$ corresponds to a spot swap, whereas $T_0 > t$ corresponds to a forward start swap.

[20] The payoff of a receiver swaption is:

$$(K - \text{Sw}(T_0))^+ \sum_{i=1}^{n} (T_i - T_{i-1}) B(T_0, T_i)$$

[21] We recall that δ_{i-1} is equal to $T_i - T_{i-1}$.

where[22]:

$$M(t) = \exp\left(\int_0^t r(s)\,\mathrm{d}s\right)$$

Under the probability measure $\mathbb{Q}$, we know that $\tilde{V}(t) = V(t)/M(t)$ is an $\mathcal{F}_t$-martingale. The money market account $M(t)$ is then the numéraire when the martingale measure is the risk-neutral probability measure[23], but other numéraires can be used in order to simplify pricing problems:

> "*The use of the risk-neutral probability measure has proved to be very powerful for computing the prices of contingent claims [...] We show here that many other probability measures can be defined in the same way to solve different asset-pricing problems, in particular option pricing. Moreover, these probability measure changes are in fact associated with numéraire changes*" (Geman *et al.*, 1995, page 443).

Let us consider another numéraire $N(t) > 0$ and the associated probability measure given by the Radon-Nikodym derivative:

$$\begin{aligned}\frac{\mathrm{d}\mathbb{Q}^\star}{\mathrm{d}\mathbb{Q}} &= \frac{N(T)/N(0)}{M(T)/M(0)} \\ &= e^{-\int_0^T r(s)\,\mathrm{d}s} \cdot \frac{N(T)}{N(0)}\end{aligned}$$

We have:

$$\begin{aligned}\mathbb{E}^{\mathbb{Q}^\star}\left[\left.\frac{V(T)}{N(T)}\right|\mathcal{F}_0\right] &= \mathbb{E}^{\mathbb{Q}}\left[\left.\frac{V(T)}{N(T)}\cdot\frac{\mathrm{d}\mathbb{Q}^\star}{\mathrm{d}\mathbb{Q}}\right|\mathcal{F}_t\right] \\ &= \frac{M(0)}{N(0)}\cdot\mathbb{E}^{\mathbb{Q}}\left[\left.\frac{V(T)}{M(T)}\right|\mathcal{F}_0\right] \\ &= \frac{M(0)}{N(0)}\cdot V(0)\end{aligned}$$

We deduce that:

$$\frac{V(0)}{N(0)} = \mathbb{E}^{\mathbb{Q}^\star}\left[\left.\frac{V(T)}{N(T)}\right|\mathcal{F}_0\right] \tag{9.17}$$

We notice that Equation (9.17) is similar to Equation (9.16), except that we have changed the numéraire ($M(t) \rightarrow N(t)$) and the probability measure ($\mathbb{Q} \rightarrow \mathbb{Q}^\star$). More generally, we have:

$$V(t) = N(t)\cdot\mathbb{E}^{\mathbb{Q}^\star}\left[\left.\frac{V(T)}{N(T)}\right|\mathcal{F}_t\right]$$

Thanks to Girsanov theorem, we also notice that $e^{-\int_0^t r(s)\,\mathrm{d}s}N(t)$ is an $\mathcal{F}_t$-martingale.

Example 84 *The forward numéraire is the zero-coupon bond price of maturity T:*

$$N(t) = B(t,T)$$

In this case, the probability measure is called the forward probability and is denoted by $\mathbb{Q}^\star(T)$. This martingale measure has been originally used by Jamshidian (1989) for pricing bond options with the Vasicek model. Another important result is that forward rates are martingales under the forward probability measure (Brigo and Mercurio, 2006).

[22] We note that $M(0) = 1$.
[23] $M(t)$ is also called the spot numéraire.

By noticing that $N(T) = B(T,T) = 1$, Equation (9.17) becomes:

$$V(t) = B(t,T)\,\mathbb{E}^{\mathbb{Q}^\star(T)}\left[V(T)\mid \mathcal{F}_t\right]$$

For instance, in the case of a caplet, we obtain:

$$\begin{aligned}
\text{Caplet}(t,T_{i-1},T_i) &= \delta_{i-1}\mathbb{E}^{\mathbb{Q}}\left[\left.\frac{M(t)}{M(T_i)}\left(L(T_{i-1},T_{i-1},T_i)-K\right)^+\right|\mathcal{F}_t\right] \\
&= \delta_{i-1}\mathbb{E}^{\mathbb{Q}^\star(T_i)}\left[\left.\frac{N(t)}{N(T_i)}\left(L(T_{i-1},T_{i-1},T_i)-K\right)^+\right|\mathcal{F}_t\right] \\
&= \delta_{i-1}B(t,T_i)\,\mathbb{E}^{\mathbb{Q}^\star(T_i)}\left[\left.\left(L(T_{i-1},T_{i-1},T_i)-K\right)^+\right|\mathcal{F}_t\right]
\end{aligned}$$

where $L(t,T_{i-1},T_i)$ is an $\mathcal{F}_t$-martingale under the forward probability measure $\mathbb{Q}^\star(T_i)$. If we use the standard Black model, we obtain:

$$\text{Caplet}(t,T_{i-1},T_i) = \delta_{i-1}B(t,T_i)\left(L(t,T_{i-1},T_i)\,\Phi(d_1) - K\Phi(d_2)\right) \tag{9.18}$$

where[24]:

$$d_1 = \frac{1}{\sigma_{i-1}\sqrt{T_{i-1}-t}}\ln\frac{L(t,T_{i-1},T_i)}{K} + \frac{1}{2}\sigma_{i-1}\sqrt{T_{i-1}-t}$$

and:

$$d_2 = d_1 - \sigma_{i-1}\sqrt{T_{i-1}-t}$$

If we consider other models, the general formula of the caplet price is[25]:

$$\text{Caplet}(t,T_{i-1},T_i) = B(t,T_i)\,\mathbb{E}^{\mathbb{Q}^\star(T_i)}\left[\left.\left(\frac{1}{B(T_{i-1},T_i)} - (1+\delta_{i-1}K)\right)^+\right|\mathcal{F}_t\right]$$

Example 85 *The annuity numéraire is equal to:*

$$N(t) = \sum_{i=1}^{n}(T_i - T_{i-1})\,B(t,T_i)$$

While the forward swap rate is a martingale under the annuity probability measure $\mathbb{Q}^\star$, the annuity numéraire is used to price a swaption (Brigo and Mercurio, 2006).

---

[24] σ_{i-1} is the volatility of the Libor rate $L(t,T_{i-1},T_i)$.

[25] We have:

$$\begin{aligned}
\delta_{i-1}\left(L(t,T_{i-1},T_i)-K\right)^+ &= \left(\frac{B(t,T_{i-1})}{B(t,T_i)} - (1+\delta_{i-1}K)\right)^+ \\
&= \frac{\left(B(t,T_{i-1}) - (1+\delta_{i-1}K)\,B(t,T_i)\right)^+}{B(t,T_i)}
\end{aligned}$$

and:

$$\delta_{i-1}\left(L(T_{i-1},T_{i-1},T_i)-K\right)^+ = \left(\frac{1}{B(T_{i-1},T_i)} - (1+\delta_{i-1}K)\right)^+$$

We deduce the following pricing formula for the swaption:

$$\begin{aligned}
\text{Swaption}(t) &= \mathbb{E}^{\mathbb{Q}}\left[\frac{M(t)}{M(T_n)}\left(\text{Sw}(T_0)-K\right)^+\sum_{i=1}^{n}\delta_{i-1}B(T_0,T_i)\,\middle|\,\mathcal{F}_t\right] \\
&= \mathbb{E}^{\mathbb{Q}^\star}\left[\frac{N(t)}{N(T_0)}\left(\text{Sw}(T_0)-K\right)^+\sum_{i=1}^{n}\delta_{i-1}B(T_0,T_i)\,\middle|\,\mathcal{F}_t\right] \\
&= N(t)\,\mathbb{E}^{\mathbb{Q}^\star}\left[\left(\text{Sw}(T_0)-K\right)^+\,\middle|\,\mathcal{F}_t\right] \\
&= N(t)\,\mathbb{E}^{\mathbb{Q}^\star}\left[\left(\frac{1-B(T_0,T_n)}{N(T_0)}-K\right)^+\,\middle|\,\mathcal{F}_t\right]
\end{aligned} \tag{9.19}$$

Using Equation (9.19), we can also find a Black formula for the swaption, in exactly the same way as caps and floors. However, we face here an issue. Indeed, it is equivalent to assume that all the forward rates are log-normal under the different forward probability measures $\mathbb{Q}^\star(T_i)$ and the swap rates are also log-normal under the annuity probability measures $\mathbb{Q}^\star$. The problem is that these different forward and swap rates are related, and their dynamics are not independent.

9.1.2.5 The HJM model

Until the beginning of the nineties, the state variable of fixed income models is the instantaneous interest rate $r(t)$. For instance, it is the case of the models of Vasicek (1977) and Cox *et al.* (1985). However, we have seen that we face some calibration issues when considering such framework. Heath *et al.* (1992) propose then that the state variables are forward rates, and not spot rates. Under the risk-neutral probability measure $\mathbb{Q}$, the dynamics of the instantaneous forward rate for the maturity T is given by:

$$f(t,T)=f(0,T)+\int_0^t\alpha(s,T)\,\mathrm{d}s+\int_0^t\sigma(s,T)\,\mathrm{d}W^{\mathbb{Q}}(s)$$

where $f(0,T)$ is the current forward rate. Therefore, the stochastic differential equation is:

$$\mathrm{d}f(t,T)=\alpha(t,T)\,\mathrm{d}t+\sigma(t,T)\,\mathrm{d}W^{\mathbb{Q}}(t) \tag{9.20}$$

Bond pricing We recall that:

$$B(t,T)=e^{-\int_t^T f(t,u)\,\mathrm{d}u}$$

If we note $X(t)=-\int_t^T f(t,u)\,\mathrm{d}u$, we have:

$$\begin{aligned}
\mathrm{d}X(t) &= f(t,t)\,\mathrm{d}t-\int_t^T\mathrm{d}f(t,u)\,\mathrm{d}u \\
&= f(t,t)\,\mathrm{d}t-\left(\int_t^T\alpha(t,u)\,\mathrm{d}u\right)\mathrm{d}t-\left(\int_t^T\sigma(t,u)\,\mathrm{d}u\right)\mathrm{d}W^{\mathbb{Q}}(t) \\
&= \left(f(t,t)+a(t,T)\right)\mathrm{d}t+b(t,T)\,\mathrm{d}W^{\mathbb{Q}}(t)
\end{aligned}$$

where:

$$a(t,T)=-\int_t^T\alpha(t,u)\,\mathrm{d}u$$

and:

$$b(t,T) = -\int_t^T \sigma(t,u)\,\mathrm{d}u$$

We deduce that:

$$\begin{aligned}
\mathrm{d}B(t,T) &= e^{X(t)}\,\mathrm{d}X(t) + \frac{1}{2}e^{X(t)}\langle \mathrm{d}X(t), \mathrm{d}X(t)\rangle \\
&= \left(f(t,t) + a(t,T) + \frac{1}{2}b^2(t,T)\right)B(t,T)\,\mathrm{d}t + \\
&\quad\; b(t,T)\,B(t,T)\,\mathrm{d}W^{\mathbb{Q}}(t)
\end{aligned}$$

Since $f(t,t)$ is equal to the spot rate $r(t)$, the HJM model implies the following restriction[26]:

$$\alpha(t,T) = \sigma(t,T)\int_t^T \sigma(t,u)\,\mathrm{d}u \tag{9.21}$$

Equation (9.21) is known as the '*drift restriction*' and is necessary to ensure no-arbitrage opportunities. In this case, we verify that the discounted zero-coupon bond is a martingale under the risk-neutral probability measure $\mathbb{Q}$:

$$\mathrm{d}B(t,T) = r(t)\,B(t,T)\,\mathrm{d}t + b(t,T)\,B(t,T)\,\mathrm{d}W^{\mathbb{Q}}(t)$$

Dynamics of spot and forward rates The drift restriction implies that the dynamics of the instantaneous forward rate $f(t,T)$ is given by:

$$\mathrm{d}f(t,T) = \left(\sigma(t,T)\int_t^T \sigma(t,u)\,\mathrm{d}u\right)\mathrm{d}t + \sigma(t,T)\,\mathrm{d}W^{\mathbb{Q}}(t)$$

Therefore, we have:

$$f(t,T) = f(0,T) + \int_0^t \left(\sigma(s,T)\int_s^T \sigma(s,u)\,\mathrm{d}u\right)\mathrm{d}s + \int_0^t \sigma(s,T)\,\mathrm{d}W^{\mathbb{Q}}(s)$$

If we are interested in the instantaneous spot rate $r(t)$, we obtain:

$$\begin{aligned}
r(t) &= f(t,t) \\
&= r(0) + \int_0^t \left(\sigma(s,t)\int_s^t \sigma(s,u)\,\mathrm{d}u\right)\mathrm{d}s + \int_0^t \sigma(s,t)\,\mathrm{d}W^{\mathbb{Q}}(s)
\end{aligned}$$

Forward probability measure We now consider the dynamics of the forward rate $f(t,T_1)$ under the forward probability measure $\mathbb{Q}^\star(T_2)$ with $T_2 \geq T_1$. We reiterate that the new numéraire $N(t)$ is given by:

$$N(t) = B(t,T_2) = e^{-\int_t^{T_2} f(t,u)\,\mathrm{d}u}$$

[26] Indeed, we must have:

$$a(t,T) + \frac{1}{2}b^2(t,T) = 0$$

or:

$$\partial_T a(t,T) = -b(t,T)\cdot\partial_T b(t,T)$$

In Exercise 9.4.5 on page 596, we show that:

$$\mathrm{d}f(t,T_1) = -\left(\sigma(t,T_1)\int_{T_1}^{T_2}\sigma(t,u)\,\mathrm{d}u\right)\mathrm{d}t + \sigma(t,T_1)\,\mathrm{d}W^{\mathbb{Q}^\star(T_2)}(t)$$

It follows that $f(t,T_1)$ is a martingale under the forward probability measure $\mathbb{Q}^\star(T_1)$:

$$\mathrm{d}f(t,T_1) = \sigma(t,T_1)\,\mathrm{d}W^{\mathbb{Q}^\star(T_1)}(t)$$

We can also show that $B(t,T_2)/B(t,T_1)$ is a martingale under $\mathbb{Q}^\star(T_1)$ and we have:

$$B(T_1,T_2) = \frac{B(t,T_2)}{B(t,T_1)}\exp\left(\int_t^{T_1} g(u)\,\mathrm{d}W^{\mathbb{Q}^\star(T_1)}(u) - \frac{1}{2}\int_t^{T_1} g^2(u)\,\mathrm{d}u\right)$$

where:

$$g(t) = b(t,T_2) - b(t,T_1)$$

Some examples If we assume that $\sigma(t,T)$ is constant and equal to σ, we obtain:

$$f(t,T) = f(0,T) + \sigma^2\left(T - \frac{t}{2}\right)t + \sigma W^{\mathbb{Q}}(t)$$

and:

$$r(t) = f(0,t) + \sigma^2\frac{t^2}{2} + \sigma W^{\mathbb{Q}}(t)$$

This case corresponds to the Gaussian model of Ho and Lee (1986).

Brigo and Mercurio (2006) consider the case of separable volatility:

$$\sigma(t,T) = \xi(t)\,\psi(T)$$

We have:

$$\begin{aligned}\mathrm{d}r(t) &= \left(\partial_t f(0,t) + \psi^2(t)\int_0^t \xi^2(s)\,\mathrm{d}s + \frac{(r(t) - f(0,t))}{\psi(t)}\psi'(t)\right)\mathrm{d}t + \\ &\quad \xi(t)\,\psi(t)\,\mathrm{d}W^{\mathbb{Q}}(t)\end{aligned}$$

For example, if we set $\sigma(t,T) = \sigma e^{-a(T-t)}$, we have $\xi(t) = \sigma e^{at}$, $\psi(T) = e^{-aT}$ and[27]:

$$\mathrm{d}r(t) = \left(\partial_t f(0,t) + \sigma^2\left(\frac{1 - e^{-2at}}{2a}\right) + a(f(0,t) - r(t))\right)\mathrm{d}t + \sigma\,\mathrm{d}W^{\mathbb{Q}}(t)$$

We retrieve the generalized Vasicek model proposed by Hull and White (1994):

$$\mathrm{d}r(t) = a(b(t) - r(t))\,\mathrm{d}t + \sigma\,\mathrm{d}W^{\mathbb{Q}}(t)$$

where $b(t)$ is given by Equation (9.15) on page 517.

[27] We have:

$$\begin{aligned}\psi^2(t)\int_0^t \xi^2(s)\,\mathrm{d}s &= \sigma^2 e^{-2at}\int_0^t e^{2as}\,\mathrm{d}s \\ &= \sigma^2\left(\frac{1 - e^{-2at}}{2a}\right)\end{aligned}$$

and:

$$\frac{\psi'(t)}{\psi(t)} = -a$$

Ritchken and Sankarasubramanian (1995) have identified necessary and sufficient conditions on the functions ξ and ψ in order to obtain a Markovian short-rate process. They showed that they must satisfy the following conditions:

$$\xi(t) = \sigma(t)\, e^{\int_0^t \kappa(s)\,\mathrm{d}s}$$

and:

$$\psi(T) = e^{-\int_0^T \kappa(s)\,\mathrm{d}s}$$

where $\sigma(t)$ and $\kappa(t)$ are two $\mathcal{F}_t$-adapted processes. In this case, we obtain:

$$\sigma(t,T) = \sigma(t)\, e^{-\int_t^T \kappa(s)\,\mathrm{d}s}$$

For instance, the generalized Vasicek model is a special case of this framework where the two functions $\sigma(t)$ and $\kappa(t)$ are constant[28].

Extension to multi-factor models We can show that the previous results can be extended when we assume that the instantaneous forward rate is given by the following SDE:

$$\mathrm{d}f(t,T) = \alpha(t,T)\,\mathrm{d}t + \sigma(t,T)^\top\,\mathrm{d}W^{\mathbb{Q}}(t)$$

where $W^{\mathbb{Q}}(t) = \left(W_1^{\mathbb{Q}}(t), \ldots, W_n^{\mathbb{Q}}(t)\right)$ is a n-dimensional Brownian motion and ρ is the correlation matrix of $W^{\mathbb{Q}}(t)$. For instance, the drift restriction (9.21) becomes:

$$\alpha(t,T) = \sigma(t,T)^\top \rho \int_t^T \sigma(t,u)\,\mathrm{d}u$$

In the two-dimensional case, we obtain:

$$\begin{aligned}
\mathrm{d}f(t,T) &= \left(\sigma_1(t,T)\int_t^T \sigma_1(t,u)\,\mathrm{d}u\right)\mathrm{d}t + \left(\sigma_2(t,T)\int_t^T \sigma_2(t,u)\,\mathrm{d}u\right)\mathrm{d}t \\
&\quad +\rho_{1,2}\left(\sigma_1(t,T)\int_t^T \sigma_2(t,u)\,\mathrm{d}u + \sigma_1(t,T)\int_t^T \sigma_2(t,u)\,\mathrm{d}u\right)\mathrm{d}t \\
&\quad \sigma_1(t,T)\,\mathrm{d}W_1^{\mathbb{Q}}(t) + \sigma_2(t,T)\,\mathrm{d}W_2^{\mathbb{Q}}(t)
\end{aligned}$$

For example, Heath *et al.* (1992) extend the Vasicek model by assuming that $\sigma_1(t,T) = \sigma_1$, $\sigma_2(t,T) = \sigma_2 e^{-a_2(T-t)}$ and $\rho_{1;2} = 0$. In this case, we obtain:

$$\begin{aligned}
r(t) &= f(0,t) + \sigma_1^2\frac{t^2}{2} + \frac{\sigma_2^2}{a_2^2}\left(\left(1 - e^{-a_2 t}\right) - \frac{1}{2}\left(1 - e^{-2a_2 t}\right)\right) + \\
&\quad \sigma_1 W_1^{\mathbb{Q}}(t) + \sigma_2\int_0^t e^{-a_2(t-s)}\,\mathrm{d}W_2^{\mathbb{Q}}(s)
\end{aligned}$$

9.1.2.6 Market models

One of the disadvantages of short-rate and HJM models is that they focus on instantaneous spot or forward interest rates. However, these quantities are unobservable. At the end of the nineties, academics have developed two families of models in order to bypass these disadvantages: the Libor market model (LMM) and the swap market model (SMM).

[28] We have $\sigma(t) = \sigma$ and $\kappa(t) = a$.

The Libor market model The Libor market model has been introduced by Brace *et al.* (1997) and is also known as the BGM model in reference to the names of Brace, Gatarek and Musiela. We recall that the Libor rate is defined as a simple forward rate:

$$L(t, T_i, T_{i+1}) = \frac{1}{T_{i+1} - T_i} \left(\frac{B(t, T_i)}{B(t, T_{i+1})} - 1 \right)$$

In order to simplify the notation, we write $L_i(t) = L(t, T_i, T_{i+1})$. Under the forward probability measure $\mathbb{Q}^\star(T_{i+1})$, the Libor rate $L_i(t)$ is a martingale:

$$\mathrm{d}L_i(t) = \gamma_i(t) L_i(t) \,\mathrm{d}W_i^{\mathbb{Q}^\star(T_{i+1})}(t) \tag{9.22}$$

Then, we can use the Black formula (9.18) on page 521 to price caplets and floorlets where the volatility σ_i is defined by:

$$\sigma_i^2 = \frac{1}{T_i - t} \int_t^{T_i} \gamma_i^2(s) \,\mathrm{d}s$$

Therefore, we can price caps and floors because they are just a sum of caplets and floorlets.

Flat or spot implied volatility We can define two surfaces of implied volatilities. Since we observe the market prices of caps and floors, we can deduce the corresponding implied volatilities by assuming that the volatility in the Black model is constant. Thus, we have:

$$\begin{aligned} \mathrm{Cap}_n(t) &= \mathrm{Cap}(t, T_0, T_1, \ldots, T_n) \\ &= \sum_{i=1}^{n} \mathrm{Caplet}(t, T_{i-1}, T_i) \\ &= \sum_{i=1}^{n} \mathrm{Caplet}_i(t) \end{aligned}$$

where $\mathrm{Caplet}_i(t) = \boldsymbol{\mathcal{C}}(L_{i-1}(t), K, \sigma_{i-1}, T_i)$ and $\boldsymbol{\mathcal{C}}(L, K, \sigma, T)$ is the Black formula with volatility σ. The implied volatility $\Sigma(K, T)$ is then obtained by solving the following equation:

$$\sum_{i=1}^{n} \boldsymbol{\mathcal{C}}(L_{i-1}(t), K, \Sigma, T_i) = \mathrm{Cap}_n(t)$$

The implied volatility is also called the '*flat*' volatility and is denoted by $\Sigma^{\mathrm{flat}}(K, T_n)$. In this case, there is a flat implied volatility for each strike K and each maturity T_n of caps/floors. However, we can also compute an implied volatility $\Sigma(K, T)$ for each caplet. We have:

$$\begin{aligned} \mathrm{Cap}_n(t) &= \mathrm{Cap}(t, T_0, T_1, \ldots, T_n) \\ &= \sum_{i=1}^{n} \mathrm{Caplet}(t, T_{i-1}, T_i) \\ &= \sum_{i=1}^{n} \boldsymbol{\mathcal{C}}(L_{i-1}(t), K, \Sigma(K, T_{i-1}), T_i) \end{aligned}$$

The estimation of the implied volatility surface is obtained by minimizing the sum of squared residuals between observed and theoretical prices. In this case, the implied volatility is called the '*spot*' volatility and is denoted by $\Sigma^{\mathrm{spot}}(K, T_{i-1})$.

Example 86 *We consider* 6 *caplets on the 3M Libor rate, whose strike is equal to* 3%*. The tenor structures are respectively (3M,6M), (6M,9M), (9M,12M), (12M,15M), (15M,18M) and (18M,21M). In the following table, we indicate the price of the six caps*[29]*, whose notional is equal to \$1 m.*

Maturity of the cap	6M	9M	12M	15M	18M	21M
Cap price	151.50	529.74	1259.38	2221.82	3295.31	4594.40

We indicate below the current value of the forward Libor rate, and also the value of the zero-coupon rate.

Start date T_{i-1}	3M	6M	9M	12M	15M	18M
Maturity T_i	6M	9M	12M	15M	18M	21M
Forward Libor rate	3.05%	3.15%	3.30%	3.40%	3.45%	3.55%
Zero-coupon rate	3.05%	3.10%	3.15%	3.20%	3.25%	3.30%

Given the term structure of the volatility, we can price the caplets and the caps[30]. Since we have the price of the caps, we can calibrate the flat and spot implied volatilities. We obtain the results given in Table 9.5.

TABLE 9.5: Calibration of $\Sigma^{\text{flat}}(K,T_n)$, $\Sigma^{\text{spot}}(K,T_i)$ and γ_i

T_n	$\Sigma^{\text{flat}}(K,T_n)$	T_i	$\Sigma^{\text{spot}}(K,T_i)$	T_i	γ_i
6M	5.000%	3M	5.000%	3M	5.000%
9M	5.083%	6M	5.199%	6M	5.391%
12M	5.130%	9M	5.449%	9M	5.918%
15M	5.158%	12M	5.497%	12M	5.637%
18M	5.192%	15M	5.557%	15M	5.794%
21M	5.214%	18M	5.616%	18M	5.899%

We consider that the functions $\gamma_i(t)$ are the same and are equal to $\gamma(t)$. If we assume that $\gamma(t)$ is a piecewise constant function, we have:

$$\gamma(t) = \begin{cases} \gamma_0 & \text{if } t \in [0, T_0[\\ \gamma_i & \text{if } t \in [T_{i-1}, T_i[\end{cases}$$

It follows that:

$$\int_0^{T_i} \gamma^2(s)\,\mathrm{d}s = \int_0^{T_i-1} \gamma^2(s)\,\mathrm{d}s + \int_{T_i-1}^{T_i} \gamma^2(s)\,\mathrm{d}s$$

or:

$$T_i \Sigma^{\text{spot}}(K,T_i)^2 = T_{i-1}\Sigma^{\text{spot}}(K,T_{i-1})^2 + (T_i - T_{i-1})\gamma_i^2$$

We deduce that:

$$\gamma_0 = \Sigma^{\text{spot}}(K,T_0)$$

[29]The i^{th} cap is the sum of the first i caplets.

[30]For instance, if we assume that the volatility σ_i for the second caplet is 5%, we obtain:

$$\text{Caplet}(0, 6\text{M}, 9\text{M}) = 10^6 \times 0.25 \times e^{-0.75\times 3.05\%} \times (3.15\% \times \Phi(d_1) - 3\% \times \Phi(d_2)) = \$394.48$$

where:

$$d_1 = \frac{1}{5\% \times \sqrt{0.5}} \ln\left(\frac{3.15\%}{3\%}\right) + \frac{1}{2} \times 5\% \times \sqrt{0.5} = 1.3977$$

and:

$$d_2 = d_1 - 5\% \times \sqrt{0.5} = 1.3623$$

and:

$$\gamma_i = \sqrt{\frac{T_i \Sigma^{\text{spot}}(K, T_i)^2 - T_{i-1}\Sigma^{\text{spot}}(K, T_{i-1})^2}{T_i - T_{i-1}}}$$

Therefore, we can use the spot volatilities to calibrate the function $\gamma(t)$ (see Table 9.5 and Figure 9.16).

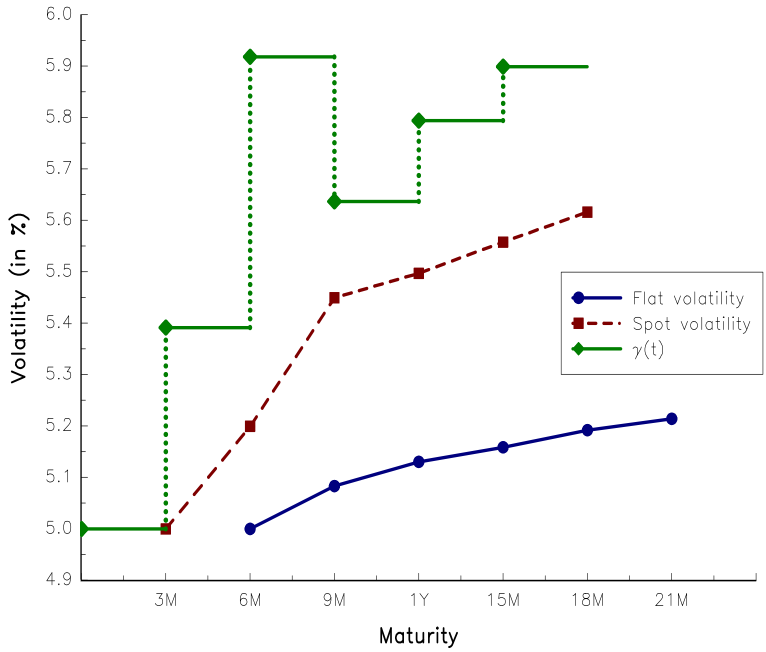

FIGURE 9.16: Flat and spot implied volatilities

Remark 102 *There is a lag between the flat volatility and the spot volatility, because we use the convention that the flat volatility is measured at the maturity date of the cap while the spot volatility is measured at the fixing date. In the previous example, the first flat volatility corresponds to the 6-month maturity date of the cap, whereas the first spot volatility corresponds to the 3-month fixing date of the caplet.*

Dynamics under other probability measures The dynamics (9.22) is valid for the Libor forward rate $L(t, T_i, T_{i+1})$. Then, we have:

$$\begin{cases} \mathrm{d}L_0(t) = \gamma_0(t) L_0(t)\, \mathrm{d}W_0^{\mathbb{Q}^\star(T_1)}(t) \\ \vdots \\ \mathrm{d}L_{n-1}(t) = \gamma_{n-1}(t) L_{n-1}(t)\, \mathrm{d}W_{n-1}^{\mathbb{Q}^\star(T_n)}(t) \end{cases}$$

It is obvious that the Wiener processes $(W_0, \ldots, W_{n-1})$ are correlated. We can show that the dynamics of $L_i(t)$ under the probability measure $\mathbb{Q}^\star(T_{k+1})$ is equal to:

$$\frac{\mathrm{d}L_i(t)}{L_i(t)} = \mu_{i,k}(t)\, \mathrm{d}t + \gamma_i(t)\, \mathrm{d}W_k^{\mathbb{Q}^\star(T_{k+1})}(t)$$

where[31]:

$$\mu_{i,k}(t) = -\gamma_i(t) \sum_{j=i+1}^{k} \rho_{i,j}\gamma_j(t) \frac{(T_{j+1} - T_j) L_j(t)}{1 + (T_{j+1} - T_j) L_j(t)} \qquad \text{if } k > i$$

and $\rho_{i,j}$ is the correlation between $W_i^{\mathbb{Q}^\star(T_{i+1})}$ and $W_j^{\mathbb{Q}^\star(T_{j+1})}$.

Brigo and Mercurio (2006) derive the risk-neutral dynamics of the forward Libor rate $L_i(t)$ when we use the spot numéraire $M(t) = \exp\left(\int_0^t r(s)\,\mathrm{d}s\right)$. However, the expression is complicated and it is not very useful from a practical point of view. This is why they define another version of the spot numéraire, when the money market account is rebalanced only on the resetting dates $T_0, T_1, \ldots, T_{n-1}$. Let $\varphi(t)$ be the next resetting date index after time t, meaning that $\varphi(t) = i$ if $T_{i-1} < t < T_i$. The spot Libor numéraire is then defined as follows:

$$M^\dagger(t) = B\left(t, T_{\varphi(t)-1}\right) \prod_{j=0}^{\varphi(t)-1} \left(1 + \delta_j L_j(T_j)\right)$$

and we have:

$$\frac{\mathrm{d}L_i(t)}{L_i(t)} = \left(\gamma_i(t) \sum_{j=\varphi(t)}^{i} \rho_{i,j}\gamma_j(t) \frac{\delta_j L_j(t)}{1 + \delta_j L_j(t)}\right) \mathrm{d}t + \gamma_i(t)\,\mathrm{d}W_k^{\mathbb{Q}}(t)$$

where $W_k^{\mathbb{Q}}(t)$ is a Brownian motion when the numéraire is $M^\dagger(t)$.

The swap market model Since forward Libor rates $L_i(t)$ are log-normal distributed, the forward swap rate $\mathrm{Sw}(t)$ cannot be log-normal. Then, the Black formula cannot be applied to price swaptions[32]. However, we can always price swaptions using Monte Carlo methods by considering the spot measure (Glasserman, 2003). To circumvent this issue, Jamshidian (1997) proposed a model where the swap rate is a martingale under the annuity probability measure $\mathbb{Q}^\star$:

$$\mathrm{d}\,\mathrm{Sw}(t) = \eta(t)\,\mathrm{Sw}(t)\,\mathrm{d}W^{\mathbb{Q}^\star}(t)$$

Again, we can use the Black formula for pricing swaptions. However, we face the same problem as previously, because forward swap and Libor rates cannot be both log-normal.

9.2 Volatility risk

In the first section of this chapter, we have seen canonical models (Black-Scholes, Black, HJM and LMM) used to price options. In fact, they are not really '*option*' pricing models in the sense that European options such as calls, puts, caps, floors and swaptions are observed in the market. Indeed, they are more '*volatility*' pricing models, because they give a price to the implied volatility of European options. Knowing the implied volatility surface, the trader can then price exotic or OTC derivatives, and more importantly, define corresponding hedging portfolios.

[31] If $k < i$, we have:

$$\mu_{i,k}(t) = \gamma_i(t) \sum_{j=k+1}^{i} \rho_{i,j}\gamma_j(t) \frac{(T_{j+1} - T_j) L_j(t)}{1 + (T_{j+1} - T_j) L_j(t)}$$

[32] Nevertheless, there exist several approximations for pricing swaptions (Rebonato, 2002).

9.2.1 The uncertain volatility model

On page 512, we have seen that the P&L of the replicating strategy is given by the formula of El Karoui *et al.* (1998):

$$V(T) - f(S(T)) = \frac{1}{2}\int_0^T e^{r(T-t)}\mathbf{\Gamma}(t)\left(\Sigma^2(T,K) - \sigma^2(t)\right)S^2(t)\,\mathrm{d}t$$

If we assume that $\sigma(t) \in [\sigma^-, \sigma^+]$, we obtain a simple rule for achieving a positive P&L:

- if $\mathbf{\Gamma}(t) \geq 0$, we have to hedge the portfolio by considering an implied volatility that is equal to the upper bound σ^+;
- if $\mathbf{\Gamma}(t) \leq 0$, we set the implied volatility to the lower bound σ^-.

This rule is valid if the gamma of the option is always positive or negative, that is when the payoff is convex. Avellaneda *et al.* (1995) extend this rule when the gamma can change its sign during the life of the option. This is the case of many exotic options, which depend on conditional events (butterfly, barrier, call spread, ratchet, etc.).

9.2.1.1 Formulation of the partial differential equation

We assume that the dynamics of the underlying price is given by the following SDE:

$$\mathrm{d}S(t) = r(t)S(t)\,\mathrm{d}t + \sigma(t)S(t)\,\mathrm{d}W^{\mathbb{Q}}(t) \tag{9.23}$$

where:

$$\sigma^- \leq \sigma(t) \leq \sigma^+ \tag{9.24}$$

Let $V(t, S(t))$ be the option price, whose payoff is $f(S(T))$. Avellaneda *et al.* (1995) show that $V(t, S(t))$ is bounded:

$$V^-(t, S(t)) \leq V(t, S(t)) \leq V^+(t, S(t))$$

where $V^-(t, S(t)) = \inf_{\mathbb{Q}(\sigma)} \mathbb{E}^{\mathbb{Q}(\sigma)}\left[\exp\left(-\int_t^T r(s)\,\mathrm{d}s\right) f(S(T))\right]$, $V^+(t, S(t)) = \sup_{\mathbb{Q}(\sigma)} \mathbb{E}^{\mathbb{Q}(\sigma)}\left[\exp\left(-\int_t^T r(s)\,\mathrm{d}s\right) f(S(T))\right]$ and $\mathbb{Q}(\sigma)$ denotes all the probability measures such that Equations (9.23) and (9.24) hold. We can then show that V^- and V^+ satisfy the HJB equation:

$$\begin{aligned}\sup_{\sigma^- \leq \sigma(t) \leq \sigma^+} / \inf \left(\frac{1}{2}\sigma^2(t)S^2\frac{\partial^2 V(t,S)}{\partial S^2} + b(t)S\frac{\partial V(t,S)}{\partial S}\right) + & \\ \frac{\partial V(t,S)}{\partial t} - r(t)V(t,S) &= 0\end{aligned}$$

Solving the HJB equation is equivalent to solve the modified Black-Scholes PDE:

$$\left\{\begin{array}{l}\frac{1}{2}\sigma^2(\mathbf{\Gamma}(t,S))S^2\partial_S^2 V(t,S) + b(t)S\partial_S V(t,S) + \partial_t V(t,S) - r(t)V(t,S) = 0 \\ V(T, S(T)) = f(S(T))\end{array}\right.$$

where:

$$\sigma(x) = \left\{\begin{array}{ll}\sigma^+ & \text{if } x \geq 0 \\ \sigma^- & \text{if } x < 0\end{array}\right. \qquad \text{for } V(t,S(t)) = V^+(t,S(t))$$

and:

$$\sigma(x) = \left\{\begin{array}{ll}\sigma^- & \text{if } x > 0 \\ \sigma^+ & \text{if } x \leq 0\end{array}\right. \qquad \text{for } V(t,S(t)) = V^-(t,S(t))$$

Since $\mathbf{\Gamma}(t,S) = \partial_S^2 V(t,S)$ may change its sign during the time interval $[t,T]$, we have to solve the PDE numerically. A solution consists in using finite difference methods described in Appendix A.1.2.4 on page 1041.

Let u_i^m be the numerical solution of $V(t_m, S_i)$. At each iteration m, we approximate the gamma coefficient by the central difference method:

$$\mathbf{\Gamma}(t_m, S_i) \simeq \frac{u_{i+1}^m - 2u_i^m + u_{i+1}^m}{h^2}$$

By assuming that:

$$\operatorname{sign}(\mathbf{\Gamma}(t_m, S_i)) \approx \operatorname{sign}(\mathbf{\Gamma}(t_{m+1}, S_i))$$

we can compute the values taken by $\sigma(\mathbf{\Gamma}(t,S))$ and solve the PDE for the next iteration $m+1$.

9.2.1.2 Computing lower and upper pricing bounds

If we consider the European call option, we have $\mathbf{\Gamma}(t,S) > 0$, meaning that:

$$V^+(t, S(t)) = C_{\mathrm{BS}}\left(t, S(t), \sigma^+\right)$$

and:

$$V^-(t, S(t)) = C_{\mathrm{BS}}\left(t, S(t), \sigma^-\right)$$

where $C_{\mathrm{BS}}(t, S, \sigma)$ is the Black-Scholes price at time t when the underlying price is equal to S and the implied volatility is equal to Σ. Then, the worst-case scenario occurs when the volatility $\sigma(t)$ reaches the upper bound σ^+.

This result is obtained because the delta of the option is a monotone function with respect to the underlying price. However, this property does not hold for many derivative contracts, in particular when the payoff is path dependent. In this case, the payoff depends on the trajectory of the underlying asset. For instance, the payoff of a barrier option depends on whether a certain barrier level was touched (or not touched) at some time during the life of the option. We give here the payoff associated to the four main types of single barrier[33]:

- down-and-in call and put options (DIC/DIP):

$$f_{\mathrm{Barrier}}(S(T)) = \mathbb{1}\left\{S_0 > L, \min_{t\in\mathcal{T}} S(t) \leq L\right\} \cdot f_{\mathrm{Vanilla}}(S(T))$$

- down-and-out call and put option (DOC/DOP):

$$f_{\mathrm{Barrier}}(S(T)) = \mathbb{1}\left\{S_0 > L, \min_{t\in\mathcal{T}} S(t) > L\right\} \cdot f_{\mathrm{Vanilla}}(S(T))$$

- up-and-in call and put options (UIC/UIP):

$$f_{\mathrm{Barrier}}(S(T)) = \mathbb{1}\left\{S_0 < H, \max_{t\in\mathcal{T}} S(t) \geq H\right\} \cdot f_{\mathrm{Vanilla}}(S(T))$$

[33]We have:

$$f_{\mathrm{Vanilla}}(S(T)) = \begin{cases} (S(T) - K)^+ & \text{for the call option} \\ (K - S(T))^+ & \text{for the put option} \end{cases}$$

- up-and-out call and put options (UOC/UOP):

$$f_{\text{Barrier}}\left(S\left(T\right)\right)=\mathbb{1}\left\{S_0<H,\max_{t\in\mathcal{T}}S\left(t\right)<H\right\}\cdot f_{\text{Vanilla}}\left(S\left(T\right)\right)$$

In the case of knocked-out barrier payoffs (DOC/DOP, UOC/UOP), the option terminates the first time the barrier is crossed, whereas knocked-in barrier options (DIC/DIP, UIC/UIP), the payoff is paid only if the underlying asset crosses the barrier. These barriers can also be combined in order to obtain double barrier options:

- double knocked-in call and put options (KIC/KIP):

$$f_{\text{Barrier}}\left(S\left(T\right)\right)=\mathbb{1}\left\{S\left(t\right)\notin\left[L,H\right],t\in\mathcal{T}\right\}\cdot f_{\text{Vanilla}}\left(S\left(T\right)\right)$$

- double knocked-out call and put option (KOC/KOP):

$$f_{\text{Barrier}}\left(S\left(T\right)\right)=\mathbb{1}\left\{S\left(t\right)\in\left[L,H\right],t\in\mathcal{T}\right\}\cdot f_{\text{Vanilla}}\left(S\left(T\right)\right)$$

These options also depend on the time monitoring $t\in\mathcal{T}$ of the barriers. In particular, we distinguish continuous ($\mathcal{T}=[0,T]$), window ($\mathcal{T}\subset[0,T]$) and discrete ($\mathcal{T}=\{t_1,t_2,\ldots,t_n\}$) barriers.

Example 87 *We consider a double KOC barrier option with the following parameters:* $K=100$*,* $L=80$*,* $H=120$*,* $T=1$*,* $b=5\%$ *and* $r=5\%$*. We assume that the volatility* $\sigma\left(t\right)$ *lies in the range of* 15% *and* 25%*.*

In the first and second panels of Figure 9.17, we report the price $V\left(T,S\right)$ of the call option for the continuous barrier ($\mathcal{T}=[0,1]$). If we use the Black-Scholes model[34], the upper bound is reached when $\sigma\left(t\right)=\sigma^-=15\%$ whereas the lower bound is reached when $\sigma\left(t\right)=\sigma^+=25\%$. We have the feeling that the barrier price is a decreasing function of the volatility. However, this is not true. Indeed, a high volatility increases the time value of the final payoff $\left(S\left(T\right)-K\right)^+$, but also decreases the probability to remain within the barrier interval $[L,H]$. Therefore, there is a trade-off between these two opposite effects. If we consider the uncertain volatility model (UVM), the upper bound is larger than this obtained with the BS model, because the worst-case scenario is to have a low volatility when the asset price is close to one barrier and a high volatility when the asset price is far way from the barriers. Therefore, the worst-case scenario at time t depends on the relative position of $S\left(t\right)$ with respect to L, H and K. If we consider a window barrier with $\mathcal{T}=[0.25,0.75]$, we obtain the third and fourth panels of Figure 9.17. We notice that the BS price is not monotone with respect to the volatility. When the current asset price S_0 is equal to the strike K, the BS price is higher when $\sigma\left(t\right)=\sigma^-=15\%$. This is not the case when $S_0=150$. The reason is that a high volatility increases the probability than the asset price is below the up barrier H when the window is triggered. A high volatility is also good when the window ends.

9.2.1.3 Application to ratchet options

Ratchet or cliquet options are financial derivatives that provide a minimum return in exchange for capping the maximum return. They are used by investors because they may

[34] Prices can be computed by numerically solving the PDE, or using the closed-form formulas of Rubinstein and Reiner (1991).

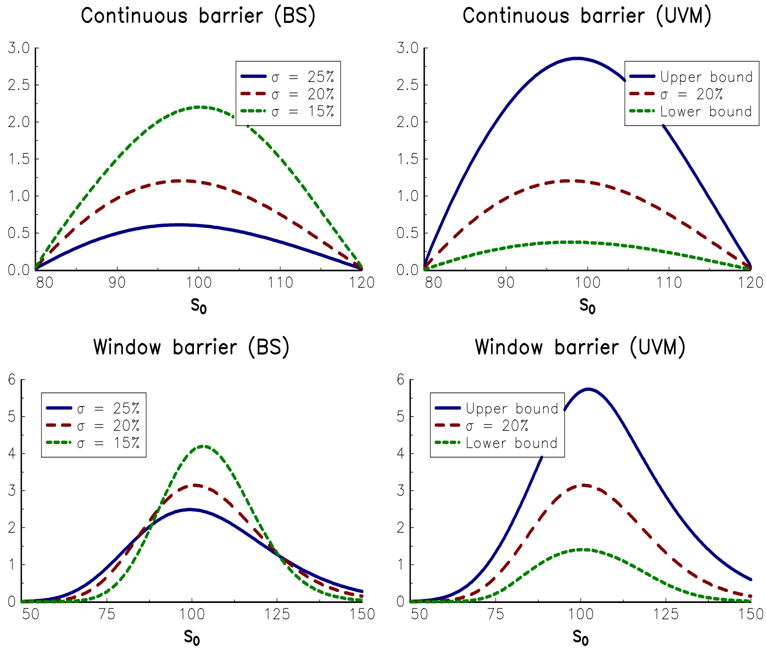

FIGURE 9.17: Comparing BS and UVM prices of the double KOC barrier option

protect them against downside risk. Let us see an example to understand the underlying mechanism of such derivative contracts.

We consider a cliquet option with a 3-year maturity on an equity index $S(t)$. The fixing dates corresponds to the end of each calendar year. We assume that the initial value S_0 of the index is equal to 100. The payoff of the cliquet option is:

$$f(S(T)) = N \cdot \left(\sum_{j=1}^{3} \max \left(0, \frac{S(T_j) - S(T_{j-1})}{S(T_{j-1})}\right)\right)$$

where $\{T_1, T_2, T_3\}$ are the fixing dates and N is the notional of the cliquet option. This cliquet option accumulates positive annual returns. In the following table, we have report four trajectories of $S(T_j)$:

$S(T_j)$	#1	#2	#3	#4
$S(0)$	100	100	100	100
$S(1)$	120	110	95	90
$S(2)$	85	125	95	50
$S(3)$	90	135	75	70
Coupon	25.9%	31.6%	0%	40%

More generally, the payoff of a ratchet is:

$$f(S(T)) = N \cdot \min \left(C_g, \max \left(F_g, \sum_{j=1}^{n} \max(F_\ell, \min(C_\ell, R_j - K_\ell)) - K_g\right)\right)$$

where C_g is the global cap, F_g is the global floor, K_g is the global strike, C_ℓ is the local cap, F_ℓ is the local floor and K_ℓ is the local strike. Here, R_j is the return between two fixing dates:

$$R_j = \frac{S(T_j) - S(T_{j-1})}{S(T_{j-1})}$$

At the maturity, the buyer of the cliquet option receives the sum of periodic returns subject to local and global caps, floors and strikes. In the market, one of the most common payoffs is the following:

$$f(S(T)) = N \cdot \max\left(F_g, \sum_{j=1}^{n} \max\left(0, \min\left(C_\ell, \frac{S(T_j)}{S(T_{j-1})} - 1\right)\right)\right)$$

With this payoff, the option buyer is hedged against the fall of the asset price and has the guarantee to have a minimum return that is equal to the global floor F_g. On the contrary, the option buyer limits the upside risk by introducing the local cap C_ℓ. Therefore, the price of the option is bounded:

$$e^{-rT} \cdot F_g \leq f(S(T)) \leq e^{-rT} \cdot \max(F_g, nC_\ell)$$

The fundamental issue of cliquet option pricing is the choice of the volatility model to price the forward call option:

$$\mathbb{E}\left[\left(\frac{S(T_j)}{S(T_{j-1})} - 1\right)^+ \middle| \mathcal{F}_0\right]$$

At first sight, we might consider the following solutions:

- we may use the implied forward volatility between T_{j-1} and T_j, which is calculated as follows:

$$T_j \cdot \Sigma^2(T_j) = T_{j-1} \cdot \Sigma^2(T_{j-1}) + (T_j - T_{j-1}) \cdot \Sigma^2(T_{j-1}, T_j)$$

- we may also use the implied volatility of maturity $T_j - T_{j-1}$ at the date T_{j-1}; this implies to have a dynamic model of the implied volatility surface.

Since the payoff is locally non-convex, it is not possible to calculate a conservative price using the Black-Scholes model. In this case, the choice of a good implied volatility is inappropriate.

Wilmott (2002) illustrates the difficulty of pricing cliquet options by comparing Black-Scholes and uncertain volatility models. The BS price can be calculated using the Monte Carlo method[35]. Another solution is to derive the corresponding PDE. In this case, we have to introduce two additional variables: $S' = S(T_{j-1})$ is the value of $S(t)$ at the previous fixing date and Q is a variable to keep track of the payoff:

$$Q = \sum_{j=1}^{n} \max\left(0, \min\left(C_\ell, \frac{S(T_j)}{S(Tt_{j-1})} - 1\right)\right)$$

The value of the option depends then on four state variables:

$$V = V(t, S, S', Q)$$

[35]For that, we simulate the asset price at the fixing dates $\{0, T_0, \ldots, T_n, T\}$ using the risk-neutral probability measure $\mathbb{Q}$ and we calculate the mean of the discounted payoff.

We deduce that $V(t, S, S', Q)$ satisfies the following PDE between two fixing dates T_{j-1} and T_j:

$$\frac{1}{2}\sigma^2 S^2 \partial_S^2 V(\cdot) + b(t) S \partial_S V(\cdot) + \partial_t V(\cdot) - r(t) V(\cdot) = 0$$

whereas the final condition is:

$$V(T, S, S', Q) = N \cdot \max(F_g, Q)$$

As noted by Wilmott (2002), $V(t, S, S', Q)$ must also satisfy the jump condition at the fixing date T_j:

$$V(T_j, S, S', Q) = V\left(T_j^+, S, S, Q + \max\left(0, \min\left(C_\ell, \frac{S}{S\prime} - 1\right)\right)\right)$$

This jump condition initializes the new value of S' for the next period $[T_{j-1}, T_j]$ and update the payoff Q. By introducing the state variable $x = S/S'$, Wilmott reduces the dimension of the problem to three variables t, x and Q:

$$\begin{cases} \frac{1}{2}\sigma^2 x^2 \partial_x^2 V(t, x, Q) + b(t) x \partial_x V(t, x, Q) + \partial_t V(t, x, Q) - r(t) V(t, x, Q) = 0 \\ V(T_j, x, Q) = V\left(T_j^+, 1, Q + \max(0, \min(C_\ell, x - 1))\right) \\ V(T, x, Q) = N \cdot \max(F_g, Q) \end{cases}$$

This PDE can easily be solved numerically and the price of the cliquet option is equal to $V(0, 1, 0)$. For the uncertain volatility model, we have exactly the same PDE, except that the quadratic term is replaced by $\frac{1}{2}\sigma^2(\mathbf{\Gamma}(t, x)) x^2 \partial_x^2 V(t, x, Q)$.

Example 88 *We consider a cliquet option with the following parameters: $r = 5\%$, $b = 5\%$, $F_g = 10\%$, $C_\ell = 12\%$ and $N = 1$. The maturity is equal to 5 years, and there are 5 annual fixing dates. The volatility $\sigma(t)$ lies in the range 20% to 30%.*

In Figure 9.18, we show the PDE solution $V(0, x, 0)$ for constant volatility and volatility ranges. We notice that the BS price is not very sensitive to the volatility. With respect to the mid volatility $\sigma = 25\%$, the BS price increases by 1.35% if the volatility is 30% and decreases by 1.57% if the volatility is 20%. On the contrary, the UVM price range $(V^+ - V^-)$ represents 34% of the BS price. This result depends on the values of the global floor and the local cap. An illustration is provided in Figure 9.19, which gives the relationship[36] between the cliquet option price $V(0, 1, 0)$ and the local cap C_ℓ.

9.2.2 The shifted log-normal model

This model assumes that the asset price $S(t)$ is a linear transformation of a log-normal random variable $X(t)$:

$$S(t) = \alpha(t) + \beta(t) X(t)$$

where $\beta(t) \geq 0$. Then, the payoff of the European call option is:

$$\begin{aligned} f(S(T)) &= (S(T) - K)^+ \\ &= (\alpha(T) + \beta(T) X(T) - K)^+ \\ &= \beta(T)\left(X(T) - \frac{K - \alpha(T)}{\beta(T)}\right)^+ \end{aligned}$$

[36] The parameters are those given in Example 88.

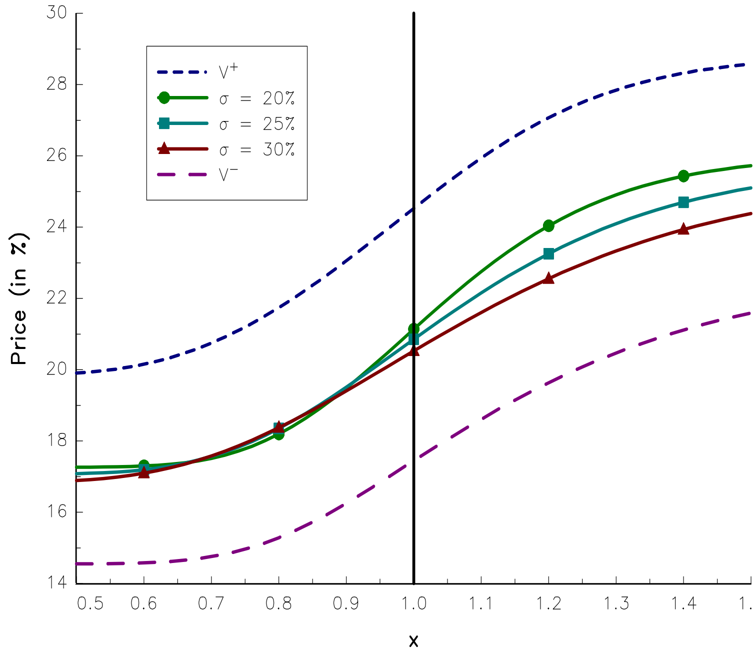

FIGURE 9.18: Comparing BS and UVM prices of the cliquet option

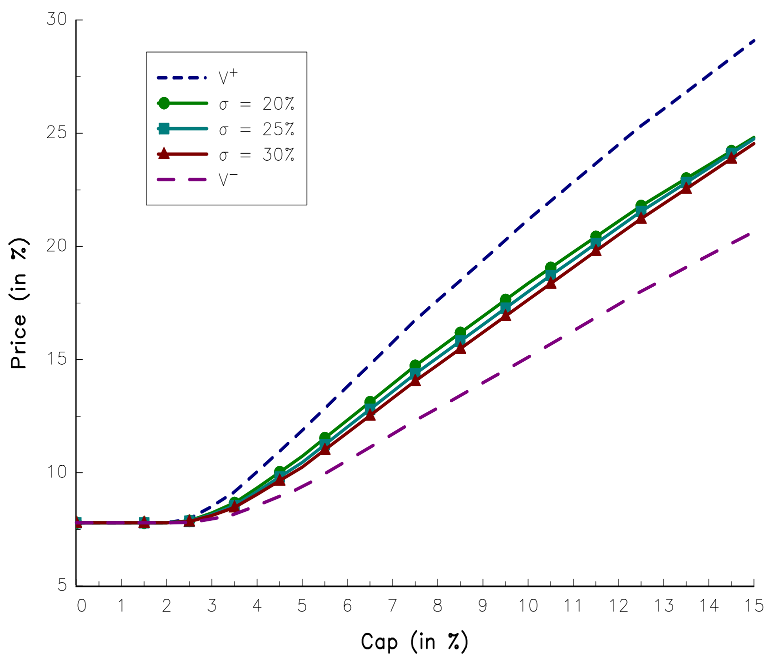

FIGURE 9.19: Influence of the local cap on the cliquet option price

This type of approach is interesting because the pricing of options can then be done using the Black-Scholes formula:

$$\mathcal{C}(0, S_0) = \beta(T) C_{\mathrm{BS}}\left(X_0, \frac{K - \alpha(T)}{\beta(T)}, \sigma_X, T, b_X, r\right)$$

where b_X and σ_X are the drift and diffusion coefficients of $X(t)$ under the risk-neutral probability measure $\mathbb{Q}$. This modeling framework has been introduced by Rubinstein (1983) and popularized by Damiano Brigo and Fabio Mercurio in a series of working papers written between 2000 and 2003[37]. This model was originally used in order to generate a volatility skew, but it is now extensively used in interest rate derivatives because it extends the Black model when facing negative interest rates.

9.2.2.1 The fixed-strike parametrization

Let us suppose that:

$$S(t) = \alpha + \beta \exp\left(\left(b^{\mathbb{Q}}(t) - \frac{1}{2}\sigma^2\right)t + \sigma W^{\mathbb{Q}}(t)\right)$$

We have $S_0 = \alpha + \beta$ meaning that:

$$S(t) = \alpha + (S_0 - \alpha)\exp\left(\left(b^{\mathbb{Q}}(t) - \frac{1}{2}\sigma^2\right)t + \sigma W^{\mathbb{Q}}(t)\right) \tag{9.25}$$

Let b the cost-of-carry parameter of the asset. Under the risk-neutral probability measure, the martingale condition is:

$$\mathbb{E}^{\mathbb{Q}}\left[e^{-bt}S(t) \mid \mathcal{F}_0\right] = S_0$$

Since we have $\mathbb{E}^{\mathbb{Q}}[S(t)] = \alpha + (S_0 - \alpha)e^{b^{\mathbb{Q}}(t)t}$, we deduce that the no-arbitrage condition implies that:

$$\alpha + (S_0 - \alpha)e^{b^{\mathbb{Q}}(t)t} = S_0 e^{bt}$$

or:

$$b^{\mathbb{Q}}(t) = \frac{1}{t}\ln\left(\frac{S_0 e^{bt} - \alpha}{S_0 - \alpha}\right)$$

The payoff of the European call option is:

$$\begin{aligned} f(S(T)) &= (S(T) - K)^+ \\ &= ((S(T) - \alpha) - (K - \alpha))^+ \end{aligned}$$

We deduce that the price of the option is given by:

$$\mathcal{C}(0, S_0) = C_{\mathrm{BS}}\left(S_0 - \alpha, K - \alpha, \sigma, T, b^{\mathbb{Q}}(T), r\right) \tag{9.26}$$

In Figure 9.20, we report the volatility skew generated by the SLN model when the current price S_0 of the asset is 100, the maturity T is one year, the cost-of-carry b is 5% and the interest rate 5 is 5%. We notice that the parameter σ of the SLN model is not of the same magnitude than the implied volatility of the BS model. This is due to the shift α. When α is positive (or negative), we have $\sigma > \Sigma(T, K)$ (or $\sigma < \Sigma(T, K)$).

[37]See Brigo and Mercurio (2002a) for a survey of their different works.

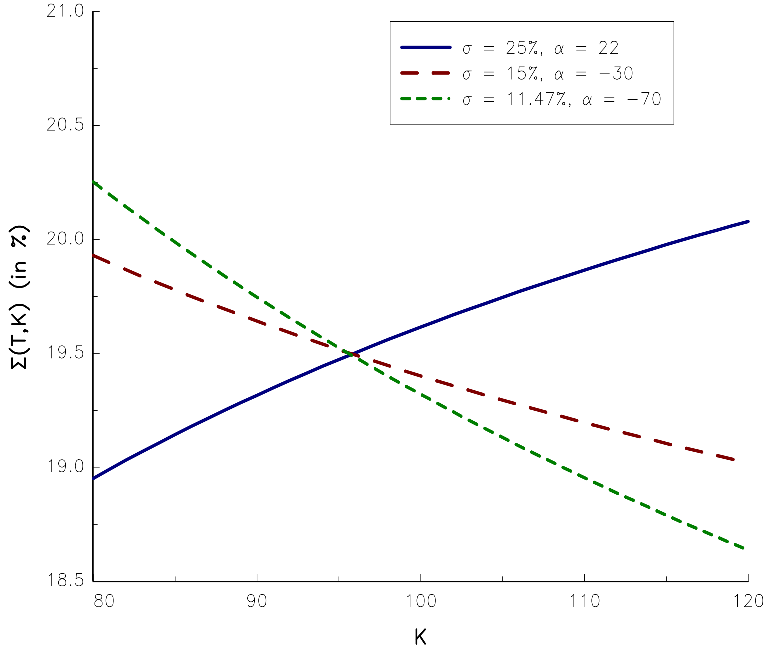

FIGURE 9.20: Volatility skew generated by the SLN model (fixed-strike parametrization)

9.2.2.2 The floating-strike parametrization

Let us now suppose that:

$$S(t) = \alpha e^{\varphi t} + \beta e^{\left(b - \frac{1}{2}\sigma^2\right)t + \sigma W^{\mathbb{Q}}(t)}$$

We have $S_0 = \alpha + \beta$ and $\mathbb{E}^{\mathbb{Q}}[S(t)] = \alpha e^{\varphi t} + \beta e^{bt}$. We deduce that the stochastic process $e^{-bt}S(t)$ is a $\mathcal{F}_t$-martingale if it is equal to:

$$S(t) = \alpha e^{bt} + (S_0 - \alpha)\, e^{\left(b - \frac{1}{2}\sigma^2\right)t + \sigma W^{\mathbb{Q}}(t)} \tag{9.27}$$

The payoff of the European call option becomes:

$$\begin{aligned} f(S(T)) &= (S(T) - K)^+ \\ &= \left(\left(S(T) - \alpha e^{bT}\right) - \left(K - \alpha e^{bT}\right)\right)^+ \end{aligned}$$

It follows that the option price is equal to:

$$\boldsymbol{\mathcal{C}}(0, S_0) = C_{\mathrm{BS}}\left(S_0 - \alpha, K - \alpha e^{bT}, \sigma, T, b, r\right) \tag{9.28}$$

Examples of Volatility skew are given in Figure 9.21 with the same parameters than those we have used in Figure 9.20.

Remark 103 *At first sight, the floating-strike parametrization seems to be different than the fixed-strike parametrization. In practice, the parameters (α, σ) are calibrated for each maturity T. This explains that the two parametrizations are very close.*

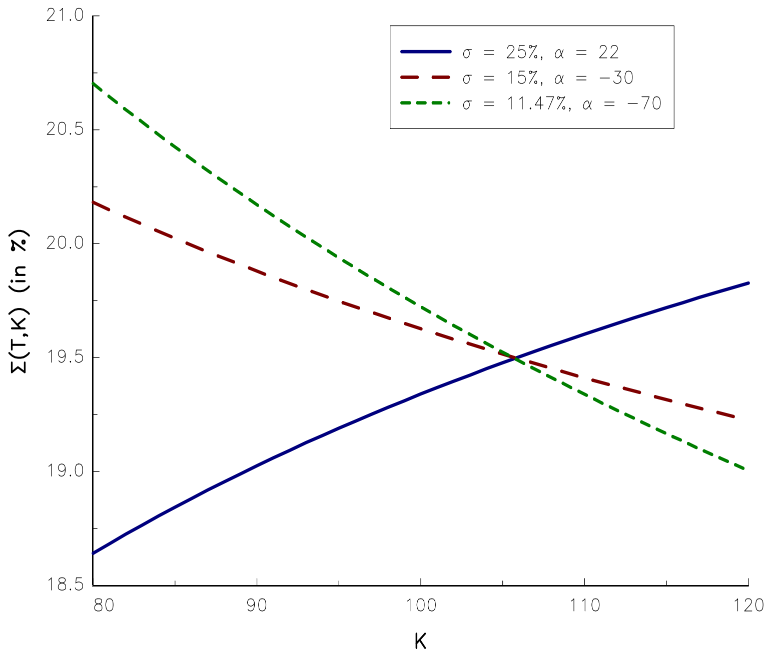

FIGURE 9.21: Volatility skew generated by the SLN model (floating-strike parametrization)

9.2.2.3 The forward parametrization

If we consider the forward price $F(t)$ instead of the spot price $S(t)$, the two models coincide because we have $b = 0$. In this case, the dynamics of the forward price is:

$$\mathrm{d}F(t) = \sigma(F(t) - \alpha)\,\mathrm{d}W^{\mathbb{Q}}(t) \tag{9.29}$$

and the price of the option is given by the Black formula[38]:

$$\mathcal{C}(0, S_0) = C_{\text{Black}}(F_0 - \alpha, K - \alpha, \sigma, T, r) \tag{9.30}$$

In Equations (9.29) and (9.30), we impose that $\alpha < F_0$ and $\alpha < K$. This implies that $F(t) \in [\alpha, \infty)$. This model is appealing for fixed income derivatives, because the interest rate may be negative when α is negative. In this case, we have:

$$\begin{aligned} \mathrm{d}F(t) &= (\sigma F(t) - \alpha\sigma)\,\mathrm{d}W^{\mathbb{Q}}(t) \\ &= (\sigma_1 F(t) + \sigma_2)\,\mathrm{d}W^{\mathbb{Q}}(t) \end{aligned}$$

where $\sigma_1 = \sigma$ and $\sigma_2 = -\alpha\sigma > 0$. We obtain a stochastic differential equation whose diffusion coefficient is a mix of log-normal and Gaussian volatilities.

[38]We recall that the Black formula can be viewed as a special case of the Black-Scholes formula when the cost-of-carry parameter b is equal to zero:

$$C_{\text{Black}}(x, K, \sigma, T, r) = C_{\text{BS}}(x, K, \sigma, T, 0, r)$$

Lee and Wang (2012) prove the following results:

- monotonicity in strike:

$$\operatorname{sign}\left(\frac{\partial\,\Sigma\left(T,K\right)}{\partial\,K}\right)=\operatorname{sign}\alpha$$

- upper and lower bounds:

$$\begin{cases}\Sigma\left(T,K\right)<\sigma & \text{if } \alpha>0\\ \Sigma\left(T,K\right)>\sigma & \text{if } \alpha<0\end{cases}$$

- sharpness of bound:

$$\lim_{K\to\infty}\Sigma\left(T,K\right)=\sigma$$

- short-expiry behavior:

$$\lim_{T\to 0}\Sigma\left(T,K\right)=\begin{cases}\dfrac{\sigma\ln\left(F_0/K\right)}{\ln\left(\left(F_0-\alpha\right)/\left(K-\alpha\right)\right)} & \text{if } K\neq F_0\\ \sigma\left(1-\alpha F_0^{-1}\right) & \text{if } K=F_0\end{cases}$$

The implied volatility formula does not depend on the maturity T and is only valid when T is equal to zero. However, it is a good approximation for other maturities as shown in Table 9.6. We use the previous parameters and three different maturities (one-month, one-year and five-year).

TABLE 9.6: Error of the SLN implied volatility formula (in bps)

K	$(\alpha=22,\sigma=25\%)$			$(\alpha=-70,\sigma=12\%)$		
	1M	1Y	5Y	1M	1Y	5Y
80	1.0	11.1	57.0	−0.9	−12.9	−66.0
90	0.7	10.6	54.1	−1.0	−11.9	−61.4
100	0.9	10.2	51.6	−1.1	−11.3	−57.3
110	1.0	9.7	49.6	−0.8	−10.8	−53.8
120	0.7	9.3	47.7	−0.6	−10.3	−51.3

9.2.2.4 Mixture of SLN distributions

One limitation of the SLN model is that it only produces a volatility skew, and not a volatility smile. In order to obtain a U-shaped curve, Brigo and Mercurio (2002b) suggest that the (risk-neutral) probability density function $f(x)$ of the asset price density is given by the mixture of known basic densities:

$$f\left(x\right)=\sum_{j=1}^{m}p_j f_j\left(x\right)$$

where f_j is the j^{th} basic density, $p_j>0$ and $\sum_{j=1}^{m}p_j=1$. Let $G\left(S\left(T\right)\right)$ be the payoff of an European option. We have:

$$\begin{aligned}\boldsymbol{\mathcal{C}}\left(0,S_0\right) &= \mathbb{E}^{\mathbb{Q}}\left[e^{-rT}G\left(S\left(T\right)\right)\,\middle|\,\mathcal{F}_0\right]\\ &= \int e^{-rT}G\left(S\left(T\right)\right)f\left(x\right)\,\mathrm{d}x\end{aligned}$$

We deduce that:

$$\begin{aligned}
\boldsymbol{\mathcal{C}}(0,S_0) &= \int e^{-rT} G(S(T)) \sum_{j=1}^{m} p_j f_j(x)\,\mathrm{d}x \\
&= \sum_{j=1}^{m} p_j \int e^{-rT} G(S(T)) f_j(x)\,\mathrm{d}x \\
&= \sum_{j=1}^{m} p_j \mathbb{E}^{\mathbb{Q}_j}\left[e^{-rT} G(S(T)) \middle| \mathcal{F}_0 \right]
\end{aligned}$$

where $\mathbb{Q}_j$ is the j^{th} probability measure. It is then straightforward to price an European option using formulas of basic models. If we consider a mixture of two shifted log-normal models, the price of the European call option is equal to:

$$\begin{aligned}
\boldsymbol{\mathcal{C}}(0,S_0) = {} & p \cdot C_{\mathrm{SLN}}(S_0, K, \sigma_1, T, b, r, \alpha_1) + \\
& (1-p) \cdot C_{\mathrm{SLN}}(S_0, K, \sigma_2, T, b, r, \alpha_2)
\end{aligned}$$

where C_{SLN} is the formula of the SLN model[39]. The model has five parameters: σ_1, σ_2, α_1, α_2 and p.

Example 89 *We consider a calibration set of five options, whose strike and implied volatilities are equal to:*

K_j	80	90	100	110	120
$\Sigma(1, K_j)$	21%	19%	18.25%	18.5%	19%

The current value of the asset price is equal to 100*, the maturity of options is one year, the cost-of-carry parameter is set to* 0 *and the interest rate is* 5%*.*

The parameters are estimated by minimizing the weighted least squares:

$$\min \sum_{j=1}^{n} w_j \left(\hat{C}_j - C_{\mathrm{SLN}}(S_0, K_j, \sigma_1, \sigma_2, T_j, b, r, \alpha_1, \alpha_2, p) \right)^2$$

where:

$$\hat{C}_j = C_{\mathrm{BS}}(S_0, K_j, \Sigma(T_j, K_j), T_j, b, r)$$

and w_j is the weight of the j^{th} option. We consider three parameterizations: (#1) the weights w_j are uniform, and we impose that $\alpha_1 = \alpha_2$ and $p = 50\%$; (#2) the weights w_j are uniform, and p is set to 25%; (#3) the weights w_j are inversely proportional to option prices $\hat{C}_j$, and p is set to 50%. Results are given in Table 9.7 and Figure 9.22. We notice that α_1 and α_2 can take large values. Shifted log-normal models are generally presented as a low perturbation of the Black-Scholes model. In practice, they are very different.

9.2.2.5 Application to binary, corridor and barrier options

One of the difficulties when using the Black-Scholes model with exotic options is the choice of the implied volatility. In the case of an European call option, it is obvious to use the implied volatility $\Sigma(T,K)$ that corresponds to the strike and the maturity of the option. In the case of a double barrier option, we can use the implied volatility $\Sigma(T,K)$

[39] It corresponds to one of the three expressions (9.26), (9.28), and (9.30).

TABLE 9.7: Calibrated parameters of the mixed SLN model

Model	#1	#2	#3
σ_1	16.5%	8.2%	10.2%
σ_2	7.3%	17.2%	21.7%
α_1	−53.3	−289.7	−145.2
α_1	−53.3	19.6	47.4
p	50.0%	25.0%	50.0%

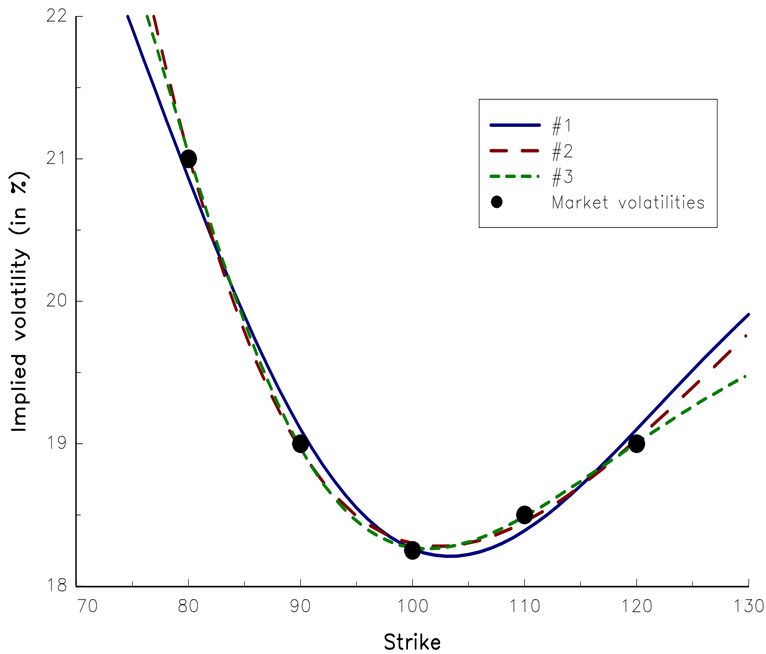

FIGURE 9.22: Implied volatility (in %) of calibrated mixed SLN models

that corresponds to the strike of the option, the implied volatility $\Sigma(T, L)$ that corresponds to the lower barrier of the option, the implied volatility $\Sigma(T, H)$ that corresponds to the higher barrier of the option, or another implied volatility. In fact, there is no satisfactory answer.

Let $S(t)$ be the asset price at time t. The payoff of the binary cash-or-nothing call option is:

$$f(S(T)) = \mathbb{1}\{S(T) > K\}$$

We deduce that:

$$\mathbf{BCC}(0, S_0) = \mathbb{E}^{\mathbb{Q}}\left[e^{-\int_0^T r(s)\,\mathrm{d}s} \cdot \mathbb{1}\{S(T) > K\} \,\middle|\, \mathcal{F}_0 \right]$$

If we consider the Black-Scholes model, we obtain:

$$\mathbf{BCC}(0, S_0) = e^{-rT}\Phi(d_2)$$

We can replicate this option by using the classical dynamic delta hedging approach presented on page 495. Here, we consider another framework, which is called the static hedging method. The hedging portfolio consists in:

- a long position on the European call option with strike K;
- a short position on the European call option with strike $K+\varepsilon$.

If the notional of each option is set to ε, the value of the hedging portfolio at time t is equal to:

$$V(t)=\frac{1}{\varepsilon}\cdot\boldsymbol{\mathcal{C}}(t,S(t),K)-\frac{1}{\varepsilon}\cdot\boldsymbol{\mathcal{C}}(t,S(t),K+\varepsilon)$$

It follows that the value of the hedging strategy is equal to:

$$X(t)=\mathbf{BCC}(t,S(t))-V(t)$$

We notice that:

$$\begin{aligned}
\lim_{\varepsilon\to 0}X(T) &= \mathbf{BCC}(T,S(T))-\lim_{\varepsilon\to 0}V(T)\\
&= \mathbb{1}\{S(T)>K\}-\lim_{\varepsilon\to 0}\frac{(S(t)-K)^{+}-(S(T)-K-\varepsilon)^{+}}{\varepsilon}\\
&= \mathbb{1}\{S(T)>K\}-\mathbb{1}\{S(T)>K\}\\
&= 0
\end{aligned}$$

The no-arbitrage condition implies that:

$$\begin{aligned}
\mathbf{BCC}(t,S(t)) &= \lim_{\varepsilon\to 0}\frac{\boldsymbol{\mathcal{C}}(t,S(t),K)-\boldsymbol{\mathcal{C}}(t,S(t),K+\varepsilon)}{\varepsilon}\\
&= -\lim_{\varepsilon\to 0}\frac{\boldsymbol{\mathcal{C}}(t,S(t),K+\varepsilon)-\boldsymbol{\mathcal{C}}(t,S(t),K)}{\varepsilon}\\
&= -\frac{\partial\,\boldsymbol{\mathcal{C}}(t,S(t),K)}{\partial\,K}
\end{aligned}$$

This result is valid only if the volatility is constant. If the volatility is not constant, the price $\mathbf{BCC}(t,S(t))$ becomes:

$$\begin{aligned}
&\lim_{\varepsilon\to 0}\frac{\boldsymbol{\mathcal{C}}(t,S(t),K,\Sigma(T,K))-\boldsymbol{\mathcal{C}}(t,S(t),K+\varepsilon,\Sigma(T,K+\varepsilon))}{\varepsilon}\\
&= -\frac{\partial\,\boldsymbol{\mathcal{C}}(t,S(t),K,\Sigma(T,K))}{\partial\,K}-\frac{\partial\,\boldsymbol{\mathcal{C}}(t,S(t),K,\Sigma(T,K))}{\partial\,\Sigma}\cdot\frac{\partial\,\Sigma(T,K)}{\partial\,K}\\
&= \mathbf{BCC}_{\mathrm{BS}}(t,S(t),\Sigma(T,K))-\boldsymbol{\upsilon}_{\mathrm{BS}}(t,S(t),\Sigma(T,K))\,\omega(T,K)
\end{aligned}$$

where $\mathbf{BCC}_{\mathrm{BS}}(t,S(t),\Sigma(T,K))$ is the Black-Scholes price with implied volatility $\Sigma(T,K)$, $\boldsymbol{\upsilon}_{\mathrm{BS}}(t,S(t),\Sigma(T,K))$ is the Black-Scholes vega for the European call option and $\omega(T,K)$ is the skew of the volatility surface:

$$\omega(T,K)=\frac{\partial\,\Sigma(T,K)}{\partial\,K}$$

This framework, called the skew-method (SM) model, shows that taking into account the volatility smile cannot be reduced to choosing the right implied volatility, because we have:

$$\mathbf{BCC}_{\mathrm{SM}}(t,S(t))\neq\mathbf{BCC}_{\mathrm{BS}}(t,S(t),\Sigma(T,K))$$

Example 90 *We price a binary call option when the underlying asset price is* 100*, the maturity of the option is* 6 *months, and the parameters b and r are equal to* 5%*. The skew $\omega(T,K)$ of the implied volatility can take the values* 0, -20 *and* $+20$ *bps. We consider two cases for the implied volatility: (1) $\Sigma(T,K)$ is equal to* 20%*, (2) $\Sigma(T,K)$ is a linear function with respect to K:*

$$\Sigma(T,K)=\Sigma(T,S_0)+\omega(T,K)\cdot(K-S_0)$$

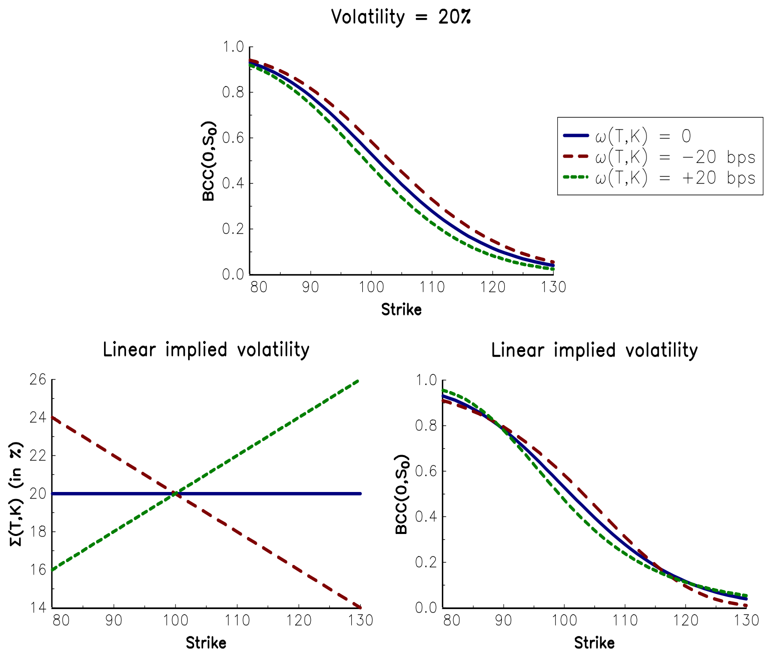

FIGURE 9.23: Impact of the implied volatility skew on the binary option price

Figure 9.23 represents the relationship between the binary call option price $\mathbf{BCC}(0, S_0)$ and the strike K. The first panel assumes that the implied volatility $\Sigma(T, K)$ is equal to 20%. We verify that:

$$\left\{ \begin{array}{l} \omega(T,K) < 0 \Rightarrow \mathbf{BCC}_{\mathrm{SM}}(0, S_0) < \mathbf{BCC}_{\mathrm{BS}}(0, S_0, \Sigma(T,K)) \\ \omega(T,K) > 0 \Rightarrow \mathbf{BCC}_{\mathrm{SM}}(0, S_0) > \mathbf{BCC}_{\mathrm{BS}}(0, S_0, \Sigma(T,K)) \end{array} \right.$$

However, the results shown in the first panel may be misleading, because it is not possible to compare the price for two different strikes. Indeed, if $K_2 > K_1$ and $\omega(T, K) > 0$ for every strike K, this implies that $\Sigma(T, K_2) > \Sigma(T, K_1)$, $\mathbf{BCC}_{\mathrm{BS}}(0, S_0, \Sigma(T, K_2)) > \mathbf{BCC}_{\mathrm{BS}}(0, S_0, \Sigma(T, K_1))$, but $\boldsymbol{\upsilon}_{\mathrm{BS}}(0, S_0, \Sigma(T, K_2)) > \boldsymbol{\upsilon}_{\mathrm{BS}}(0, S_0, \Sigma(T, K_1))$. A higher implied volatility increases the binary option price thanks to the impact on the Black-Scholes price, but also reduces it thanks to the impact on the vega. Therefore, the second and third panels are more useful to understand the dynamics of the binary option price with respect to the strike. We observe that it is more complex because of the two contrary effects.

We now assume that the shifted log-normal model is the right model. We have:

$$\begin{array}{rcl} \mathbb{1}\{S(T) > K\} & \Leftrightarrow & \mathbb{1}\{\alpha(T) + \beta(T) X(T) > K\} \\ & \Leftrightarrow & \mathbb{1}\left\{(S_0 - \alpha) e^{\left(b - \frac{1}{2}\sigma^2\right)T + \sigma W^{\mathbb{Q}}(T)} > K - \alpha e^{bT}\right\} \end{array}$$

We deduce that:

$$\mathbf{BCC}_{\mathrm{SLN}}(0, S_0) = f_{\mathrm{BS}}\left(S_0 - \alpha, K - \alpha e^{bT}, \sigma, T, b, r\right) \tag{9.31}$$

where f_{BS} is the Black-Scholes formula of the BCC option. Equation (9.31) is equivalent to shift the current price and the option strike.

TABLE 9.8: Price of the binary call option ($\alpha = -50, \sigma = 15\%$)

K	$\Sigma(T,K)$	$\omega(T,K)$	BS	SLN	SM
80	23.64	−5.47	0.8087	0.8184	0.8184
90	23.14	−4.57	0.6761	0.6895	0.6895
100	22.72	−3.87	0.5160	0.5306	0.5306
110	22.36	−3.34	0.3582	0.3715	0.3715
120	22.05	−2.92	0.2271	0.2374	0.2374

TABLE 9.9: Price of the binary call option ($\alpha = 50, \sigma = 40\%$)

K	$\Sigma(T,K)$	$\omega(T,K)$	BS	SLN	SM
80	16.71	17.25	0.8937	0.8780	0.8780
90	18.21	13.13	0.7390	0.7055	0.7055
100	19.39	10.51	0.5364	0.4971	0.4971
110	20.34	8.69	0.3546	0.3202	0.3202
120	21.14	7.35	0.2209	0.1953	0.1953

We consider the following parameters: $S_0 = 100$, $T = 1$, $b = 5\%$ and $r = 5\%$. The SLN parameters α and σ are equal to -50 and 15%. In Table 9.8, we price the binary call option with three models: the Black-Scholes model with the implied volatility $\Sigma(T,K)$, the SLN model and the SM approximation using the implied volatility $\Sigma(T,K)$ and the volatility skew $\omega(T,K)$. We remark that the Black-Scholes model produces bad option prices, whereas the SM prices are equal to those obtained with the SLN model. We obtain the same conclusion with an increasing smile as shown in Table 9.9.

The previous analysis can be extended to many other payoffs including corridor and barrier options. For instance, the holder of a corridor option receives a coupon at maturity, the magnitude of which depends on the behavior of a specified spot rate during the lifetime of the corridor. A special case is the range binary corridor option that pays a fixed coupon c if the asset stays within the range $[L, H]$:

$$f(S(T)) = c \sum_{j=1}^{n} \mathbb{1}\{S(T_j) \in [L, H]\}$$

where $\{T_1, \ldots, T_n\}$ are the fixing dates of the corridor option. Since we have:

$$\begin{aligned} \mathbb{1}\{S(T_j) \in [L, H]\} &\Leftrightarrow \mathbb{1}\{L \le S(T_j) \le H\} \\ &\Leftrightarrow \mathbb{1}\{S(T_j) \ge L\} - \mathbb{1}\{S(T_j) \ge H\} \end{aligned}$$

we deduce that the price $\mathbf{CC}(0, S_0)$ is related to a series of BCC cash flows:

$$\mathbf{CC}(0, S_0) = c \sum_{j=1}^{n} (\mathbf{BCC}(0, S_0, L) - \mathbf{BCC}(0, S_0, H))$$

where $\mathbf{BCC}(0, S_0, K)$ is the price of the cash-or-nothing binary call option, whose strike is K. We can then use SLN, mixed-SLN or SM models in order to take into account the volatility smile.

Remark 104 *In the case of barrier options, we can use the Black-Scholes formulas of Rubinstein and Reiner (1991) by shifting the parameters S_0, K, L and H:*

$$\begin{cases} S_0 \to S_0 - \alpha \\ K \to K - \alpha_0 e^{bT} \\ L \to L - \alpha_0 e^{bT} \\ H \to H - \alpha_0 e^{bT} \end{cases}$$

9.2.3 Local volatility model

The local volatility model has been proposed by Dupire (1994) using continuous-time modeling and, Derman and Kani (1994) in a binomial tree framework. It is one of the most famous smile models with Heston and SABR models. We assume that the risk-neutral dynamics of the asset price is given by the following SDE:

$$\mathrm{d}S(t) = bS(t)\,\mathrm{d}t + \sigma(t, S(t))\,S(t)\,\mathrm{d}W^{\mathbb{Q}}(t)$$

We can then retrieve the local volatility surface $\sigma(t, S)$ from the implied volatility surface $\Sigma(T, K)$, because the knowledge of all European option prices is sufficient to estimate the unique risk-neutral diffusion (Dupire, 1994).

9.2.3.1 Derivation of the forward equation

The Fokker-Planck equation Using Appendix A.3.6 on page 1072, the risk-neutral probability density function $q_t(T, S)$ of the asset price $S(T)$ satisfies the forward Chapman-Kolmogorov equation:

$$\frac{\partial\, q_t(T,S)}{\partial\, T} = -\frac{\partial\,[bSq_t(T,S)]}{\partial\, S} + \frac{1}{2}\frac{\partial^2\,\left[\sigma^2(T,S)\,S^2 q_t(T,S)\right]}{\partial\, S^2}$$

The initial condition is:

$$q_t(t,S) = \mathbb{1}\{S = S_t\}$$

where S_t is the value of $S(t)$ that is known at time t.

The Breeden-Litzenberger formulas On page 508, we have seen that the risk-neutral probability measure is related to the prices of European options. In particular, we have found that:

$$\begin{aligned}
\boldsymbol{\mathcal{C}}_t(T,K) &= e^{-r(T-t)}\int_K^\infty (S-K)\,q_t(T,S)\,\mathrm{d}S \\
\frac{\partial\,\boldsymbol{\mathcal{C}}_t(T,K)}{\partial\, K} &= -e^{-r(T-t)}\int_K^\infty q_t(T,S)\,\mathrm{d}S \\
\frac{\partial^2\,\boldsymbol{\mathcal{C}}_t(T,K)}{\partial\, K^2} &= e^{-r(T-t)} q_t(T,K)
\end{aligned}$$

Main result We also have:

$$\begin{aligned}
\frac{\partial\,\boldsymbol{\mathcal{C}}_t(T,K)}{\partial\, T} &= -r\boldsymbol{\mathcal{C}}_t(T,K) + e^{-r(T-t)}\int_K^\infty (S-K)\,\frac{\partial\, q_t(T,S)}{\partial\, T}\,\mathrm{d}S \\
&= -r\boldsymbol{\mathcal{C}}_t(T,K) + e^{-r(T-t)}\mathcal{I}
\end{aligned}$$

Using the Fokker-Planck equation, we obtain:

$$\begin{aligned}
\mathcal{I} &= \int_K^\infty (S-K)\left(\frac{1}{2}\frac{\partial^2\left[\sigma^2(T,S)S^2 q_t(T,S)\right]}{\partial S^2} - \frac{\partial\left[bSq_t(T,S)\right]}{\partial S}\right)\mathrm{d}S \\
&= \frac{1}{2}\int_K^\infty (S-K)\frac{\partial^2\left[\sigma^2(T,S)S^2 q_t(T,S)\right]}{\partial S^2}\mathrm{d}S - \\
&\quad \int_K^\infty (S-K)\frac{\partial\left[bSq_t(T,S)\right]}{\partial S}\mathrm{d}S \\
&= \frac{1}{2}\mathcal{I}_1 - \mathcal{I}_2
\end{aligned}$$

Using an integration by parts, we have:

$$\begin{aligned}
\mathcal{I}_1 &= \int_K^\infty (S-K)\frac{\partial^2\left[\sigma^2(T,S)S^2 q_t(T,S)\right]}{\partial S^2}\mathrm{d}S \\
&= \left[(S-K)\frac{\partial\left[\sigma^2(T,S)S^2 q_t(T,S)\right]}{\partial S}\right]_K^\infty - \\
&\quad \int_K^\infty \frac{\partial\left[\sigma^2(T,S)S^2 q_t(T,S)\right]}{\partial S}\mathrm{d}S \\
&= 0 - \left[\sigma^2(T,S)S^2 q_t(T,S)\right]_K^\infty \\
&= \sigma^2(T,K)K^2 q_t(T,K)
\end{aligned}$$

We notice that[40]:

$$\begin{aligned}
\mathcal{I}_2 &= \int_K^\infty (S-K)\frac{\partial\left[bSq_t(T,S)\right]}{\partial S}\mathrm{d}S \\
&= \left[(S-K)bSq_t(T,S)\right]_K^\infty - b\int_K^\infty Sq_t(T,S)\,\mathrm{d}S \\
&= -b\int_K^\infty Sq_t(T,S)\,\mathrm{d}S \\
&= -be^{r(T-t)}\left(\boldsymbol{\mathcal{C}}_t(T,K) + K\frac{\partial\boldsymbol{\mathcal{C}}_t(T,K)}{\partial K}\right)
\end{aligned}$$

The expression of $\mathcal{I}$ is then equal to:

$$\mathcal{I} = \frac{1}{2}\sigma^2(T,K)K^2 q_t(T,K) + be^{r(T-t)}\left(\boldsymbol{\mathcal{C}}_t(T,K) - K\frac{\partial\boldsymbol{\mathcal{C}}_t(T,K)}{\partial K}\right)$$

[40] Using Breeden-Litzenberger formulas, we have:

$$\begin{aligned}
e^{r(T-t)}\boldsymbol{\mathcal{C}}_t(T,K) &= \int_K^\infty (S-K)\,q_t(T,S)\,\mathrm{d}S \\
&= \int_K^\infty Sq_t(T,S)\,\mathrm{d}S - K\int_K^\infty q_t(T,S)\,\mathrm{d}S \\
&= \int_K^\infty Sq_t(T,S)\,\mathrm{d}S - Ke^{r(T-t)}\frac{\partial\boldsymbol{\mathcal{C}}_t(T,K)}{\partial K}
\end{aligned}$$

It follows that:

$$\begin{aligned}\frac{\partial \boldsymbol{\mathcal{C}}_t(T,K)}{\partial T} &= -r\boldsymbol{\mathcal{C}}_t(T,K) + \frac{1}{2}\sigma^2(T,K)K^2\frac{\partial^2 \boldsymbol{\mathcal{C}}_t(T,K)}{\partial K^2} + \\ & \quad b\left(\boldsymbol{\mathcal{C}}_t(T,K) - K\frac{\partial \boldsymbol{\mathcal{C}}_t(T,K)}{\partial K}\right)\end{aligned}$$

We conclude that:

$$\begin{aligned}&\frac{1}{2}\sigma^2(T,K)K^2\frac{\partial^2 \boldsymbol{\mathcal{C}}_t(T,K)}{\partial K^2} - bK\frac{\partial \boldsymbol{\mathcal{C}}_t(T,K)}{\partial K} - \\ &\qquad \frac{\partial \boldsymbol{\mathcal{C}}_t(T,K)}{\partial T} + (b-r)\boldsymbol{\mathcal{C}}_t(T,K) = 0 \end{aligned} \tag{9.32}$$

Differences between backward and forward PDE approaches Equation (9.32) is very important because it can be interpreted as the dual of the backward PDE (9.2):

$$\begin{cases} \frac{1}{2}\sigma^2(t,S)S^2\partial_S^2 V(t,S) + bS\partial_S V(t,S) + \partial_t V(t,S) - rV(t,S) = 0 \\ V(T,S(T)) = f(T,S(T),K) \end{cases}$$

where $V(t,S)$ is the price of the European option, whose terminal payoff is $f(T,S(T),K)$. In the case of Dupire model, the pricing formula becomes:

$$\begin{cases} \frac{1}{2}\sigma^2(T,K)K^2\partial_K^2 V(T,K) - bK\partial_K V(T,K) - \\ \qquad\qquad \partial_T V(T,K) + (b-r)V(T,K) = 0 \\ V(t,K) = f(t,S_t,K) \end{cases}$$

where $V(T,S)$ is the price of the European option, whose initial payoff is $f(t,S_t,K)$. In the backward formulation, the state variables are t and S, whereas the fixed variables are T and K. In the backward formulation, the state variables become T and K, whereas the fixed variables are now the current time[41] t and the current asset price S_t. This is not the only difference between the two approaches. Indeed, the backward PDE approach suggests that we can hedge the option using a dynamic portfolio of the underlying asset, whereas the forward PDE approach suggests that we can hedge the option using a static portfolio of call and put options.

We consider the pricing of an European call option with the following parameters: $S_0 = 100$, $K = 100$, $\sigma(t,S) = 20\%$, $T = 0.5$, $b = 2\%$ and $r = 5\%$. In the case of the backward PDE, we consider the usual boundary conditions:

$$\begin{cases} \boldsymbol{\mathcal{C}}(t,S) = 0 \\ \partial_S \boldsymbol{\mathcal{C}}(t,+\infty) = 1 \end{cases}$$

For the forward PDE, the boundary conditions are[42]:

$$\begin{cases} \partial_K \boldsymbol{\mathcal{C}}(T,0) = -1 \\ \boldsymbol{\mathcal{C}}(T,+\infty) = 0 \end{cases}$$

In Figure 9.24, we show the relative error (expressed in bps) of numerical solutions when considering the Crank-Nicholson scheme. In the case of the backward PDE, the state variable

[41] t can be equal to zero.

[42] We can also use the following specifications:

$$\begin{cases} \boldsymbol{\mathcal{C}}(T,0) = e^{(b-r)T}S_0 \\ \partial_K \boldsymbol{\mathcal{C}}(T,+\infty) = 0 \end{cases}$$

is the current asset price S_0, and we obtain all the option prices when the strike is equal to 100. In the case of the forward PDE, the state variable is the strike K, and we obtain all the option prices when the current asset price is equal to 100. We notice that the relative errors are equivalent when S_0 is equal to K. In fact, the efficiency of the numerical algorithms will depend on the relative position between S_0 and K.

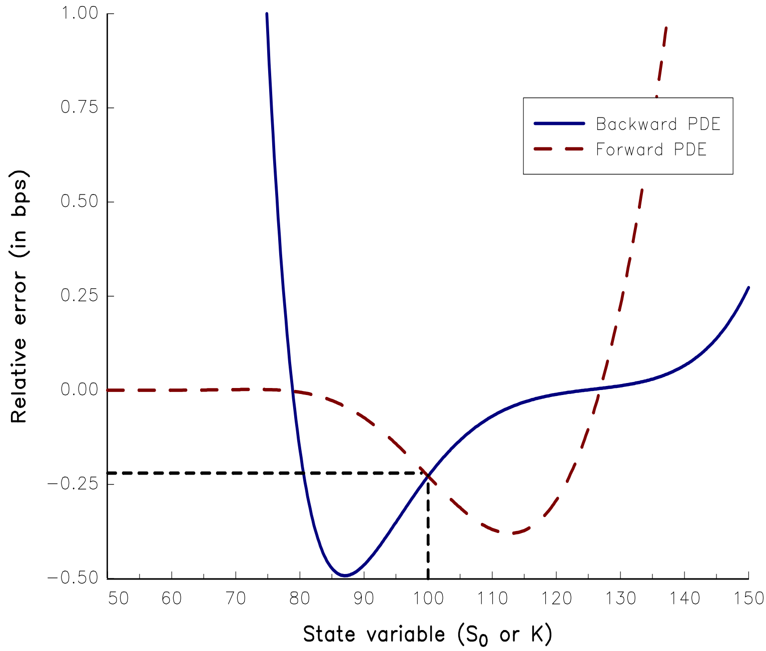

FIGURE 9.24: Relative error of backward and forward PDE numerical solutions

9.2.3.2 Duality between local volatility and implied volatility

We can inverse Equation (9.32) in order to relate the expression of the local volatility and the price of the call option:

$$\sigma^2(T,K) = 2\frac{bK\partial_K \boldsymbol{\mathcal{C}}(T,K) + \partial_T \boldsymbol{\mathcal{C}}(T,K) - (b-r)\boldsymbol{\mathcal{C}}(T,K)}{K^2\partial_K^2 \boldsymbol{\mathcal{C}}(T,K)}$$

In Exercise 9.4.8 on page 599, we show that $\sigma(T,K)$ can also be written with respect to the implied volatility $\Sigma(T,K)$:

$$\sigma(T,K) = \sqrt{\frac{A(T,K)}{B(T,K)}} \tag{9.33}$$

where:

$$\begin{aligned} A(T,K) &= \Sigma^2(T,K) + 2bKT\Sigma(T,K)\partial_K\Sigma(T,K) + \\ & \quad 2T\Sigma(T,K)\partial_T\Sigma(T,K) \end{aligned}$$

and:

$$\begin{aligned} B(T,K) &= 1 + 2K\sqrt{T}d_1\partial_K\Sigma(T,K) + K^2T\Sigma(T,K)\partial_K^2\Sigma(T,K) + \\ & \quad K^2Td_1d_2(\partial_K\Sigma(T,K))^2 \end{aligned}$$

Equation (9.33) is the key finding of Dupire (1994). Indeed, knowing the implied volatility surface, we can retrieve the unique local volatility function that matches the set of all European call and put option prices.

Many results have been derived from Equation (9.33). For instance, if there is no skew[43], the local volatility function does not depend on the strike[44]:

$$\sigma^2(T) = \Sigma^2(T) + 2T\Sigma(T)\frac{\partial\,\Sigma(T)}{\partial\,T} \tag{9.34}$$

On the contrary, the local volatility always depends on the maturity T even if there is no time-variation in the implied volatility[45].

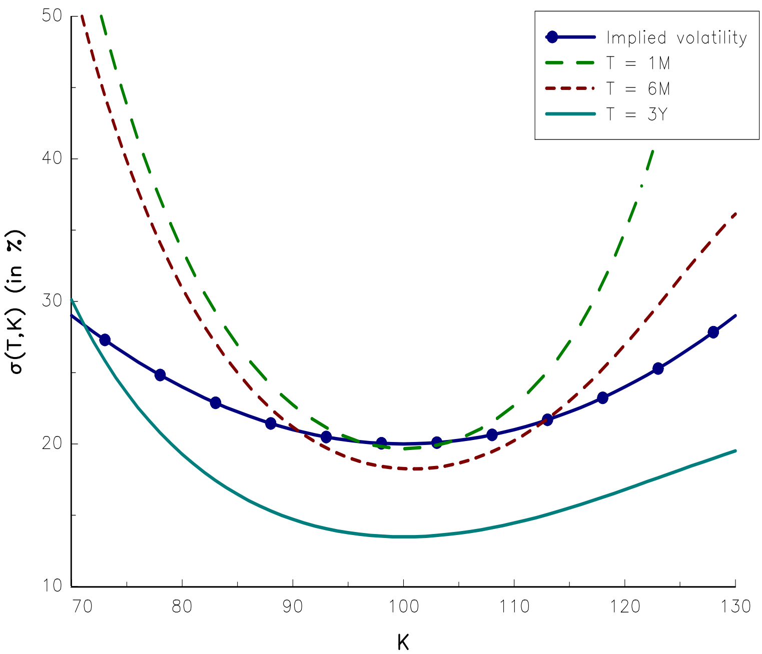

FIGURE 9.25: Calibrated local volatility $\sigma(T,S)$ (in %)

Example 91 *We assume that the implied volatility is equal to:*

$$\Sigma(T,K) = \Sigma_0 + \alpha(S_0 - K)^2$$

where $\Sigma_0 = 20\%$, $\alpha = 1$ *bp*, $S_0 = 100$ *and* $b = 5\%$.

Figure 9.25 shows the calibrated local volatility for different values of T. We verify the time-variation property of the local volatility. We notice that Equation (9.34) is equivalent to:

$$\sigma^2(T) = \frac{\partial\,T\Sigma^2(T)}{\partial\,T}$$

or:

$$\Sigma^2(T) = \frac{1}{T}\int_0^T \sigma^2(t)\;\mathrm{d}t$$

The implied variance is then the time series average of the local variance.

[43]We have $\Sigma(T,K) = \Sigma(T)$.

[44]This result is obtained by setting $\partial_K\Sigma(T,K)$ and $\partial_K^2\Sigma(T,K)$ equal to 0 in Equation (9.33).

[45]We have $\Sigma(T,K) = \Sigma(K)$.

Another important result concerns the behavior of the implied volatility near expiry. Let x be the log-moneyness:

$$\begin{aligned} x &= \varphi(T, K) \\ &= \ln \frac{S_0}{K} + bT \end{aligned}$$

We introduce the functions $\tilde{\Sigma}$ and $\tilde{\sigma}$ such that $\Sigma(T, K) = \tilde{\Sigma}(T, \varphi(T, K))$ and $\sigma(T, K) = \tilde{\sigma}(T, \varphi(T, K))$. Berestycki *et al.* (2002) showed that the implied volatility is the harmonic mean of the local volatility[46]:

$$\frac{1}{\tilde{\Sigma}(0, x)} = \int_0^1 \frac{\mathrm{d}y}{\tilde{\sigma}(0, xy)}$$

It follows that:

$$\frac{\partial\, \tilde{\Sigma}(0, 0)}{\partial\, x} = \frac{1}{2} \frac{\partial\, \tilde{\sigma}(0, 0)}{\partial\, x}$$

The ATM slope of the implied volatility near expiry is equal to one half the slope of the local volatility.

9.2.3.3 Dupire model in practice

One of the problems is the availability of the call/put prices for all maturities and all strikes. In practice, we only know the option price for some maturities T_m and some strikes K_i. This is why we have to use a calibration method to obtain the continuous volatility surface $\Sigma(T, K)$.

Time interpolation We note $\upsilon(T, K)$ the total implied variance:

$$\upsilon(T, K) = T\Sigma^2(T, K)$$

The linear interpolation of the total implied variance gives:

$$\upsilon(T, K) = w \cdot \upsilon(T_m, K_m(T)) + (1 - w) \cdot \upsilon(T_{m+1}, K_{m+1}(T))$$

where $T \in [T_m, T_{m+1}]$ and:

$$w = \frac{T_{m+1} - T}{T_{m+1} - T_m}$$

We deduce that:

$$\begin{aligned} \Sigma^2(T, K) &= \frac{T_m(T_{m+1} - T)}{T(T_{m+1} - T_m)} \Sigma^2(T_m, K_m(T)) + \\ &\quad \frac{T_{m+1}(T - T_m)}{T(T_{m+1} - T_m)} \Sigma^2(T_{m+1}, K_{m+1}(T)) \\ &= a_m(T)\, \Sigma^2(T_m, K_m(T)) + b_{m+1}(T)\, \Sigma^2(T_{m+1}, K_{m+1}(T)) \end{aligned}$$

where:

$$a_m(T) = \frac{T_m(T_{m+1} - T)}{T(T_{m+1} - T_m)}$$

[46] See Exercise 9.4.8 on page 599 for the proof of this result.

and:

$$b_{m+1}(T) = \frac{T_{m+1}(T - T_m)}{T(T_{m+1} - T_m)} = 1 - a_m(T)$$

In the previous scheme, we interpolate the total variance for the strike K and the maturity T by considering the pairs $(T_m, K_m(T))$ and $(T_{m+1}, K_{m+1}(T))$. Generally, the strikes $K_m(T)$ and $K_{m+1}(T)$ are a translation of the strike K:

$$\begin{cases} K_m(T) = k_m \cdot (T) K \\ K_{m+1}(T) = k_{m+1} \cdot (T) K \end{cases}$$

with $k_m(T_m) = 1$ and $k_{m+1}(T_{m+1}) = 1$. The simplest rule is $k_m(T) = k_{m+1}(T) = 1$. Another method is to define $k_m(T_m) = e^{-b(T-T_m)} \leq 1$ and $k_{m+1}(T_{m+1}) = e^{b(T_{m+1}-T)} \geq 1$.

Example 92 *We assume that the implied volatility is equal to:*

$$\Sigma(T_m, K) = \Sigma_m + \alpha_m (K - 100)^2$$

where $\Sigma_m = 20\% + 0.005 \cdot (T_m - 1.0)$, $\alpha_m = 0.05 \cdot T_m$ *bps and* T_m *is equal to* 1, 2, 3, 4 *and* 5 *years. The cost-of-carry parameter* b *is set to* 5%.

We have represented the implied volatility $\Sigma(T_m, K)$ in the first panel in Figure 9.26. We can then compute the volatility surface. When T is lower than the first observed maturity or higher than the last observed maturity, we can extrapolate the implied volatility in several ways. The simplest method is to assume that the implied volatility is constant. In the third panel, we have reported the interpolated implied volatility with respect to the maturity T for three different strikes. We notice that it is curved between two interpolating knots due to the effect of the square root transformation.

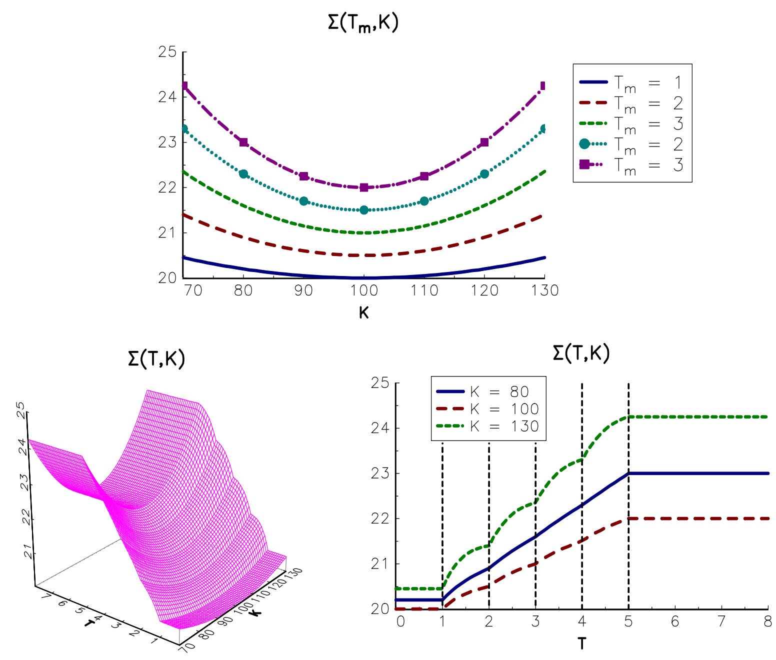

FIGURE 9.26: Time interpolation of the implied volatility

Non-parametric interpolation We note $\mathcal{S}_m(K)$ the non-parametric function that give the value of $\Sigma(T_m, K)$ for all values of strike K. The calculation of the local volatility surface implies to calculate the quantities $\partial_K \Sigma(T,K)$, $\partial_K^2 \Sigma(T,K)$ and $\partial_T \Sigma(T,K)$. We use the shortened notations: $\mathcal{S}_m = \mathcal{S}_m(K_m(T))$, $\mathcal{S}'_m = \mathcal{S}'_m(K_m(T))$, $\mathcal{S}''_m = \mathcal{S}''_m(K_m(T))$, $\mathcal{S}_{m+1} = \mathcal{S}_{m+1}(K_{m+1}(T))$, $\mathcal{S}'_{m+1} = \mathcal{S}'_{m+1}(K_{m+1}(T))$ and $\mathcal{S}''_{m+1} = \mathcal{S}''_{m+1}(K_{m+1}(T))$. We have:

$$\begin{aligned}
\Sigma(T,K)\,\partial_K \Sigma(T,K) &= \frac{1}{2}\partial_K \Sigma^2(T,K) \\
&= a_m(T)\,k_m(T)\,\mathcal{S}_m\mathcal{S}'_m + \\
&\quad\; b_{m+1}(T)\,k_{m+1}(T)\,\mathcal{S}_{m+1}\mathcal{S}'_{m+1}
\end{aligned}$$

For the second term, we obtain:

$$\begin{aligned}
\Sigma(T,K)\,\partial_K^2 \Sigma(T,K) &= \frac{1}{2}\partial_K^2 \Sigma^2(T,K) - \left(\partial_K \Sigma(T,K)\right)^2 \\
&= a_m(T)\,k_m^2(T)\left(\mathcal{S}_m\mathcal{S}''_m + \left(\mathcal{S}'_m\right)^2\right) + \\
&\quad\; b_{m+1}(T)\,k_{m+1}^2(T)\left(\mathcal{S}_{m+1}\mathcal{S}''_{m+1} + \left(\mathcal{S}'_{m+1}\right)^2\right) - \\
&\quad\; \left(\partial_K \Sigma(T,K)\right)^2
\end{aligned}$$

Since we have:

$$a'_m(T) = \frac{-T_m T_{m+1}}{T^2\left(T_{m+1} - T_m\right)}$$

and:

$$b'_{m+1}(T) = \frac{T_m T_{m+1}}{T^2\left(T_{m+1} - T_m\right)}$$

we deduce that the last term is equal to[47]:

$$\begin{aligned}
\Sigma(T,K)\,\partial_T \Sigma(T,K) &= \frac{1}{2}\partial_T \Sigma^2(T,K) \\
&= \frac{1}{2}a'_m(T)\,\Sigma^2(T_m, K_m(T)) + \\
&\quad\; \frac{1}{2}b'_{m+1}(T)\,\Sigma^2(T_{m+1}, K_{m+1}(T)) + \\
&\quad\; a_m(T)\,\Sigma(T_m, K_m(T))\,\partial_T \Sigma(T_m, K_m(T)) + \\
&\quad\; b_{m+1}(T)\,\Sigma(T_{m+1}, K_{m+1}(T))\,\partial_T \Sigma(T_{m+1}, K_{m+1}(T)) \\
&= \frac{1}{2}\left(\mathcal{S}_{m+1} - \mathcal{S}_m\right)\frac{T_m T_{m+1}}{T^2\left(T_{m+1} - T_m\right)} + \\
&\quad\; a_m(T)\,\mathcal{S}_m\mathcal{S}'_m K\partial_T k_m(T) + \\
&\quad\; b_m(T)\,\mathcal{S}_{m+1}\mathcal{S}'_{m+1} K\partial_T k_{m+1}(T)
\end{aligned}$$

In the case where $k_m(T) = k_{m+1}(T) = 1$, the previous formula reduces to:

$$\Sigma(T,K)\,\partial_T \Sigma(T,K) = \frac{1}{2}\left(\mathcal{S}_{m+1} - \mathcal{S}_m\right)\frac{T_m T_{m+1}}{T^2\left(T_{m+1} - T_m\right)}$$

In practice, we don't observe the function $\mathcal{S}_m(K)$, but only few values of $\Sigma(T_m, K_i)$ for some maturities T_m and some strikes K_i. An example is given in Table 9.10. We assume that

[47] We use the fact that $\partial_T K_m(T) = K\partial_T k_m(T)$ and $\partial_T K_{m+1}(T) = K\partial_T k_{m+1}(T)$.

TABLE 9.10: Calibration set

$T_m = 1/12$									
K_i	87.0	92.0	96.0	98.0	100.0	103.0	106.0	110.0	116.0
$\Sigma(T_m, K_i)$	13.7	13.7	13.3	13.2	13.0	13.1	13.2	13.5	13.5
$T_m = 3/12$									
K_i	77.0	85.0	93.0	97.0	101.0	106.0	111.0	121.0	134.0
$\Sigma(T_m, K_i)$	14.9	14.9	14.1	14.0	13.5	13.8	14.2	15.1	15.1
$T_m = 6/12$									
K_i	66.0	78.0	89.0	96.0	102.0	111.0	119.0	136.0	161.0
$\Sigma(T_m, K_i)$	16.8	16.8	15.5	15.0	14.5	15.0	15.5	16.8	16.8
$T_m = 1$									
K_i	53.0	69.0	86.0	96.0	104.0	119.0	133.0	166.0	217.0
$\Sigma(T_m, K_i)$	19.0	19.0	17.0	16.0	15.5	16.5	17.5	18.5	18.5
$T_m = 2$									
K_i	37.0	56.0	80.0	96.0	103.0	137.0	163.0	229.0	347.0
$\Sigma(T_m, K_i)$	21.9	21.9	20.0	18.5	18.5	19.0	19.5	20.8	20.8

five maturities are quoted (1M, 3M, 6M, 1Y and 2Y). For each maturity, we observe the implied volatility (expressed in %) for 9 strikes. This is why we have to use an interpolation method. In Figure 9.27, we have represented the function $\mathcal{S}_m(K)$ obtained with the cubic spline method[48]. One of the issues is the interpolated implied volatility on the wings. Here, we have chosen to keep the cubic spline values, but an alternative approach is to assume that the smile is constant before the first strike and after the last strike. Let us assume that $S_0 = 100$, $b = 5\%$ and $r = 5\%$. Using the time approximation approach, we obtain the implied volatility surface given in Figure 9.28. The implied volatility is constant when $T \leq 1/12$ and $T \geq 2$. Finally, the local volatility surface is reported in Figure 9.29. We notice that it is not a smooth function. This is why we can use cubic spline approximation or other smoothing methods in place of cubic spline interpolation[49]. However, we not not retrieve exactly the quoted implied volatilities with this approach.

Remark 105 *In real life, the number of strikes may be different from one maturity to another, and may be smaller. For example, in the case of currency options*[50]*, we generally have* 5 *quoted options (ATM,* 10*-delta call,* 25*-delta call,* 10*-delta put and* 25*-delta put).*

Parametric calibration In the previous section, $\Sigma(T, K)$ and $\sigma(T, K)$ are calibrated using non-parametric approaches such as the cubic spline method. This produces a disorderly local volatility surface. In order to avoid this problem, we can use a parametric framework. For instance, we can calibrate $\Sigma(T, K)$ using the SABR model. Another popular approach is to consider the stochastic volatility inspired or SVI parametrization.

We recall that the total implied variance is equal to:

$$\upsilon(T, K) = T\Sigma^2(T, K)$$

We assume that $\upsilon(T, K) = \tilde{\upsilon}(T, x)$ and $\Sigma(T, K) = \tilde{\Sigma}(T, x)$ where x is the log-moneyness:

$$x = \varphi(T, K) = \ln \frac{K}{F(T)} = \ln \frac{K}{S_0 e^{bT}}$$

[48] See Appendix A.1.2.1 on page 1035.

[49] See Crépey (2003) and Fengler (2009).

[50] FX vanilla options are generally quoted in terms of volatility with respect to a fixed delta, and not in terms of premium with respect to a given strike.

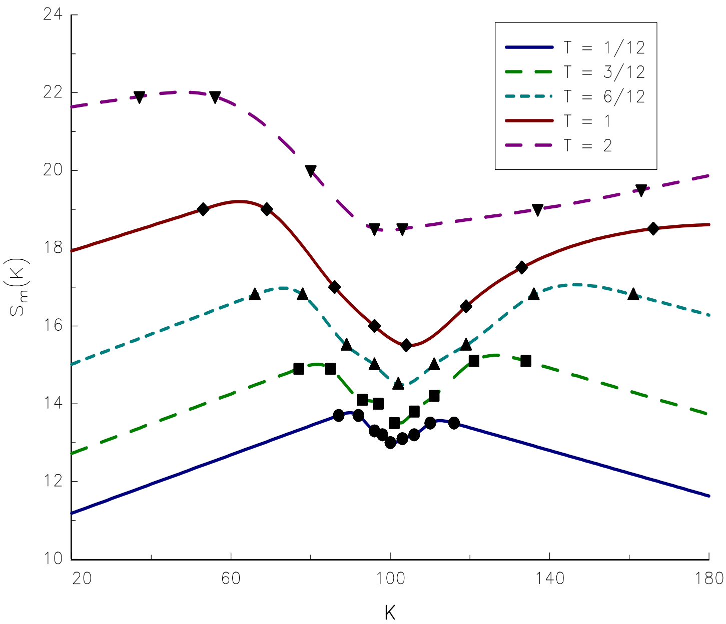

FIGURE 9.27: Cubic spline interpolation $\mathcal{S}_m(K)$ (in %)

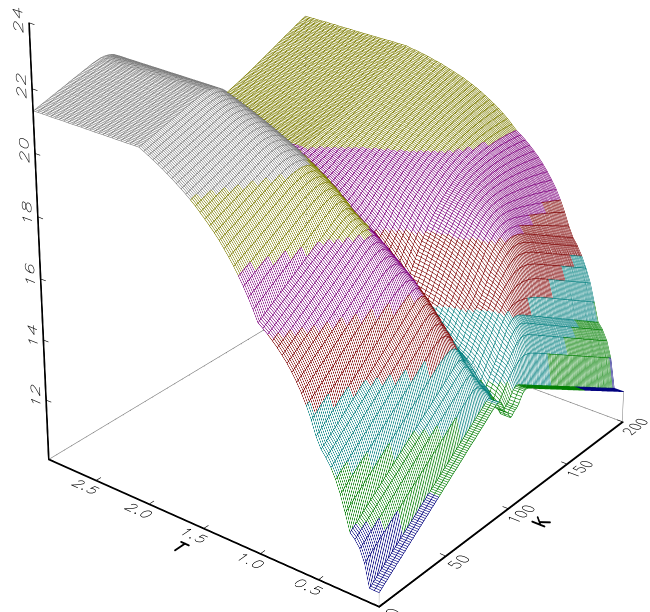

FIGURE 9.28: Implied volatility surface $\Sigma(T, K)$ (in %)

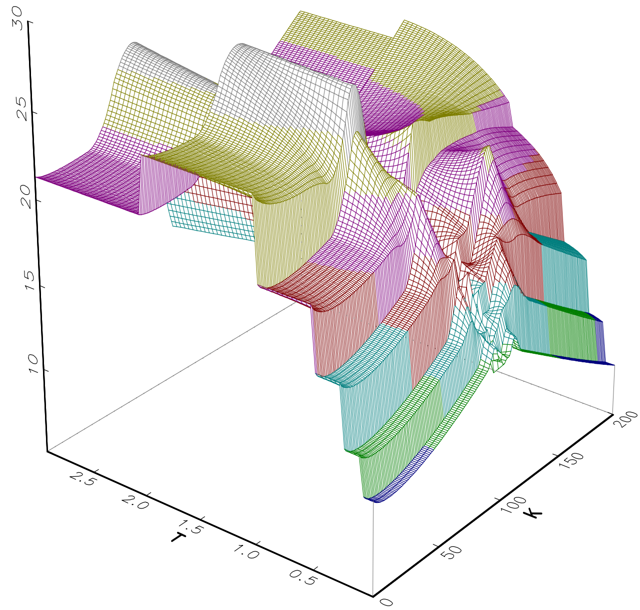

FIGURE 9.29: Local volatility surface $\sigma(T, K)$ (in %)

Let $\tilde{\upsilon}_T(x) = \tilde{\upsilon}(T, x)$ be the total implied variance for a given maturity slice. Gatheral (2004) introduces the following SVI parametrization:

$$\tilde{\upsilon}_T(x) = \alpha + \beta\left(\rho(x - m) + \sqrt{(x - m)^2 + \sigma^2}\right)$$

where $\beta > 0$, $\sigma > 0$ and $\rho \in [-1, 1]$. We have:

$$\tilde{\upsilon}_T(m) = \alpha + \beta\sigma$$

and:

$$\begin{cases} \lim_{x\to-\infty} \tilde{\upsilon}_T(x) = \alpha - \beta(1 - \rho)(x - m) \\ \lim_{x\to\infty} \tilde{\upsilon}_T(x) = \alpha + \beta(1 + \rho)(x - m) \end{cases}$$

Gatheral deduces that α controls the general level, β influences the slope of the wings, σ changes the curvature of the smile, ρ impacts the symmetry of the smile while m shifts the smile.

Example 93 *We assume that $\alpha = 2\%$, $\beta = 0.3$, $\sigma = 10\%$, $\rho = -40\%$ and $m = 0$. Figure 9.30 shows the impact of each parameter on the total variance $\tilde{\upsilon}_T(x)$.*

Gatheral and Jacquier (2014) show that a volatility surface is free of static arbitrage if and only if it is free of calendar spread arbitrage[51] and each time slice is free of butterfly arbitrage[52]. The first property implies that:

$$\partial_T \tilde{\upsilon}(T, x) \geq 0$$

[51]This means that the price of an European option is monotone with the maturity.
[52]This means that the probability density function is non-negative for any given maturity T.

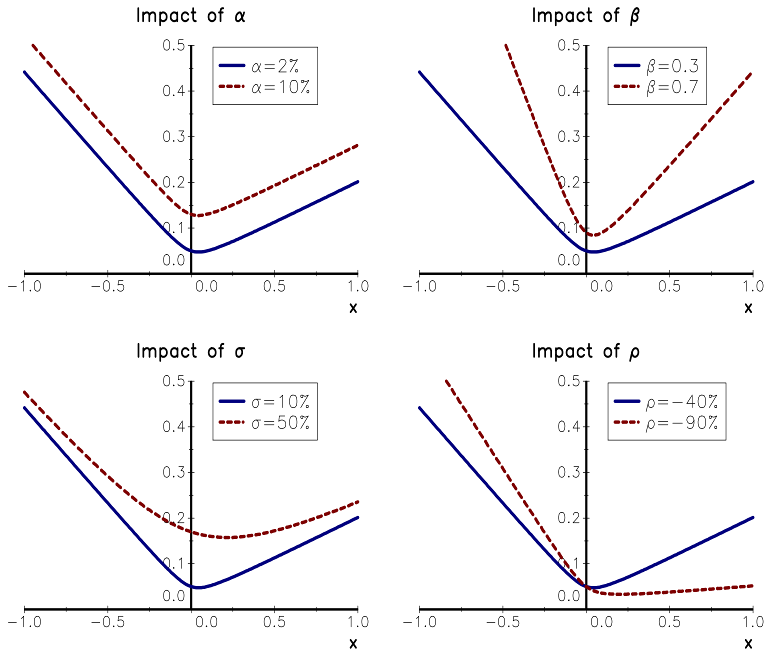

FIGURE 9.30: Impact of SVI parameters on the total variance $\tilde{\upsilon}_T(x)$

for all $x \in \mathbb{R}$. Thanks to Breeden and Litzenberger (1978), the second property is equivalent to verify that[53]:

$$\frac{\partial^2 \mathcal{C}(T,K)}{\partial K^2} \geq 0$$

These authors deduce then how the absence of static arbitrage impacts SVI parameters.

We consider the calibration set defined in Table 9.10 on page 554. We delete the two extreme strikes of each maturity[54]. In Figure 9.31, we show the SVI parametrization for each maturity. By considering the time interpolation presented previously, we can define the implied volatility surface $\Sigma(T,K)$ and then calculate the local $\sigma(T,K)$. These two volatility surfaces are reported in Figure 9.31.

Hedging coefficients Let $\Sigma(T,K,S_t)$ and $\sigma(T,K,S_t)$ be the implied and local volatility surfaces that depend on the current price S_t. We also write the value of the option $V(T,K,S_t)$ as a function of the maturity T, the strike K and the current price S_t. The delta of the option is then equal to:

$$\boldsymbol{\Delta}_t = \frac{\partial V(T,K,S_t)}{\partial S_t}$$

If we use the finite difference approximation, we obtain:

$$\boldsymbol{\Delta} \approx \frac{V(T,K,S_t+\varepsilon) - V(T,K,S_t-\varepsilon)}{2\varepsilon}$$

[53]See Section 9.1.1.4 on page 508.

[54]In fact, we have added these two points in the calibration set in order to stabilize the non-parametric calibration. However, this approach is not adequate because volatility smile is linear and not constant at extreme strikes (Lee, 2004).

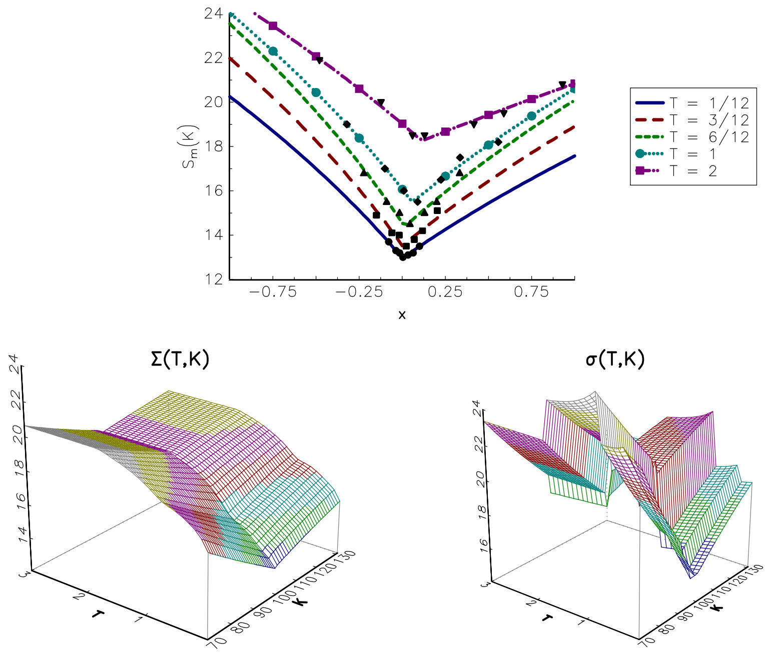

FIGURE 9.31: SVI parametrization, implied volatility $\Sigma(T,K)$ and local volatility $\sigma(T,K)$ (in %)

Computing the option price and its corresponding delta require then to calculate three local volatility surfaces[55] and solve the forward PDE three times[56]. This method can also be used to calculate the gamma of the option, because we have:

$$\boldsymbol{\Gamma} \approx \frac{V(T,K,S_t+\varepsilon) - 2V(T,K,S_t) + V(T,K,S_t-\varepsilon)}{\varepsilon^2}$$

The vega coefficient in a local volatility model is not well-defined. It can be measured with respect to the local volatility $\sigma(T,K,S_t)$ or the implied volatility $\Sigma(T,K,S_t)$. The most frequent approach is to measure the vega as the sensitivity of the price to a parallel shift of $\Sigma(T,K,S_t)$. We have:

$$\boldsymbol{\upsilon} = \frac{V'(T,K,S_t) - V(T,K,S_t)}{\varepsilon'}$$

where $V'(T,K,S_t)$ is the option price obtained when the implied volatility surface is $\Sigma(T,K,S_t) + \varepsilon'$.

One of the issues with the local volatility model is that greeks are not easy to compute and are not stable in the time and across strikes. This is a severe disadvantage, since the hedging of the option is not straightforward and generally less efficient than the hedging portfolio given by the Black-Scholes model:

> "*Market smiles and skews are usually managed by using local volatility models* a la *Dupire. We discover that the dynamics of the market smile predicted by local vol models is opposite of observed market behavior: when the price of the underlying decreases, local vol models predict that the smile shifts to higher*

[55] We have to calculate $\sigma(T,K,S_t-\varepsilon)$, $\sigma(T,K,S_t)$ and $\sigma(T,K,S_t+\varepsilon)$.
[56] We have to calculate $V(T,K,S_t-\varepsilon)$, $V(T,K,S_t)$ and $V(T,K,S_t+\varepsilon)$.

prices; when the price increases, these models predict that the smile shifts to lower prices. Due to this contradiction between model and market, delta and vega hedges derived from the model can be unstable and may perform worse than naive Black-Scholes' hedges" (Hagan *et al.*, 2002, page 84).

9.2.3.4 Application to exotic options

Another shortcoming of the local volatility model is the unrealistic probability distribution of the conditional random variable $S(t_2) \mid S(t_1)$. This is why this model is only used for European options, and not for path-dependent derivatives. In particular, it has been popular in the 1990s and 2000s for pricing European barrier options.

We consider the calibration set given in Table 9.10 on page 554. We assume that S_0, $b = 5\%$ and $5 = 5\%$. We price different payoffs given in Table 9.11, whose parameters are $K = 100$, $L = 90$ and $H = 115$. The maturity is set to one year. Prices are calculated with a Crank-Nicholson scheme with 2 000 discretization points[57] in space, 2 000 discretization points in time and traditional boundary conditions[58]. Results are given in column LV. We can compare them with Black-Scholes prices calculated with implied volatilities[59] $\Sigma_1 = 16\%$ and $\Sigma_2 = 15.5\%$. For each payoff and each value of implied volatility, we report two values of the option price: one obtained by solving the PDE and another one calculated with the analytical formulas of Rubinstein and Reiner (1991). We observe some differences between the two prices, because the PDE price depends on the choice of the discretization scheme and the boundary conditions. We notice that the prices DOC, UOC, KOC and BCC calculated with the local volatility model are not in the interval of BS prices.

TABLE 9.11: Barrier option pricing with the local volatility model

Option	Payoff	LV	BS-PDE		BS-RR	
			Σ_1	Σ_2	Σ_1	Σ_2
Call	$(S(T)-K)^+$	8.85	8.96	8.78	8.96	8.78
Put	$(K-S(T))^+$	3.97	4.08	3.90	4.08	3.90
DOC	$\mathbb{1}\{S(t)>L\}\cdot(S(T)-K)^+$	7.98	8.14	8.05	8.11	8.02
DOP	$\mathbb{1}\{S(t)>L\}\cdot(K-S(T))^+$	0.26	0.27	0.28	0.25	0.27
UOC	$\mathbb{1}\{S(t)<H\}\cdot(S(T)-K)^+$	0.99	0.88	0.94	0.83	0.89
UOP	$\mathbb{1}\{S(t)<H\}\cdot(K-S(T))^+$	3.81	3.90	3.75	3.89	3.74
KOC	$\mathbb{1}\{S(t)\in[L,H]\}\cdot(S(T)-K)^+$	0.65	0.56	0.64	0.52	0.59
KOP	$\mathbb{1}\{S(t)\in[L,H]\}\cdot(K-S(T))^+$	0.20	0.20	0.22	0.19	0.21
BCC	$\mathbb{1}\{S(T)\geq K\}$	0.58	0.56	0.57	0.56	0.57
BCP	$\mathbb{1}\{S(T)\leq K\}$	0.37	0.39	0.38	0.39	0.38

[57] We assume that $S(t) \in [0, 200]$.

[58] We use the following Dirichlet and Neumann conditions:

$V(t,S^-)=0$	$V(t,S^+)=0$	$\partial_S V(t,S^-)=-1$	$\partial_S V(t,S^+)=0$
Call, BCC DOC, DOP, UOC KOC, KOP	Put, BCP DOP, UOC, UOP KOC, KOP	Put, BCP UOP	Call, BCC DOC

where $S^- = 0$ and $S^+ = 200$.

[59] $\Sigma_1 = 16\%$ and $\Sigma_2 = 15.5\%$ correspond to the two implied volatilities of strikes 96 and 104 for the one-year maturity.

9.2.4 Stochastic volatility models

The most popular approach to model the volatility smile is to consider that the volatility is not constant, but stochastic. In this case, we obtain a model with two state variables, which are the spot price $S(t)$ and the volatility $\sigma(t)$. After deriving the general formula of the fundamental pricing equation, we present Heston and SABR models, which are the two most important parametrizations of this class of models.

9.2.4.1 General analysis

Pricing formula We assume that the joint dynamics of the spot price $S(t)$ and the stochastic volatility $\sigma(t)$ is:

$$\begin{cases} \mathrm{d}S(t) = \mu(t) S(t)\,\mathrm{d}t + \sigma(t) S(t)\,\mathrm{d}W_1(t) \\ \mathrm{d}\sigma(t) = \zeta(\sigma(t))\,\mathrm{d}t + \xi(\sigma(t))\,\mathrm{d}W_2(t) \end{cases}$$

where $\mathbb{E}[W_1(t) W_2(t)] = \rho t$. $S(t)$ is a geometric Brownian motion with time-varying parameters $\mu(t)$ and $\sigma(t)$, whereas $\sigma(t)$ follows a general diffusion that does not depend on $S(t)$. In the Black-Scholes model, the volatility has the status of parameter. In this new approach, the volatility is a second state variable. The SV model is defined by the functions $\zeta(y)$ and $\xi(y)$.

Using Itô's lemma, we can show that the fundamental pricing equation defined on page 492 becomes[60]:

$$\begin{aligned} \frac{1}{2}\sigma^2 S^2 \partial_S^2 V(t,S,\sigma) + \rho\sigma S \xi(\sigma)\,\partial_{S,\sigma}^2 V(t,S,\sigma) + \frac{1}{2}\xi^2(\sigma)\,\partial_\sigma^2 V(t,S,\sigma) & \\ + (\mu - \lambda_S \sigma) S \partial_S V(t,S,\sigma) + (\zeta(\sigma) - \lambda_\sigma \xi(\sigma))\,\partial_\sigma V(t,S,\sigma) & \\ + \partial_t V(t,S,\sigma) - rV(t,S,\sigma) & = 0 \end{aligned}$$

where $V(t,S,\sigma)$ is the price of the contingent claim, $V(T,S(T)) = f(S(T))$ and $f(S(T))$ is the option payoff. As previously, the market price of the spot risk $W_1(t)$ is:

$$\lambda_S(t) = \frac{\mu(t) - b(t)}{\sigma(t)}$$

By introduction the function $\zeta'(y)$:

$$\zeta'(\sigma(t)) = \zeta(\sigma(t)) - \lambda_\sigma(t)\,\xi(\sigma(t))$$

we obtain the following PDE:

$$\begin{aligned} \frac{1}{2}\sigma^2 S^2 \partial_S^2 V(t,S,\sigma) + \rho\sigma S \xi(\sigma)\,\partial_{S,\sigma}^2 V(t,S,\sigma) + \frac{1}{2}\xi^2(\sigma)\,\partial_\sigma^2 V(t,S,\sigma) & \\ + bS\partial_S V(t,S,\sigma) + \zeta'(\sigma)\,\partial_\sigma V(t,S,\sigma) + \partial_t V(t,S,\sigma) - rV(t,S,\sigma) & = 0 \end{aligned} \tag{9.35}$$

Equation (9.35) is the equivalent of Equation (9.2) on page 492 when the volatility is stochastic.

Using the Girsanov theorem, we deduce that the risk-neutral dynamics is:

$$\begin{cases} \mathrm{d}S(t) = b(t) S(t)\,\mathrm{d}t + \sigma(t) S(t)\,\mathrm{d}W_1^{\mathbb{Q}}(t) \\ \mathrm{d}\sigma(t) = \zeta'(\sigma(t))\,\mathrm{d}t + \xi(\sigma(t))\,\mathrm{d}W_2^{\mathbb{Q}}(t) \end{cases}$$

[60] We omit the dependence in t in order to simplify the notation.

The martingale solution is then equal to:

$$V_0 = \mathbb{E}^{\mathbb{Q}} \left[e^{-\int_0^T r(t)\,\mathrm{d}t} f\left(S\left(T\right)\right) \middle| \mathcal{F}_0 \right]$$

We retrieve the formula obtained in the one-dimensional case. However, the computation of the expected value is now more complex since $S\left(T\right)$ depends on the trajectory of the volatility $\sigma\left(t\right)$.

Hedging portfolio The computation of greek coefficients is more complex in SV models. This is why the definition of the hedging portfolio is not straightforward and depends on the assumption on the smile dynamics. In the case of the Black-Scholes model, delta and vega sensitivities are equal to:

$$\boldsymbol{\Delta}_{\mathrm{BS}} = \frac{\partial\, V_{\mathrm{BS}}\left(S_0, K, \Sigma, T\right)}{\partial\, S_0}$$

and:

$$\boldsymbol{\upsilon}_{\mathrm{BS}} = \frac{\partial\, V_{\mathrm{BS}}\left(S_0, K, \Sigma, T\right)}{\partial\, \Sigma}$$

In the case of the stochastic volatility model, we have:

$$\boldsymbol{\Delta}_{\mathrm{SV}} = \frac{\partial\, V_{\mathrm{SV}}\left(S_0, K, \sigma_0, T\right)}{\partial\, S_0}$$

If we assume that $V_{\mathrm{SV}}\left(S_0, K, \sigma_0, T\right) = V_{\mathrm{BS}}\left(S_0, K, \Sigma_{\mathrm{SV}}\left(T, S_0\right), T\right)$, we obtain:

$$\begin{aligned}
\boldsymbol{\Delta}_{\mathrm{SV}} &= \frac{\partial\, V_{\mathrm{BS}}\left(S_0, K, \Sigma_{\mathrm{SV}}, T\right)}{\partial\, S_0} + \frac{\partial\, V_{\mathrm{BS}}\left(S_0, K, \Sigma_{\mathrm{SV}}, T\right)}{\partial\, \Sigma_{\mathrm{SV}}} \cdot \frac{\partial\, \Sigma_{\mathrm{SV}}\left(T, S_0\right)}{\partial\, S_0} \\
&= \boldsymbol{\Delta}_{\mathrm{BS}} + \boldsymbol{\upsilon}_{\mathrm{BS}} \cdot \frac{\partial\, \Sigma_{\mathrm{SV}}\left(T, S_0\right)}{\partial\, S_0}
\end{aligned}$$

Therefore, the delta of the SV model depends on the BS vega. Generally, we have $\partial_{S_0} \Sigma_{\mathrm{SV}}\left(T, S_0\right) \geq 0$ implying that $\boldsymbol{\Delta}_{\mathrm{SV}} \geq \boldsymbol{\Delta}_{\mathrm{BS}}$.

The calculation of the vega coefficient is a second issue. Indeed, the natural hedging portfolio should consist in two long/short exposures since we have two risk factors $S\left(t\right)$ and $\sigma\left(t\right)$. Therefore, we can define the vega sensitivity as follows:

$$\boldsymbol{\upsilon}_{\mathrm{SV}} = \frac{\partial\, V_{\mathrm{SV}}\left(S_0, K, \sigma_0, T\right)}{\partial\, \sigma_0}$$

However, this definition has no interest since the stochastic volatility $\sigma\left(t\right)$ cannot be directly or even indirectly trade. This is why most of traders prefer to use a BS vega:

$$\boldsymbol{\upsilon}_{\mathrm{SV}} = \frac{\partial\, V_{\mathrm{BS}}\left(S_0, K, \Sigma_{\mathrm{SV}}\left(T, S_0\right), T\right)}{\partial\, \Sigma_{\mathrm{SV}}}$$

Here, we make the assumption that the vega is calculated with respect to the implied volatility $\Sigma_{\mathrm{SV}}\left(T, S_0\right)$ deduced from the stochastic volatility model. It can be viewed as a pure Black-Scholes vega, but most of times, it corresponds to a shift of the implied volatility surface. This approach requires a new calibration of the stochastic volatility parameters. In some sense, the vega can be viewed as the difference between the prices obtained with two stochastic volatility models.

9.2.4.2 Heston model

Heston (1993) assumes that the stochastic differential equation of the spot price is equal to:

$$\begin{cases} \mathrm{d}S(t) = \mu S(t)\,\mathrm{d}t + \sqrt{v(t)}S(t)\,\mathrm{d}W_1(t) \\ \mathrm{d}v(t) = \kappa(\theta - v(t))\,\mathrm{d}t + \xi\sqrt{v(t)}\,\mathrm{d}W_2(t) \end{cases}$$

where $S(0) = S_0$, $v(0) = v_0$ and $W(t) = (W_1(t), W_2(t))$ is a two-dimensional Wiener process with $\mathbb{E}[W_1(t)W_2(t)] = \rho t$. We notice that the stochastic variance $v(t)$ follows a CIR process: θ is the long-run variance, κ is the mean-reverting parameter and ξ is the volatility of the variance (also called the vovol parameter).

Remark 106 *We have $\sigma(t) = \sqrt{v(t)}$ and:*

$$\mathrm{d}\sigma(t) = \left(\left(\frac{\kappa\theta}{2} - \frac{\xi^2}{8}\right)\frac{1}{\sigma(t)} - \frac{1}{2}\kappa\sigma(t)\right)\mathrm{d}t + \frac{1}{2}\xi\,\mathrm{d}W_2(t)$$

The stochastic volatility is then an Ornstein-Uhlenbeck process if we impose $\theta = \xi^2/(4\kappa)$.

As the second state variable of the Heston model is the stochastic variance $v(t)$, the price $V(t, S, v)$ of the option must satisfy the PDE[61]:

$$\begin{array}{rcl} \frac{1}{2}vS^2\partial_S^2 V + \rho\xi v S\partial_{S,v}^2 V + \frac{1}{2}\xi^2 v\partial_v^2 V & & \\ +bS\partial_S V + (\kappa(\theta - v(t)) - \lambda v)\partial_v V + \partial_t V - rV & = & 0 \end{array}$$

It follows that the risk-neutral dynamics is:

$$\begin{cases} \mathrm{d}S(t) = bS(t)\,\mathrm{d}t + \sqrt{v(t)}S(t)\,\mathrm{d}W_1^{\mathbb{Q}}(t) \\ \mathrm{d}v(t) = (\kappa(\theta - v(t)) - \lambda v(t))\,\mathrm{d}t + \xi\sqrt{v(t)}\,\mathrm{d}W_2^{\mathbb{Q}}(t) \end{cases}$$

In the case of European call and put options, Heston (1993) gives a closed-form solution of the price:

$$\begin{array}{rcl} \mathcal{C}_0 & = & S_0 e^{(b-r)T} P_1 - K e^{-rT} P_2 \\ \mathcal{P}_0 & = & S_0 e^{(b-r)T}(P_1 - 1) - K e^{-rT}(P_2 - 1) \end{array}$$

where the probabilities P_1 and P_2 satisfy:

$$\begin{array}{l} P_j = \frac{1}{2} + \frac{1}{\pi}\int_0^\infty \mathrm{Re}\left(\frac{e^{-i\phi\ln K}\varphi_j(S_0, v_0, T, \phi)}{i\phi}\right)\mathrm{d}\phi \\ \varphi_j(S_0, v_0, T, \phi) = \exp\left(C_j(T,\phi) + D_j(T,\phi)v_0 + i\phi\ln S_0\right) \\ C_j(T,\phi) = ib\phi T + \frac{a_j}{\xi^2}\left((b_j - i\rho\xi\phi + d_j)T - 2\ln\left(\frac{1 - g_j e^{d_j T}}{1 - g_j}\right)\right) \\ D_j(T,\phi) = \frac{b_j - i\rho\xi\phi + d_j}{\xi^2}\left(\frac{1 - e^{d_j T}}{1 - g_j e^{d_j T}}\right) \\ g_j = \frac{b_j - i\rho\xi\phi + d_j}{b_j - i\rho\xi\phi - d_j} \\ d_j = \sqrt{(i\rho\xi\phi - b_j)^2 - \xi^2(2iu_j\phi - \phi^2)} \end{array}$$

where $a_1 = a_2 = \kappa\theta$, $b_1 = \kappa + \lambda - \rho\xi$, $b_2 = \kappa + \lambda$, $u_1 = 1/2$ and $u_2 = -1/2$.

[61] Heston (1993) makes the assumption that $\lambda_v(t) \propto \sqrt{v}$.

The existence of these semi-analytical formulas for European options is one of the main factors for explaining the popularity of the Heston model. However, the implementation of the formulas is not straightforward since it requires computing the integral of the inverse Fourier transform. In particular, Kahl and Jäckel (2005) show that the evaluation of logarithms with complex arguments may produce a numerical instability. Numerical softwares will generally do the following computation:

$$\ln\left(\frac{1-g_j e^{d_j T}}{1-g_j}\right)=\ln|r|+i\varphi$$

where:

$$r=\left|\frac{1-g_j e^{d_j T}}{1-g_j}\right|$$

and:

$$\varphi=\arg\left(\frac{1-g_j e^{d_j T}}{1-g_j}\right)$$

However, the fact that $\varphi\in[-\pi,\pi]$ will create a discontinuity when integrating the function. In order to circumvent this problem, we note:

$$g_j=r\left(g_j\right)e^{i\varphi\left(g_j\right)}$$

and:

$$d_j=a\left(d_j\right)+ib\left(d_j\right)$$

Kahl and Jäckel (2005) deduce that:

$$\begin{aligned} g_j-1 &= r\left(g_j\right)e^{i\varphi\left(g_j\right)}-1 \\ &= \tilde{r}e^{i\left(\tilde{\varphi}_j+2\pi\tilde{m}\right)} \end{aligned}$$

where $\tilde{m}=\left\lfloor(2\pi)^{-1}\left(\varphi\left(g_j\right)+\pi\right)\right\rfloor$, $\tilde{\varphi}_j=\arg\left(g_j-1\right)$ and $\tilde{r}=\left|g_j-1\right|$. They also found that:

$$\begin{aligned} g_j e^{d_j T}-1 &= r\left(g_j\right)e^{i\varphi\left(g_j\right)}e^{a\left(d_j\right)T+ib\left(d_j\right)T}-1 \\ &= r\left(g_j\right)e^{a\left(d_j\right)T}e^{i\left(\varphi\left(g_j\right)+b\left(d_j\right)T\right)}-1 \\ &= \breve{r}e^{i\left(\breve{\varphi}_j+2\pi\breve{m}\right)} \end{aligned}$$

where $\breve{m}=\left\lfloor(2\pi)^{-1}\left(\varphi\left(g_j\right)+b\left(d_j\right)T+\pi\right)\right\rfloor$, $\breve{\varphi}_j=\arg\left(g_j e^{d_j T}-1\right)$ and $\breve{r}=\left|g_j e^{d_j T}-1\right|$. Finally, they obtain:

$$\ln\left(\frac{1-g_j e^{d_j T}}{1-g_j}\right)=\ln\frac{\breve{r}}{\tilde{r}}+i\left(\breve{\varphi}_j-\tilde{\varphi}_j+2\pi\breve{m}-2\pi\tilde{m}\right)$$

In Figure 9.32, we show the functions $f_1(u)$ and $f_2(u)$ defined by:

$$f_j(u)=\operatorname{Re}\left(\frac{e^{-iu\ln K}\varphi_j\left(S_0,v_0,T,u\right)}{iu}\right)$$

The parameters are $S_0=100$, $K=100$, $T=30$, $b=0.00$, $v_0=0.2$, $\kappa=1$, $\theta=0.2$, $\xi=0.5$ and $\lambda=0$. For $f_1(u)$, we use $\rho=30\%$ whereas ρ is set to -30% for the function $f_2(u)$. We see the discontinuity produced by numerical softwares. The Kahl-Jäckel method produces continuous functions without jumps. The problem can sometimes affect the two functions $f_1(u)$ and $f_2(u)$. This is the case in Figure 9.33 with the following parameters $S_0=100$, $K=100$, $T=30$, $b=0.05$, $v_0=4\%$, $\kappa=0.5$, $\theta=4\%$, $\xi=0.7$, $\rho=-0.80$ and $\lambda=0$. Again, the Kahl-Jäckel method performs the good correction.

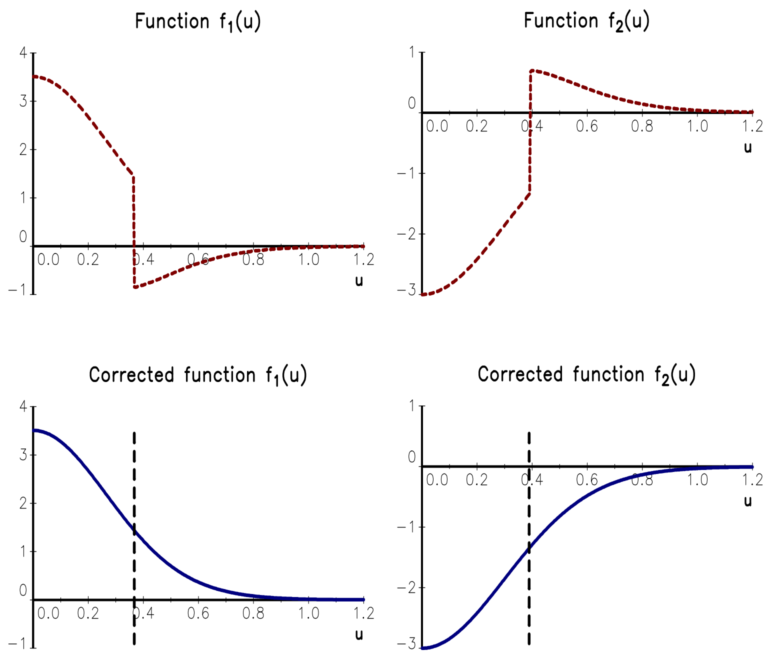

FIGURE 9.32: Functions $f_1(u)$ and $f_2(u)$ ($\kappa = 1$)

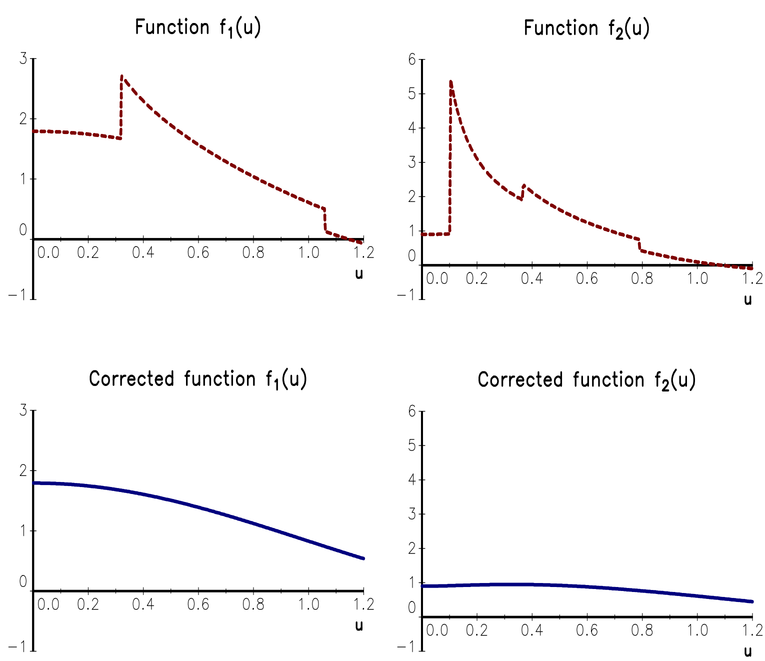

FIGURE 9.33: Functions $f_1(u)$ and $f_2(u)$ ($\kappa = 0.5$)

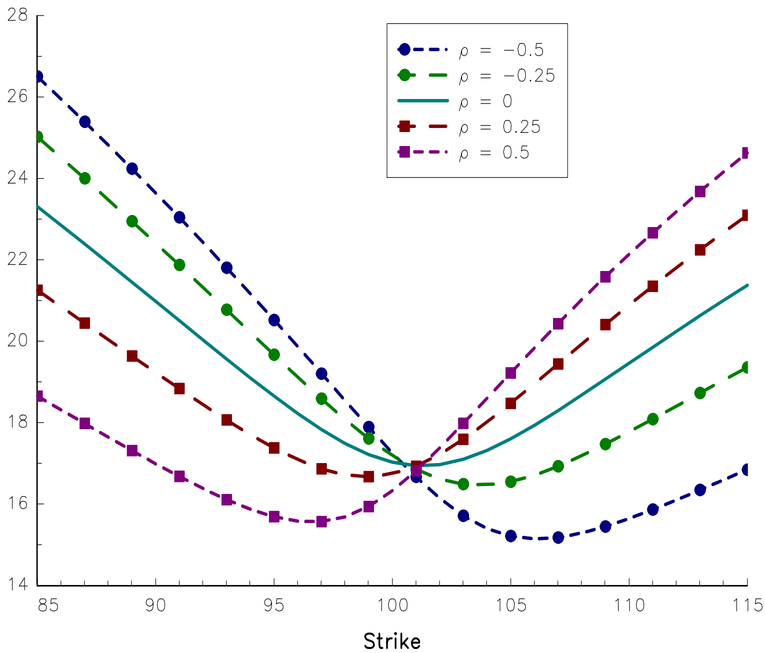

FIGURE 9.34: Implied volatility of the Heston model (in %)

Example 94 *The parameters are equal to* $S_0 = 100$, $b = r = 5\%$, $v_0 = \theta = 4\%$, $\kappa = 0.5$, $\xi = 0.9$ *and* $\lambda = 0$. *We consider the pricing of the European call option, whose maturity is three months.*

Figure 9.34 shows the implied volatility for different values of the strike K and the correlation ρ. We notice that the Heston model can produce different shapes of the volatility surface. In Figure 9.35, we have reported the skew of the implied volatility defined by:

$$\omega(T, K) = \frac{\partial\,\Sigma(T, K)}{\partial\, K}$$

Several authors have proposed approximations of the Heston implied volatility $\Sigma_t(T, K)$. We can cite Schönbucher (1999), Forde and Jacquier (2009), and Gatheral and Jacquier (2011). A more general approach has been proposed by Durrleman (2010), who assumes that the dynamics of S_t is Markovian with:

$$S(t) = S_0 \exp\left(\int_0^t \sigma(s)\, \mathrm{d}W(s) - \frac{1}{2}\int_0^t \sigma^2(s)\, \mathrm{d}s\right)$$

and:

$$\begin{cases} \mathrm{d}\sigma^2(t) = \mu(t)\, \mathrm{d}t - 2\sigma(t)\left(a(t)\, \mathrm{d}W(t) + \tilde{a}(t)\, \mathrm{d}\tilde{W}(t)\right) \\ \mathrm{d}\mu(t) = (\cdot)\, \mathrm{d}t + \omega(t)\, \mathrm{d}W(t) + (\cdot)\, \mathrm{d}\tilde{W}(t) \\ \mathrm{d}a(t) = m(t)\, \mathrm{d}t + u(t)\, \mathrm{d}W(t) + \tilde{u}(t)\, \mathrm{d}\tilde{W}(t) \\ \mathrm{d}\tilde{a}(t) = (\cdot)\, \mathrm{d}t + v(t)\, \mathrm{d}W(t) + (\cdot)\, \mathrm{d}\tilde{W}(t) \\ \mathrm{d}u(t) = (\cdot)\, \mathrm{d}t + x(t)\, \mathrm{d}W(t) + (\cdot)\, \mathrm{d}\tilde{W}(t) \end{cases}$$

where $(\cdot)$ is a generic symbol for a continuous adapted process. Durrleman (2010) shows that:

$$\Sigma_t^2(T, K) \simeq \sigma^2(t) + a(t)\, s(t) + \frac{b(t)\,\tau}{2} + \frac{c(t)\, s^2(t)}{2} + \frac{d(t)\, s(t)\,\tau}{2} + \frac{e(t)\, s^3(t)}{6}$$

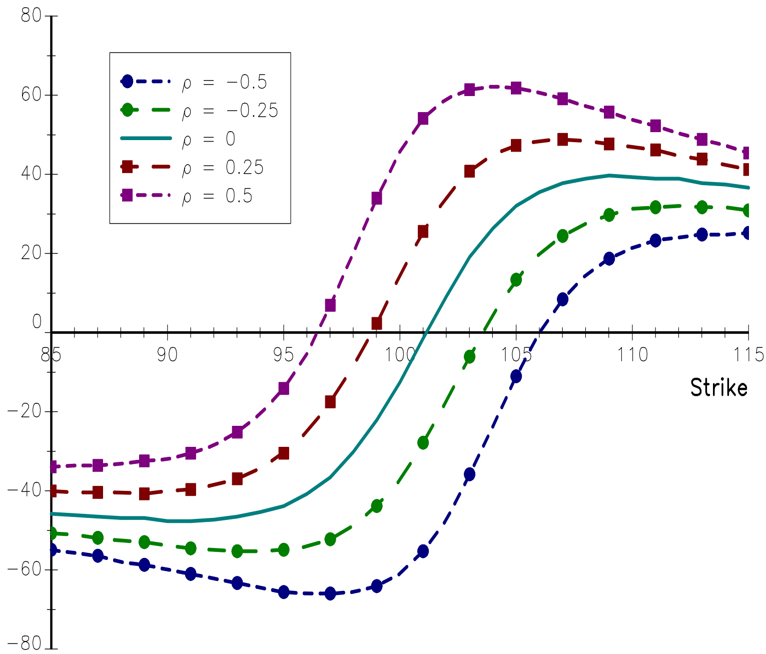

FIGURE 9.35: Skew of the Heston model (in bps)

where $\tau = T - t$ and $s(t) = \ln S(t) - \ln K$. The coefficients $b(t)$, $c(t)$, $d(t)$ and $e(t)$ are given by:

$$b(t) = \mu(t) - \frac{a^2(t)}{2} - \frac{2\tilde{a}^2(t)}{3} - a(t)\sigma^2(t) + \frac{2u(t)\sigma(t)}{3}$$

and:

$$\begin{aligned} c(t) &= -\frac{2u(t)}{3\sigma(t)} - \frac{a^2(t)}{2\sigma^2(t)} + \frac{2\tilde{a}^2(t)}{3\sigma^2(t)} \\ d(t) &= \frac{2m(t)}{3} - \frac{\omega(t)}{3\sigma(t)} - \frac{x(t)}{2} - \frac{a(t)\mu(t)}{3\sigma^2(t)} + \frac{\tilde{a}(t)\tilde{u}(t)}{6\sigma(t)} + \frac{\tilde{a}(t)v(t)}{\sigma(t)} + \\ &\quad \frac{2a(t)\tilde{a}^2(t)}{3\sigma^2(t)} + \frac{2u(t)\sigma(t)}{3} - \frac{a^2(t)}{3} \\ e(t) &= \frac{x(t)}{2\sigma^2(t)} + \frac{2a(t)u(t)}{\sigma^3(t)} - \frac{3\tilde{a}(t)\tilde{u}(t)}{2\sigma^3(t)} - \frac{\tilde{a}(t)v(t)}{\sigma^3(t)} + \frac{3a^3(t)}{2\sigma^4(t)} - \\ &\quad \frac{4a(t)\tilde{a}^2(t)}{\sigma^4(t)} \end{aligned}$$

In the case of the Heston model, we have:

$$\begin{cases} \mathrm{d}S(t) = \sigma(t)S(t)\ \mathrm{d}W(t) \\ \mathrm{d}\sigma^2(t) = \kappa\left(\theta - \sigma^2(t)\right)\ \mathrm{d}t + \xi\sigma(t)\ \left(\rho\,\mathrm{d}W_t + \sqrt{1-\rho^2}\,\mathrm{d}\tilde{W}_t\right) \end{cases}$$

It follows that $a(t) = -\frac{\xi\rho}{2}$, $\tilde{a}(t) = -\frac{\xi\sqrt{1-\rho^2}}{2}$ and $\omega(t) = m(t) = u(t) = \tilde{u}(t) = v(t) = x(t) = 0$. We deduce that:

$$\begin{aligned}
b(t) &= \kappa\left(\theta - \sigma^2(t)\right) + \frac{\xi\rho\sigma^2(t)}{2} - \frac{\xi^2}{6}\left(1 - \frac{\rho^2}{4}\right) \\
c(t) &= \frac{\xi^2}{6\sigma^2(t)}\left(1 - \frac{7\rho^2}{4}\right) \\
d(t) &= \frac{\kappa\xi\rho}{6}\left(\frac{\theta}{\sigma_t^2} - 1\right) - \frac{\xi^2\rho}{12}\left(\rho + \frac{\xi\left(1-\rho^2\right)}{\sigma^2(t)}\right) \\
e(t) &= \frac{\xi^3\rho}{2\sigma^4(t)}\left(1 - \frac{11\rho^2}{8}\right)
\end{aligned}$$

In Figure 9.36, we have generated the volatility surface using the Durrleman formula of the Heston model approximation. The parameters are $S(t) = 100$, $\sigma(t) = 20\%$, $\kappa = 0.5$, $\theta = 4\%$ and $\xi = 0.2$. We consider different values for the correlation parameter ρ and the maturity T. We notice that the Durrleman formula does not fit correctly the Heston smile when the absolute value $|\rho|$ of the correlation is high.

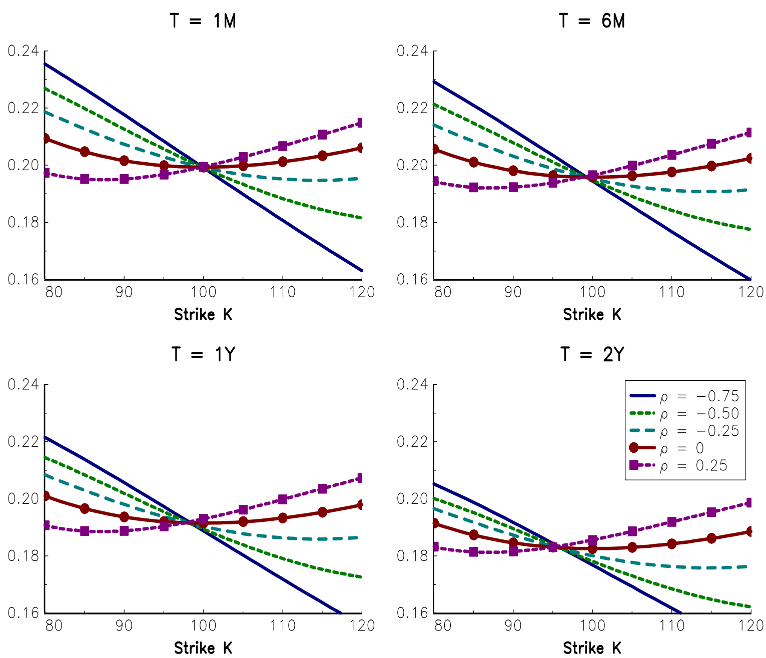

FIGURE 9.36: Implied volatility of the Durrleman formula (in %)

Example 95 *We assume that $S(t) = 100$ and $T = 0.5$. The volatility smile is given by the following values:*

K	90.00	95.00	100.00	105.00	110.00
$\Sigma_t(T,K)$ *(in %)*	20.25	19.92	19.67	19.49	19.38

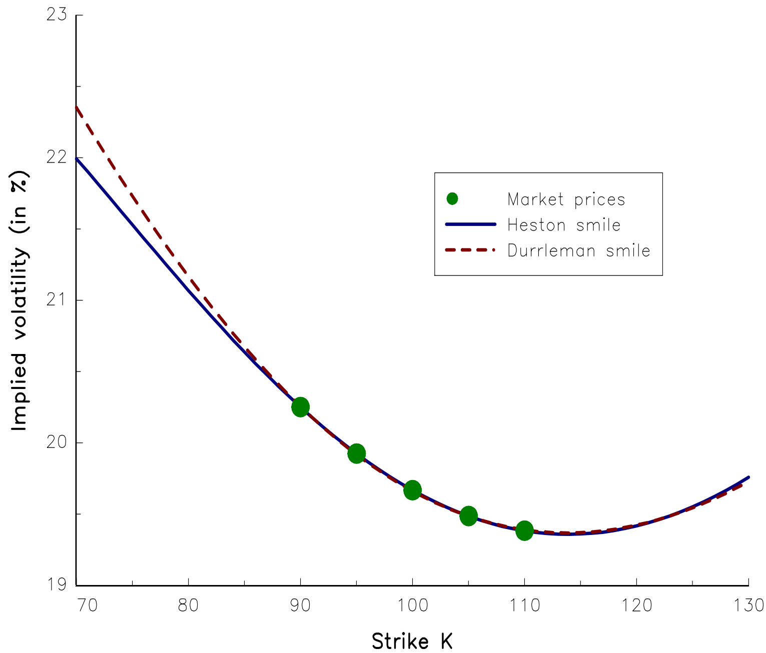

FIGURE 9.37: Calibration of the smile by the Heston model and the Durrleman formula

The calibration of the smile gives the following result[62]:

Model	$\sigma(t)$	κ	θ	ξ	ρ
Heston	0.201	0.980	0.040	0.192	-0.207
Durrleman	0.222	1.000	0.014	0.191	-0.193

The volatility surface of each calibrated model is represented in Figure 9.37. The results are very similar.

Remark 107 *The Heston model was very popular in the 2000s. Nevertheless, even if we have an analytical formula for the call and put prices, the absence of a true implied volatility formula was an obstacle of its development, and the use of the Heston model is today less frequent. The Heston model has then been replaced by the SABR model, because of the availability of an implied volatility formula.*

9.2.4.3 SABR model

Hagan *et al.* (2002) suggest using the SABR[63] model to take into account the smile effect. The dynamics of the forward rate $F(t)$ is given by:

$$\left\{ \begin{array}{l} \mathrm{d}F(t) = \alpha(t) F(t)^{\beta} \, \mathrm{d}W_1^{\mathbb{Q}}(t) \\ \mathrm{d}\alpha(t) = \nu \alpha(t) \, \mathrm{d}W_2^{\mathbb{Q}}(t) \end{array} \right.$$

where $\mathbb{E}\left[W_1^{\mathbb{Q}}(t) W_2^{\mathbb{Q}}(t)\right] = \rho t$. Since $\beta \in [0,1]$, $\alpha(t)$ is not necessarily the instantaneous volatility of $F(t)$ except in the cases $\beta = 0$ (Gaussian volatility) and $\beta = 1$ (log-normal

[62] It consists of minimizing the sum of squared errors between observed implied volatilities and theoretical implied volatilities deduced from the option model.

[63] This is the acronym of stochastic $-\alpha-\beta-\rho$.

volatility). The model has also 4 parameters: α the current value of $\alpha(t)$, β the exponent of the forward rate, ν the log-normal volatility of $\alpha(t)$ and ρ the correlation between the two Brownian motions. One of the big interests of the SABR model is that we have an approximate formula of the implied Black volatility:

$$\begin{aligned}\Sigma_B(T,K) &= \frac{\alpha}{(F_0K)^{(1-\beta)/2}\left(1+\frac{(1-\beta)^2}{24}\ln^2\frac{F_0}{K}+\frac{(1-\beta)^4}{1920}\ln^4\frac{F_0}{K}\right)}\left(\frac{z}{\chi(z)}\right)\cdot\\ &\quad \left(1+\left(\frac{(1-\beta)^2\alpha^2}{24(F_0K)^{1-\beta}}+\frac{\rho\alpha\nu\beta}{4(F_0K)^{(1-\beta)/2}}+\frac{2-3\rho^2}{24}\nu^2\right)T\right)\end{aligned}$$

where $z=\nu\alpha^{-1}(F_0K)^{(1-\beta)/2}\ln\dfrac{F_0}{K}$ and $\chi(z)=\ln\left(\sqrt{1-2\rho z+z^2}+z-\rho\right)-\ln(1-\rho)$.

Let us see the interpretation of the parameters[64]. We have represented their impact in Figures[65] 9.38 and 9.39. The parameter β allows to define a stochastic log-normal model when β is equal to 1, or a stochastic normal model when β is equal to 0, or an hybrid model. The choice of β is generally exogenous. The main reason is that β is highly related to the dynamics of the ATM implied volatility. If β is equal to 1, we observe a simple translation of the smile when the forward rate moves (first panel in Figure 9.38). If β is equal to 0, the ATM implied volatility decreases when the forward rates increases (second panel in Figure 9.38). This explains the behavior of the backbone, which represents the dynamics of the ATM implied volatility when the forward rate varies (third panel in Figure 9.38).

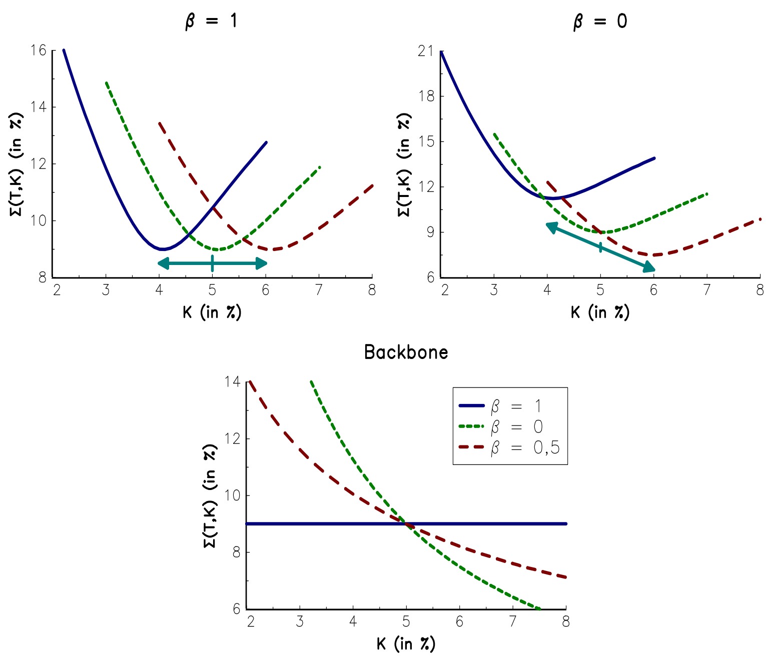

FIGURE 9.38: Impact of the parameter β

[64] In the following examples, we consider a one-year option, whose current forward rate F_0 is equal to 5%.
[65] The default values are $\alpha = 10\%$, $\beta = 1$, $\nu = 50\%$ and $\rho = 0$.

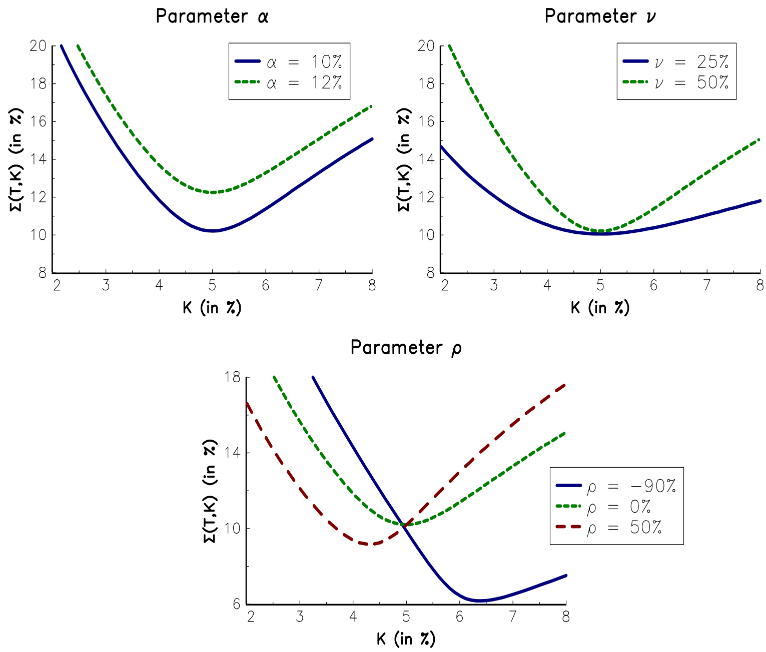

FIGURE 9.39: Impact of the parameters α, ν and ρ

The parameter α controls the level of implied volatilities (see Panel 1 in Figure 9.39). In particular, α is close to the value of the ATM volatility when β is equal to one[66]. ν is called the vovol (or vol-vol) parameter, because it measures the volatility of the volatility. ν impacts then the stochastic property of the volatility $\alpha(t)$. The limit case $\nu = 0$ corresponds to the constant volatility and we obtain the classical Black model[67]. An increase of ν tends to increase the slope of the implied volatility (see Panel 2 in Figure 9.39). The asymmetry of the smile is due to the parameter ρ. For instance, if ρ is negative, the skew is more important in the left side than in the right side (see Panel 3 in Figure 9.39).

Remark 108 *The parameters β and ρ impact the slope of the smile in a similar way. Then, they cannot be jointly identifiable. For example, let us consider the following smile when F_0 is equal to 5%: $\Sigma_B(1, 3\%) = 13\%$, $\Sigma_B(1, 4\%) = 10\%$, $\Sigma_B(1, 5\%) = 9\%$ and $\Sigma_B(1, 7\%) = 10\%$. If we calibrate this smile for different values of β, we obtain the following solutions:*

β	α	ν	ρ
0.0	0.0044	0.3203	0.2106
0.5	0.0197	0.3244	0.0248
1.0	0.0878	0.3388	−0.1552

We have represented the corresponding smiles in Figure 9.40 and we verify that the three sets of calibrated parameters give the same smile.

[66]In this case, we have:

$$\Sigma_B(T, F_0) = \alpha \left(1 + \left(\frac{\rho\alpha\nu}{4} + \frac{2 - 3\rho^2}{24}\nu^2\right) T\right)$$

It follows that $\Sigma_B(T, F_0)$ is exactly equal to α when ρ is equal to zero.

[67]When β is equal to one of course.

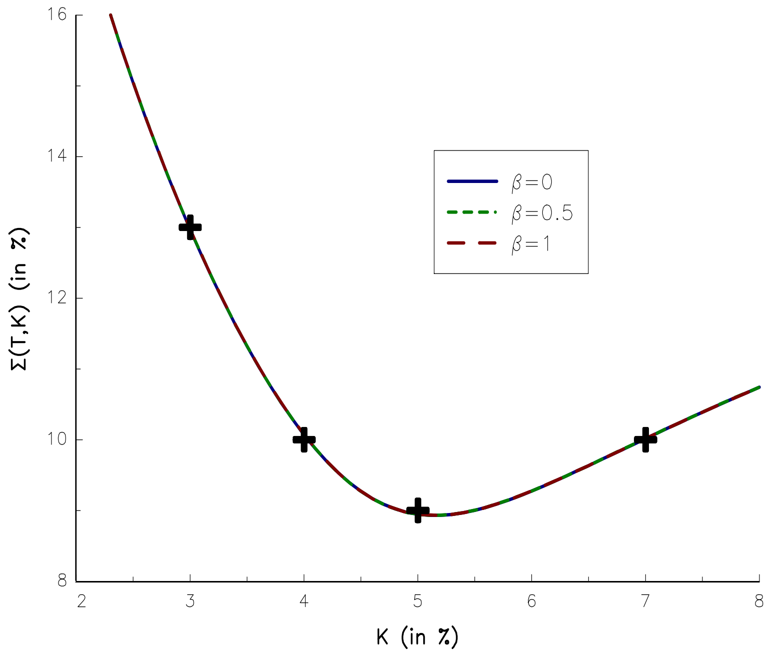

FIGURE 9.40: Implied volatility for different parameter sets (β, ρ)

We have seen that the choice of β is not important for calibrating the SABR model for a given maturity. We have already seen that the parameter β has a great impact on the dynamics on the backbone. Therefore, there are two approaches for estimating β:

1. β can be chosen from prior beliefs ($\beta = 0$ for the normal model, $\beta = 0.5$ for the CIR model and $\beta = 1$ for the log-normal model);

2. β can be statistically estimated by considering the dynamics of the forward rate.

TABLE 9.12: Calibration of the parameter β in the SABR model

Rate	Level		Difference		Empirical quantile of $\hat{\beta}_{t,t+h}$				
	$\hat{\beta}$	R_c^2	$\hat{\beta}$	R_c^2	10%	25%	50%	75%	90%
1y1y	−0.06	0.91	0.59	0.15	−2.01	−0.14	0.71	1.00	2.17
1y5y	−0.29	0.87	0.32	0.27	−1.80	−0.28	0.73	1.11	2.76
1y10y	−0.37	0.80	0.34	0.22	−2.04	−0.23	0.71	1.11	2.69
5y1y	0.42	0.29	0.35	0.22	−1.58	−0.31	0.71	1.00	2.38
5y5y	−0.01	0.73	0.23	0.28	−2.12	−0.36	0.61	1.00	2.52
5y10y	−0.10	0.69	0.27	0.23	−1.99	−0.30	0.70	1.05	2.58
10y1y	0.96	0.00	0.28	0.20	−1.88	−0.20	0.80	1.07	2.43
10y5y	−0.10	0.65	0.28	0.20	−2.02	−0.29	0.73	1.02	2.76
10y10y	−0.47	0.73	0.27	0.20	−1.71	−0.24	0.85	1.07	2.93

The second approach is based on the approximation of the ATM volatility:

$$\Sigma_t(T, F_t) \simeq \frac{\alpha}{F_t^{1-\beta}}$$

We have:

$$\ln \Sigma_t(T, F_t) = \ln \alpha + (\beta - 1) \ln F_t + u_t \tag{9.36}$$

We can then estimate β by considering the linear regression of the logarithm of the ATM volatility on the logarithm of the forward rate. However, these two variables are generally integrated of order one or $I(1)$. A better approach is then to consider the alternative linear regression[68]:

$$\ln \Sigma_{t+h}(T, F_{t+h}) - \ln \Sigma_t(T, F_t) = c + (\beta - 1)(\ln F_{t+h} - \ln F_t) + u_t \tag{9.37}$$

where c is a constant. In this case, the linear regression is performed using the difference and not the level of implied volatilities. Using the Libor EUR rates between 2000 and 2003, we obtain results given in Table 9.12. In the first column, we indicate the maturity and the tenor of the forward rate. The next two columns report the estimate $\hat{\beta}$ and the R-squared coefficient R_c^2 for the regression model (9.36). Then, we have the values of $\hat{\beta}$ and R_c^2 for the regression model[69] (9.37). We observe some strong differences between the two approaches (see also the probability density function of $\hat{\beta}$ in Figure 9.41). These results show that the regression model (9.36) produces bad results. However, it does not mean that the second regression model (9.36) is more robust. Indeed, we can calculate the exact value $\hat{\beta}_{t,t+h}$ that explains the dynamics of the ATM volatility from time t to time $t+h$:

$$\hat{\beta}_{t,t+h} = \frac{\ln(F_{t+h} \cdot \Sigma_{t+h}(T, F_{t+h})) - \ln(F_t \cdot \Sigma_t(T, F_t))}{\ln F_{t+h} - \ln F_t}$$

In Table 9.12, we notice the wide dispersion of $\hat{\beta}_{t,t+h}$. On average, the parameter β is around 70%, but it can also take some large negative or positive values. This is why β is generally chosen from prior beliefs.

Once we have set the value of β, we estimate the parameters (α, ν, ρ) by fitting the observed implied volatilities. However, we have seen that α is highly related to the ATM volatility. Indeed, we have:

$$\Sigma_B(T, F_0) = \frac{\alpha}{F_0^{1-\beta}} \left(1 + \left(\frac{(1-\beta)^2 \alpha^2}{24 F_0^{2-2\beta}} + \frac{\rho\alpha\nu\beta}{4F_0^{1-\beta}} + \frac{2-3\rho^2}{24}\nu^2\right) T\right)$$

We deduce that:

$$\alpha^3 \left(\frac{(1-\beta)^2 T}{24 F_0^{2-2\beta}}\right) + \alpha^2 \left(\frac{\rho\nu\beta T}{4F_0^{1-\beta}}\right) + \alpha\left(1 + \frac{2-3\rho^2}{24}\nu^2 T\right) - \Sigma_B(T, F_0) F_0^{1-\beta} = 0$$

Let $\alpha = g_\alpha(\Sigma_B(T, F_0), \nu, \rho)$ be the positive root of the cubic equation. Therefore, imposing that the smile passes through the ATM volatility $\Sigma_B(T, F_0)$ allows to reduce the calibration to two parameters (ν, ρ).

Example 96 *We consider the following smile:*

K *(in %)*	2.8	3.0	3.5	3.7	4.0	4.5	5.0	7.0
$\Sigma(T, K)$ *(in %)*	13.2	12.8	12.0	11.6	11.0	10.0	9.0	10.0

The maturity T is equal to one year and the forward rate F_0 is set to 5%.

[68] We have:

$$\frac{\Sigma_{t+h}(T, F_{t+h})}{\Sigma_t(T, F_t)} \simeq \left(\frac{F_{t+h}}{F_t}\right)^{\beta-1}$$

[69] In this case, we set h to one trading day.

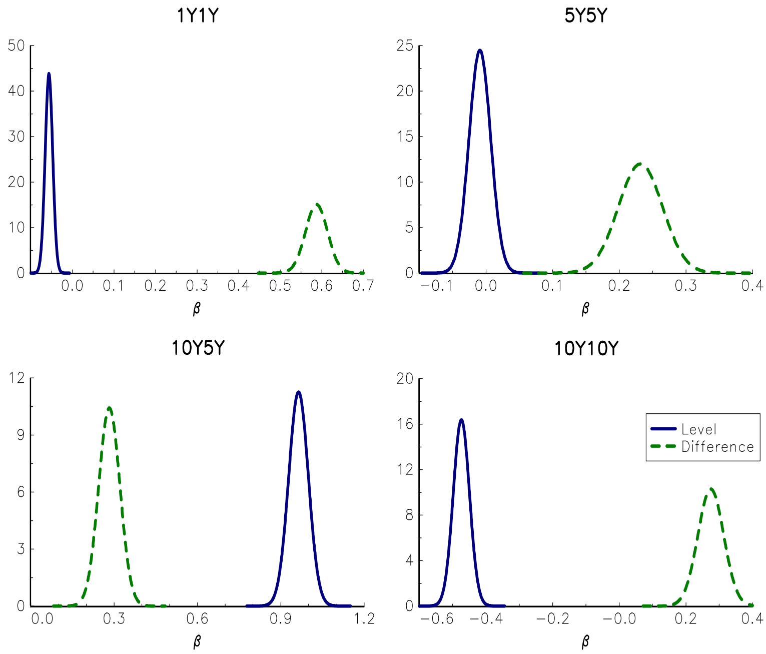

FIGURE 9.41: Probability density function of the estimate $\hat{\beta}$ (SABR model)

If we consider a stochastic log-normal model ($\beta = 1$), we obtain the following results:

Calibration	α (in %)	β	ν	ρ (in %)	RSS	Σ_{ATM} (in %)
#1	9.466	1.00	0.279	−23.70	0.630	9.51
#2	8.944	1.00	0.322	−22.90	1.222	9.00

RSS indicates the residual sum of squares (expressed in bps). In the first calibration, we estimate the three parameters α, ν and ρ. In this case, the residual sum of squares is equal to 0.63 bps, but the SABR ATM volatility is equal to 9.51%, which is far from the market ATM volatility. In the second calibration, we estimate the two parameters ν and ρ, whereas α is the solution of the cubic equation that fits the ATM volatility. We notice that the residual sum of squares has increased from 0.63 bps to 1.222 bps, but the SABR ATM volatility is exactly equal to the market ATM volatility. The two calibrated smiles are reported in Figure 9.42.

Remark 109 *One of the issues with implied volatility calibration is that we generally have more market prices for the put (or left) wing of the smile than its call (or right) wing. This implies that the put wing is better calibrated than the call wing, and we may observe a large difference between the calibrated ATM volatility and the market ATM volatility. Therefore, professionals prefer the second calibration.*

The sensitivities correspond to the following formulas[70]:

$$\boldsymbol{\Delta} = \frac{\partial\, \mathcal{C}_B}{\partial\, F_0} + \frac{\partial\, \mathcal{C}_B}{\partial\, \Sigma} \cdot \frac{\partial\, \Sigma_B\,(T, K)}{\partial\, F_0}$$

[70]If we consider the parametrization $\alpha = g_\alpha\left(\Sigma_{\text{ATM}}, \nu, \rho\right)$, we have:

$$\boldsymbol{\Delta} = \frac{\partial\, \mathcal{C}_B}{\partial\, F_0} + \frac{\partial\, \mathcal{C}_B}{\partial\, \Sigma} \cdot \left(\frac{\partial\, \Sigma_B\,(T, K)}{\partial\, F_0} + \frac{\partial\, \Sigma_B\,(T, K)}{\partial\, \alpha} \cdot \frac{\partial\, g_\alpha\left(\Sigma_{\text{ATM}}, \nu, \rho\right)}{\partial\, F_0}\right)$$

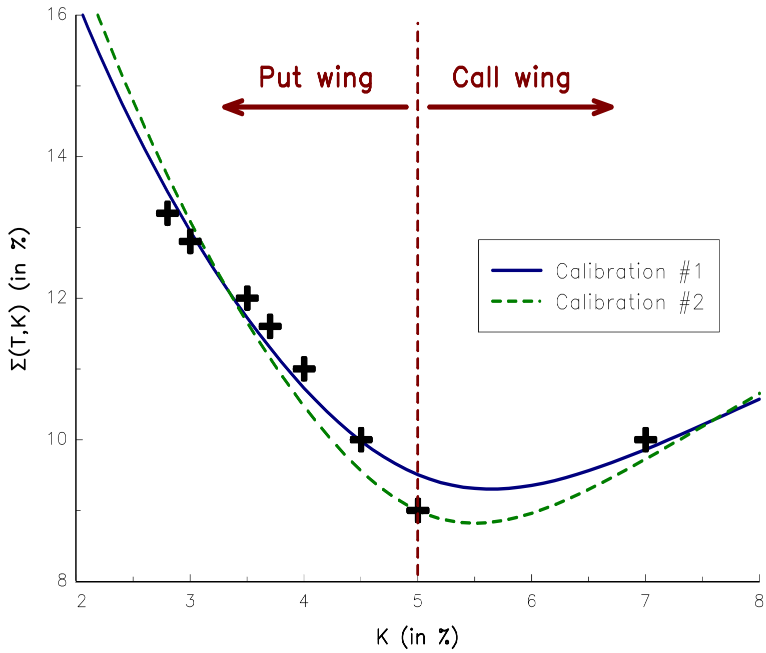

FIGURE 9.42: Calibration of the SABR model

and:

$$\boldsymbol{\upsilon} = \frac{\partial \boldsymbol{\mathcal{C}}_B}{\partial \Sigma} \cdot \frac{\partial \Sigma_B (T, K)}{\partial \alpha}$$

To obtain these formulas, we apply the chain rule on the Black formula by assuming that the volatility Σ is not constant and depends on F_0 and α.

Remark 110 *We notice that the vega is defined with respect to the parameter α. This approach is little used in practice, because it is difficult to hedge this model parameter. This is why traders prefer to compute the vega with respect to the ATM volatility:*

$$\boldsymbol{\upsilon} = \frac{\partial \boldsymbol{\mathcal{C}}_B}{\partial \Sigma} \cdot \frac{\partial \Sigma_B (T, K)}{\partial \alpha} \cdot \frac{\partial \alpha}{\partial \Sigma_{\mathrm{ATM}}}$$

where $\Sigma_{\mathrm{ATM}} = \Sigma_B (T, F_0)$.

Remark 111 *Bartlett (2006) proposes a refinement for computing the delta. Indeed, a shift in F_0 produces a shift in α, because the two processes $F(t)$ and $\alpha(t)$ are correlated. Since we have:*

$$\begin{aligned} \mathrm{d}\alpha (t) &= \nu \alpha (t) \, \mathrm{d}W_2^Q (t) \\ &= \nu \alpha (t) \left(\rho \, \mathrm{d}W_1^Q (t) + \sqrt{1 - \rho^2} \, \mathrm{d}W (t) \right) \end{aligned}$$

and:

$$\mathrm{d}W_1^Q (t) = \frac{\mathrm{d}F (t)}{\alpha (t) F (t)^{\beta}}$$

we deduce that:

$$\mathrm{d}\alpha (t) = \frac{\nu \rho}{F (t)^{\beta}} \, \mathrm{d}F (t) + \nu \alpha (t) \sqrt{1 - \rho^2} \, \mathrm{d}W (t)$$

The new delta is then:

$$\begin{aligned}
\boldsymbol{\Delta}^{\star} &= \frac{\partial \boldsymbol{\mathcal{C}}_B}{\partial F_0} + \frac{\partial \boldsymbol{\mathcal{C}}_B}{\partial \Sigma} \left(\frac{\partial \Sigma_B (T,K)}{\partial F_0} + \frac{\partial \Sigma_B (T,K)}{\partial \alpha} \cdot \frac{\partial \alpha}{\partial F_0} \right) \\
&= \frac{\partial \boldsymbol{\mathcal{C}}_B}{\partial F_0} + \frac{\partial \boldsymbol{\mathcal{C}}_B}{\partial \Sigma} \left(\frac{\partial \Sigma_B (T,K)}{\partial F_0} + \frac{\nu \rho}{F(t)^{\beta}} \frac{\partial \Sigma_B (T,K)}{\partial \alpha} \right) \\
&= \boldsymbol{\Delta} + \frac{\nu \rho}{F(t)^{\beta}} \boldsymbol{\upsilon}
\end{aligned}$$

Therefore, this approach is particularly useful when we consider a delta hedging instead of a delta-vega hedging, since the new delta risk incorporates a part of the vega risk.

9.2.5 Factor models

Factor models are extensively used for modeling fixed income derivatives (Vasicek, CIR, HJM, etc.). They assume that interest rates are linked to some factors $X(t)$, which can be observable or not observable. For instance, the factor is directly the instantaneous interest rate $r(t)$ in Vasicek or CIR models. However, a one-factor model is generally limited and is not enough rich to fit the yield curve and the basic asset prices (caplets and swaptions). During a long time, academics have developed multi-factor models by considering explicit factors (level, slope, convexity, etc.). For instance, Brennan and Schwartz (1979) consider the short-term interest rate and the long-term interest rate, whereas Longstaff and Schwartz (1992) use the short-term interest rate and its volatility. Today, this type of approach is outdated and is replaced by a more pragmatic approach based on non-explicit factors.

9.2.5.1 Linear and quadratic Gaussian models

Let us assume that the instantaneous interest rate $r(t)$ is linked to the factors $X(t)$ under the risk-neutral probability $\mathbb{Q}$ as follows:

$$r(t) = \alpha(t) + \beta(t)^{\top} X(t) + X(t)^{\top} \Gamma(t) X(t)$$

where $\alpha(t)$ is a scalar, $\beta(t)$ is a $n \times 1$ vector and $\Gamma(t)$ is a $n \times n$ matrix. This parametrization encompasses different specific cases: one-factor model, affine model and quadratic model[71]. We also assume that the factors follow an Ornstein-Uhlenbeck process:

$$\mathrm{d}X(t) = (a(t) + B(t) X(t))\, \mathrm{d}t + \Sigma(t)\, \mathrm{d}W^{\mathbb{Q}}(t)$$

where $a(t)$ is a $n \times 1$ vector, $B(t)$ is a $n \times n$ matrix, $\Sigma(t)$ is a $n \times n$ matrix and $W^{\mathbb{Q}}(t)$ is a standard n-dimensional Brownian motion.

El Karoui *et al.* (1992a) show that there exists a family of $\hat{\alpha}(t,T)$, $\hat{\beta}(t,T)$ and $\hat{\Gamma}(t,T)$ such that the price of the zero-coupon bond $B(t,T)$ is given by:

$$B(t,T) = \exp\left(-\hat{\alpha}(t,T) - \hat{\beta}(t,T)^{\top} X(t) - X(t)^{\top} \hat{\Gamma}(t,T) X(t)\right)$$

[71] As shown by Filipović (2002), it is not necessary to use higher order because the only consistent polynomial term structure approaches are the affine and quadratic term structure models.

where $\hat{\alpha}(t,T)$, $\hat{\beta}(t,T)$ and $\hat{\Gamma}(t,T)$ solve a system of Riccati equations. If we assume that the matrix $\hat{\Gamma}(t,T)$ is symmetric, we obtain:[72]:

$$\begin{aligned}
\partial_t \hat{\alpha}(t,T) &= -\operatorname{tr}\left(\Sigma(t)\Sigma(t)^\top \hat{\Gamma}(t,T)\right) - \hat{\beta}(t,T)^\top a(t) + \\
&\quad \frac{1}{2}\hat{\beta}(t,T)^\top \Sigma(t)\Sigma(t)^\top \hat{\beta}(t,T) - \alpha(t) \\
\partial_t \hat{\beta}(t,T) &= -B(t)^\top \hat{\beta}(t,T) + 2\hat{\Gamma}(t,T)\Sigma(t)\Sigma(t)^\top \hat{\beta}(t,T) - \\
&\quad 2\hat{\Gamma}(t,T)a(t) - \beta(t) \\
\partial_t \hat{\Gamma}(t,T) &= 2\hat{\Gamma}(t,T)\Sigma(t)\Sigma(t)^\top \hat{\Gamma}(t,T) - \\
&\quad 2\hat{\Gamma}(t,T)B(t) - \Gamma(t)
\end{aligned}$$

with the boundary conditions $\hat{\alpha}(T,T) = \hat{\beta}(T,T) = \hat{\Gamma}(T,T) = \mathbf{0}$. We notice that the expression of the forward interest rate $F(t,T_1,T_2)$ is given by:

$$\begin{aligned}
F(t,T_1,T_2) &= -\frac{1}{T_2 - T_1}\ln\frac{B(t,T_2)}{B(t,T_1)} \\
&= \frac{\hat{\alpha}(t,T_2) - \hat{\alpha}(t,T_1) + \left(\hat{\beta}(t,T_2) - \hat{\beta}(t,T_2)\right)^\top X(t)}{T_2 - T_1} + \\
&\quad \frac{X(t)^\top \left(\hat{\Gamma}(t,T_2) - \hat{\Gamma}(t,T_1)\right)X(t)}{T_2 - T_1}
\end{aligned}$$

We deduce that the instantaneous forward rate is equal to:

$$f(t,T) = \alpha(t,T) + \beta(t,T)^\top X(t) + X(t)^\top \Gamma(t,T)X(t)$$

where $\alpha(t,T) = \partial_T \hat{\alpha}(t,T)$, $\beta(t,T) = \partial_T \hat{\beta}(t,T)$ and $\Gamma(t,T) = \partial_T \hat{\Gamma}(t,T)$. It follows that $\alpha(t) = \alpha(t,t) = \partial_t \hat{\alpha}(t,t)$, $\beta(t) = \beta(t,t) = \partial_t \hat{\beta}(t,t)$ and $\Gamma(t) = \Gamma(t,t) = \partial_t \hat{\Gamma}(t,t)$.

Let $V(t,X)$ be the price of the option, whose payoff is $f(x)$. It satisfies the following PDE:

$$\begin{aligned}
&\frac{1}{2}\operatorname{trace}\left(\Sigma(t)\partial_X^2 V(t,X)\Sigma(t)^\top\right) + (a(t) + B(t)X)\partial_X V(t,X) + \\
&\quad \partial_t V(t,X) - \left(\alpha(t) + \beta(t)^\top X + X^\top \Gamma(t)X\right)V(t,X) = 0
\end{aligned} \tag{9.38}$$

Once we have specified the functions $\alpha(t)$, $\beta(t)$, $\Gamma(t)$, $a(t)$, $B(t)$ and $\Sigma(t)$, we can then price the option by solving numerically the previous multidimensional PDE with the terminal condition $V(T,X) = f(X)$. Most of the time, the payoff is not specified with respect to the state variables X, but depends on the interest rate $r(t)$. In this case, we use the following transformation:

$$f(r) = f\left(\alpha(T) + \beta(T)^\top X + X^\top \Gamma(T)X\right)$$

Remark 112 *We can also calculate the price of the option by Monte Carlo methods. This approach is generally more efficient when the number of factors is larger than* 2.

[72] See Exercise 9.4.10 on page 601 and Ahn *et al.* (2002) for the derivation of the Riccati equations.

9.2.5.2 Dynamics of risk factors under the forward probability measure

We have:

$$\frac{\mathrm{d}B(t,T)}{B(t,T)} = r(t)\,\mathrm{d}t - \left(2\hat{\Gamma}(t,T)X(t) + \hat{\beta}(t,T)\right)^{\top}\Sigma(t)\,\mathrm{d}W^{\mathbb{Q}}(t)$$

We deduce that:

$$W^{\mathbb{Q}^\star(T)}(t) = W^{\mathbb{Q}}(t) + \int_0^t \Sigma(s)^{\top}\left(2\hat{\Gamma}(s,T)X(s) + \hat{\beta}(s,T)\right)\mathrm{d}s$$

defines a Brownian motion under $\mathbb{Q}^\star(T)$. It follows that:

$$\mathrm{d}X(t) = \left(\tilde{a}(t) + \tilde{B}(t)X(t)\right)\mathrm{d}t + \Sigma(t)\,\mathrm{d}W^{\mathbb{Q}^\star(T)}(t)$$

where:

$$\tilde{a}(t) = a(t) - \Sigma(t)\Sigma(t)^{\top}\hat{\beta}(t,T)$$

and:

$$\tilde{B}(t) = B(t) - 2\Sigma(t)\Sigma(t)^{\top}\hat{\Gamma}(t,T)$$

We conclude that $X(t)$ is Gaussian under any forward probability measure $\mathbb{Q}^\star(T)$:

$$X(t) \sim \mathcal{N}(m(0,t), V(0,t))$$

El Karoui *et al.* (1992a) show that the conditional mean and variance satisfies the following forward differential equations:

$$\left\{\begin{array}{lcl} \partial_T m(t,T) & = & a(T) + B(T)m(t,T) - 2V(t,T)\Gamma(T)m(t,T) - \\ & & V(t,T)\beta(T) \\ \partial_T V(t,T) & = & V(t,T)B(T)^{\top} + B(T)V(t,T) - 2V(t,T)\Gamma(T)V(t,T) + \\ & & \Sigma(T)\Sigma(T)^{\top} \end{array}\right.$$

If t is equal to zero, the initial conditions are $m(0,0) = X(0) = \mathbf{0}$ and $V(0,0) = \mathbf{0}$. If $t \neq 0$, we proceed in two steps: first, we calculate numerically the solutions $m(0,t)$ and $V(0,t)$, and second, we initialize the system with $m(t,t) = m(0,t)$ and $V(t,t) = V(0,t)$.

Remark 113 *In fact, the previous forward differential equations are not obtained under the traditional forward probability measure $\mathbb{Q}^\star(T)$, but under the probability measure $\mathbb{Q}^\star(t,T)$ defined by the following Radon-Nykodin derivative:*

$$\frac{\mathrm{d}\mathbb{Q}^\star(t,T)}{\mathrm{d}\mathbb{P}} = e^{-\int_0^T r(s)\,\mathrm{d}s}e^{\int_t^T f(t,s)\,\mathrm{d}s}$$

The reason is that we would like to price at time t any caplet with maturity T. Therefore, this is the maturity T and not the filtration $\mathcal{F}_t$ that moves.

9.2.5.3 Pricing caplets and swaptions

We reiterate that the formula of the Libor rate $L(t,T_{i-1},T_i)$ at time t between the dates T_{i-1} and T_i is:

$$L(t,T_{i-1},T_i) = \frac{1}{T_i - T_{i-1}}\left(\frac{B(t,T_{i-1})}{B(t,T_i)} - 1\right)$$

It follows that the price of the caplet is given by:

$$\text{Caplet} = B(0,t)\,\mathbb{E}^{\mathbb{Q}^\star(t)}\left[\left(B(t,T_{i-1}) - (1 + (T_i - T_{i-1})K)B(t,T_i)\right)^+\right]$$

where $\mathbb{Q}^\star(t)$ is the forward probability measure. We can then calculate the price using two approaches:

1. we can solve the partial differential equation;
2. we can calculate the mathematical expectation using numerical integration.

In the first approach, we consider the PDE (9.38) with the following payoff:

$$f(X) = \max(0, g(X))$$

where:

$$\begin{aligned} g(X) &= \exp\left(-\hat{\alpha}(t, T_{i-1}) - \hat{\beta}(t, T_{i-1})^\top X - X^\top \hat{\Gamma}(t, T_{i-1}) X\right) - \\ & \quad (1 + \delta_{i-1} K) \exp\left(-\hat{\alpha}(t, T_i) - \hat{\beta}(t, T_i)^\top X - X^\top \hat{\Gamma}(t, T_i) X\right) \end{aligned}$$

In the second approach, we have $X(t) \sim \mathcal{N}(m(0,t), V(0,t))$ under the forward probability $\mathbb{Q}^\star(t)$. We deduce that:

$$\text{Caplet}(t, T_{i-1}, T_i) = B(0,t) \int f(x)\, \phi_n(x; m(0,t), V(0,t))\, \mathrm{d}x$$

This integral can be computed numerically using Gauss-Legendre quadrature methods.

For the swaption, the payoff is:

$$\begin{aligned} f(X) &= (\mathrm{Sw}(T_0) - K)^+ \sum_{i=1}^n (T_i - T_{i-1}) B(T_0, T_i) \\ &= \left(B(T_0, T_0) - B(T_0, T_n) - K \sum_{i=1}^n (T_i - T_{i-1}) B(T_0, T_i)\right)^+ \\ &= \max(0, g(X)) \end{aligned}$$

where:

$$\begin{aligned} g(X) &= \exp\left(-\hat{\alpha}(T_0, T_0) - \hat{\beta}(T_0, T_0)^\top X - X^\top \hat{\Gamma}(T_0, T_0) X\right) - \\ & \quad \exp\left(-\hat{\alpha}(T_0, T_n) - \hat{\beta}(T_0, T_n)^\top X - X^\top \hat{\Gamma}(T_0, T_n) X\right) - \\ & \quad K \sum_{i=1}^n \delta_{i-1} \exp\left(-\hat{\alpha}(T_0, T_i) - \hat{\beta}(T_0, T_i)^\top X - X^\top \hat{\Gamma}(T_0, T_i) X\right) \end{aligned}$$

As previously, we can price the swaption by solving the PDE with the payoff $f(X)$ or by calculating the following integral:

$$\text{Swaption} = B(0, T_0) \int f(x)\, \phi_n(x; m(0, T_0), V(0, T_0))\, \mathrm{d}x$$

9.2.5.4 Calibration and practice of factor models

The calibration of the model consists in fitting the functions $\alpha(t)$, $\beta(t)$, $\Gamma(t)$, $a(t)$, $B(t)$ and $\Sigma(t)$. Generally, professionals assume that $a(t) = 0$ and $B(t) = \mathbf{0}$. Indeed, if we consider the following transformation:

$$\tilde{X}(t) = e^{-\int_0^t B(s)\,\mathrm{d}s} X(t) - \int_0^t a(s)\, e^{-\int_0^s B(u)\,\mathrm{d}u}\, \mathrm{d}s$$

we obtain:

$$\begin{array}{rcl} \mathrm{d}\tilde{X}(t) & = & e^{-\int_0^t B(s)\,\mathrm{d}s}\Sigma(t)\ \mathrm{d}W^{\mathbb{Q}}(t) \\ & = & \tilde{\Sigma}(t)\ \mathrm{d}W(t) \end{array}$$

Without loss of generality, we can then set $\mathrm{d}X(t) = \Sigma(t)\ \mathrm{d}W^{\mathbb{Q}}(t)$, and the Riccati equations are simplified as follows:

$$\left\{ \begin{array}{l} \partial_t\hat{\alpha}(t,T) = -\operatorname{tr}\left(\Sigma(t)\Sigma(t)^\top \hat{\Gamma}(t,T)\right) + \frac{1}{2}\hat{\beta}(t,T)^\top \Sigma(t)\Sigma(t)^\top \hat{\beta}(t,T) - \alpha(t) \\ \partial_t\hat{\beta}(t,T) = 2\hat{\Gamma}(t,T)^\top \Sigma(t)\Sigma(t)^\top \hat{\beta}(t,T) - \beta(t) \\ \partial_t\hat{\Gamma}(t,T) = 2\hat{\Gamma}(t,T)^\top \Sigma(t)\Sigma(t)^\top \hat{\Gamma}(t,T) - \Gamma(t) \end{array} \right.$$

If we consider an affine model, we retrieve the formula of Duffie and Huang (1996):

$$B(t,T) = \exp\left(-\hat{\alpha}(t,T) - \hat{\beta}(t,T)^\top X(t)\right)$$

where[73]:

$$\left\{ \begin{array}{l} \partial_t\hat{\alpha}(t,T) = \frac{1}{2}\hat{\beta}(t,T)^\top \Sigma(t)\Sigma(t)^\top \hat{\beta}(t,T) - \alpha(t) \\ \partial_t\hat{\beta}(t,T) = -\beta(t) \end{array} \right.$$

First, we must fit the initial yield curve, which is noted $B(0,T)$. If we assume that $X(0) = \mathbf{0}$, we obtain:

$$\hat{\alpha}(t,T) = -\ln\frac{B(0,T)}{B(0,t)}$$

We notice that the computation of $\hat{\alpha}(t,T)$ allows to define $\alpha(t)$:

$$\alpha(t) = -\operatorname{tr}\left(\Sigma(t)\Sigma(t)^\top \hat{\Gamma}(t,T)\right) + \frac{1}{2}\hat{\beta}(t,T)^\top \Sigma(t)\Sigma(t)^\top \hat{\beta}(t,T) - \partial_t\hat{\alpha}(t,T)$$

because $\partial_t\hat{\alpha}(t,T)$ can be calculated using finite differences. Therefore, the problem dimension is reduced and the calibration depends on $\beta(t)$, $\Gamma(t)$ and $\Sigma(t)$. In order to calibrate these functions, we need to fit other products like caplets and swaptions. We have shown that these products can be priced using numerical integration. Therefore, the calibration of $\beta(t)$, $\Gamma(t)$ and $\Sigma(t)$ can be done without solving the PDE, which is time-consuming.

Let us now see what type of volatility smile is generated by quadratic and linear Gaussian factor models. We assume that the functions $\beta(t)$, $\Gamma(t)$ and $\Sigma(t)$ are piecewise constant functions, whose knots are $t_1^\star = 0.5$ and $t_2^\star = 0.5$. For instance, the function $\beta(t)$ is given by:

$$\beta(t) = \left\{ \begin{array}{ll} \beta_1 & \text{if } t \in [0, 0.5[\\ \beta_2 & \text{if } t \in [0.5, 1[\\ \beta_3 & \text{if } t \in [1, \infty) \end{array} \right.$$

where β_1, β_2 and β_3 are three scalars. Therefore, $\beta(t)$ is defined by the vector $(\beta_1, \beta_2, \beta_3)$. In a similar way, $\Gamma(t)$ and $\Sigma(t)$ are defined by the vectors $(\Gamma_1, \Gamma_2, \Gamma_3)$ and $(\Sigma_1, \Sigma_2, \Sigma_3)$. We

[73]In the general case $a(t) \neq 0$ and $B(t) \neq \mathbf{0}$, we have:

$$\left\{ \begin{array}{l} \partial_t\hat{\alpha}(t,T) = -\hat{\beta}(t,T)^\top a(t) + \frac{1}{2}\hat{\beta}(t,T)^\top \Sigma(t)\Sigma(t)^\top \hat{\beta}(t,T) - \alpha(t) \\ \partial_t\hat{\beta}(t,T) = -B(t)^\top \hat{\beta}(t,T) - \beta(t) \end{array} \right.$$

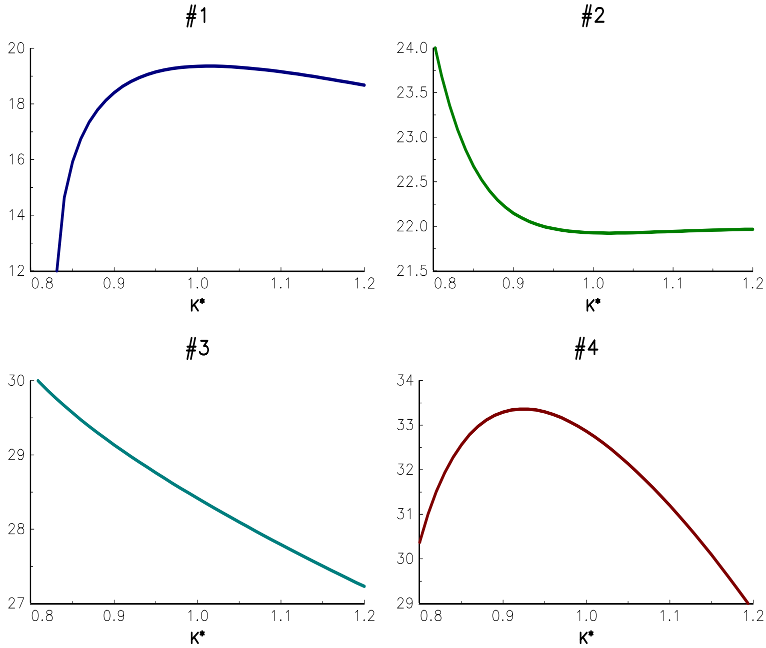

FIGURE 9.43: Volatility smiles generated by the quadratic Gaussian model

consider 4 parameter sets[74]:

Set	$(\beta_1, \beta_2, \beta_3)$	$(\Gamma_1, \Gamma_2, \Gamma_3)$	$(\Sigma_1, \Sigma_2, \Sigma_3)$
#1	$(0.3, 0.4, 0.5)$	$(-20, -10, 10)$	$(3, 3.2, 3.5)$
#2	$(0.3, 0.4, 0.5)$	$(20, 15, 10)$	$(3, 3.2, 3.5)$
#3	$(0.3, 0.4, 0.5)$	$(5, 5, 5)$	$(4, 3.5, 3)$
#4	$(0.3, 0.4, 0.5)$	$(-10, -10, -10)$	$(6, 5, 4)$

We also assume that the yield curve is flat and is equal to 5%. We consider the pricing of a caplet with $T_0 = T_1 - 2/365$, $T_1 = 0.5$ and $T_2 = 1.5$ for different strikes $K_i = K_i^\star \cdot \mathrm{Sw}(T_0)$ where $K_i^\star \in [0.8, 1.2]$. In Figure 9.43, we have reported the implied Black volatilities (in %) generated by the quadratic Gaussian model with the four parameter sets. We notice that the quadratic Gaussian model can generate different forms of volatility smiles. Since it is a little more flexible than the linear Gaussian model, we can obtained U-shaped and even reverse U-shaped volatility smiles.

9.3 Other model risk topics

In this section, we consider other risks than the volatility risk. In particular, we study the impact of dividends on option premia, the pricing of basket options and the liquidity risk.

[74]The volatilities $(\Sigma_1, \Sigma_2, \Sigma_3)$ are normalized by the factor $\sqrt{260} \times 10^{-4}$.

9.3.1 Dividend risk

9.3.1.1 Understanding the impact of dividends on option prices

Let us consider that the underlying asset pays a continuous dividend yield d during the life of the option. We have seen that the risk-neutral dynamics become:

$$\mathrm{d}S(t) = (r-d)\,S(t)\,\mathrm{d}t + \sigma S(t)\,\mathrm{d}W(t)$$

We deduce that the Black-Scholes formula is equal to:

$$\mathcal{C}_0 = S_0 e^{-dT}\Phi(d_1) - Ke^{-rT}\Phi(d_2)$$

where:

$$\begin{aligned} d_1 &= \frac{1}{\sigma\sqrt{T}}\left(\ln\frac{S_0}{K} + (r-d)\,T\right) + \frac{1}{2}\sigma\sqrt{T} \\ d_2 &= d_1 - \sigma\sqrt{T} \end{aligned}$$

We can also show that $\lim_{d\to\infty}\mathcal{C}_0 = 0$. In Figure 9.44, we report the price of the option when $K = 100$, $\sigma = 20\%$, $r = 5\%$ and $T = 0.5$. We consider different level of the dividend yield d. We notice that the call price is a decreasing function of the continuous dividend. If we consider put options instead of call options, the function becomes increasing.

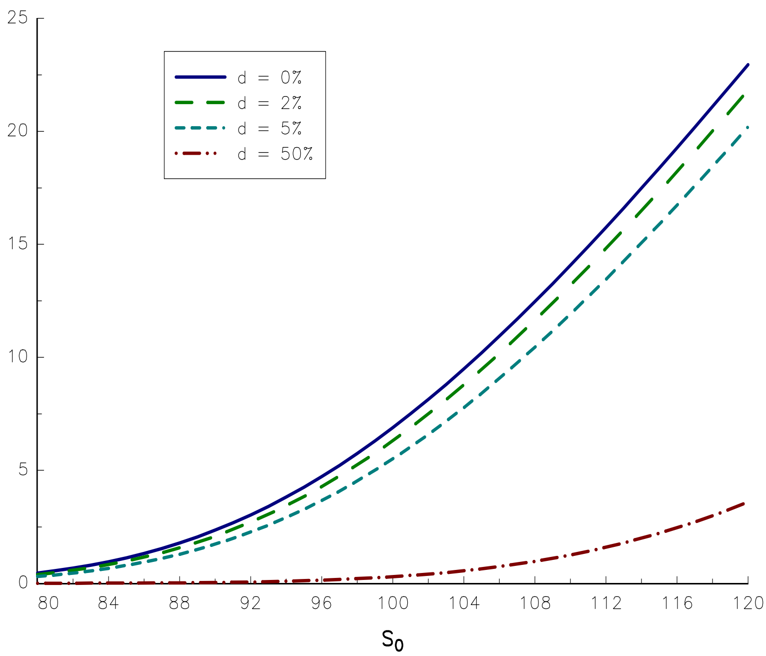

FIGURE 9.44: Impact of dividends on the call option price

We generally explain the impact of dividends because stock prices generally fall by the amount of the dividend on the ex-dividend date. Let $S(t)$ denote the value of the underlying asset at time t and D the discrete dividend paid at time t_D. We have:

$$S(t_D) = S\left(t_D^-\right) - D$$

The impact on the payoff is not the unique effect. Indeed, we recall that the option price is the cost of the replication portfolio. When the trader hedges the call option, he has a long exposure on the asset since the delta is positive. This implies that he receives the dividend of the asset. Therefore, the hedging cost of the call option is reduced. In the case of a put option, the trader has a short exposure and has to pay the dividend. As a result, the hedging cost of the put option is increased.

9.3.1.2 Models of discrete dividends

We denote by $S(t)$ the market price and $Y(t)$ an additional process that is assumed to be a geometric Brownian motion:

$$\mathrm{d}Y(t) = rY(t)\,\mathrm{d}t + \sigma Y(t)\,\mathrm{d}W^{\mathbb{Q}}(t)$$

Following Frishling (2002), there are three main approaches to take into account discrete dividends. In the first approach, $Y(t)$ is the capital price process excluding the dividends and the market price $S(t)$ is equal to the sum of the capital price and the discounted value of future dividends:

$$S(t) = Y(t) + \sum_{t_k \in [t,T]} D(t_k)\, e^{-r(t_k - t)}$$

To price European options, we then replace the price S_0 by the adjusted price $Y_0 = S_0 - \sum_{t_k \leq T} D(t_k)\, e^{-rt_k}$. In the second approach, we define $D(t)$ as the sum of capitalized dividends paid until time t:

$$D(t) = \sum \mathbb{1}\{t_k < t\} \cdot D(t_k)\, e^{r(t-t_k)}$$

The market price $S(t)$ is equal to the difference between the cum-dividend price $Y(t)$ and the capitalized dividends (Haug *et al.*, 2003):

$$S(t) = Y(t) - D(t)$$

We deduce that:

$$\begin{aligned} (S(T) - K)^+ &= (Y(T) - D(T) - K)^+ \\ &= (Y(T) - (K + D(T)))^+ \\ &= (Y(T) - K')^+ \end{aligned}$$

In the case of European options, we replace the strike K by the adjusted strike $K' = K + \sum_{t_k \leq T} D(t_k)\, e^{r(T-t_k)}$. The last approach considers the market price process as a discontinuous process:

$$\begin{cases} \mathrm{d}S(t) = rS(t)\,\mathrm{d}t + \sigma S(t)\,\mathrm{d}W^{\mathbb{Q}}(t) & \text{if } t_{k-1} < t < t_k \\ S(t) = S\left(t_k^-\right) - D(t_k) & \text{if } t = t_k \end{cases}$$

Therefore, we calculate the option price using finite differences or Monte Carlo simulations.

Remark 114 *The three models can be used to price exotic options, and not only European options. Generally, we do not have closed-form formulas and we calculate the price with numerical methods. For that, we have to define the risk-neural dynamics of $S(t)$. For instance, we have for the second model*[75]*:*

$$\mathrm{d}S(t) = \left(rS(t) - \sum \mathbb{1}\{t_k = t\} \cdot D(t_k)\, e^{r(t-t_k)}\right)\mathrm{d}t + \sigma\left(S(t) + D(t)\right)\mathrm{d}W^{\mathbb{Q}}(t)$$

[75] We notice that:

$$\mathrm{d}D(t) = \left(rD(t) + \sum \mathbb{1}\{t_k = t\} \cdot D(t_k)\, e^{r(t-t_k)}\right)\mathrm{d}t$$

Example 97 *We assume that $S_0 = 100$, $K = 100$, $\sigma = 30\%$, $T = 1$, $r = 5\%$ and $b = 5\%$. A dividend $D(t_1)$ will be paid at time $t_1 = 0.5$.*

Table 9.13 compares option prices when we use the three previous models. When $D(t_1)$ is equal to zero, the three models give the same price: the call option is equal to 14.23 whereas the put option is equal to 9.35. When the asset pays a dividend, the three models give different option prices. For instance, if the dividend is equal to 3, the call option is equal to 12.46 for Model #1, 12.81 for Model #2 and 12.69 for Model #3. We notice that the three models produce very different option prices[76]. Therefore, the choice of the dividend model has a big impact on the pricing of derivatives.

TABLE 9.13: Impact of the dividend on the option price

	Call			Put		
$D(t_1)$	(#1)	(#2)	(#3)	(#1)	(#2)	(#3)
0	14.23	14.23	14.23	9.35	9.35	9.35
3	12.46	12.81	12.69	10.51	10.86	10.64
5	11.34	11.92	11.69	11.34	11.92	11.59
10	8.78	9.93	9.42	13.66	14.80	14.20

Remark 115 *The previous models assume that dividends are not random at the inception date of the option. In practice, only the first dividend can be known if it has been announced before the inception date. This implies that dividends are generally unknown. Some authors have proposed option models with stochastic dividends, but they are not used by professionals. Most of the time, they use a very basic model. For instance, the Gordon growth model assumes that dividends increase at a constant rate g:*

$$D(t_k) = (1+g)^{(t_k - t_1)} D(t_1)$$

The parameter g can be calibrated in order to match the forward prices.

9.3.2 Correlation risk

Until now, we have studied the pricing and hedging of options that are based on one underlying asset. Banks have also developed derivatives with several underlying assets. In this case, the option price is sensitive to the covariance risk, which may be split between volatility risk and correlation risk. Here, we face two issues: the determination of implied correlations, and the hedging of the correlation risk.

9.3.2.1 The two-asset case

Pricing of basket options We consider the example of a basket option on two assets. Let $S_i(t)$ be the price process of asset i at time t. According to the Black-Scholes model, we have:

$$\begin{cases} \mathrm{d}S_1(t) = b_1 S_1(t)\,\mathrm{d}t + \sigma_1 S_1(t)\,\mathrm{d}W_1^{\mathbb{Q}}(t) \\ \mathrm{d}S_2(t) = b_2 S_2(t)\,\mathrm{d}t + \sigma_2 S_2(t)\,\mathrm{d}W_2^{\mathbb{Q}}(t) \end{cases}$$

where b_i and σ_i are the cost-of-carry and the volatility of asset i. Under the risk-neutral probability measure $\mathbb{Q}$, $W_1^{\mathbb{Q}}(t)$ and $W_2^{\mathbb{Q}}(t)$ are two correlated Brownian motions:

$$\mathbb{E}\left[W_1^{\mathbb{Q}}(t)\,W_2^{\mathbb{Q}}(t)\right] = \rho\, t$$

[76] We also notice that the price given by the third model is between the two prices calculated with the first and second models.

The option price associated to the payoff $(\alpha_1 S_1(T) + \alpha_2 S_2(T) - K)^+$ is the solution of the two-dimensional PDE:

$$\begin{aligned} \frac{1}{2}\sigma_1^2 S_1^2 \partial_{S_1}^2 \mathcal{C} + \frac{1}{2}\sigma_2^2 S_2^2 \partial_{S_2}^2 \mathcal{C} + \rho\sigma_1\sigma_2 S_1 S_2 \partial_{S_1,S_2}^2 \mathcal{C} + & \\ b_1 S_1 \partial_{S_1} \mathcal{C} + b_2 S_2 \partial_{S_2} \mathcal{C} + \partial_t \mathcal{C} - r\mathcal{C} &= 0 \end{aligned}$$

with the terminal condition:

$$\mathcal{C}(T, S_1, S_2) = (\alpha_1 S_1 + \alpha_2 S_2 - K)^+$$

Using the Feynman-Kac representation theorem, we have:

$$\mathcal{C}_0 = \mathbb{E}^{\mathbb{Q}}\left[e^{-\int_0^T r\,\mathrm{d}t}\left(\alpha_1 S_1(T) + \alpha_2 S_2(T) - K\right)^+\right]$$

The value $\mathcal{C}_0$ can be calculated using numerical integration techniques such as Gauss-Legendre or Gauss-Hermite quadrature methods. In some cases, the two-dimensional problem can be reduced to one-dimensional integration. For instance, if $\alpha_1 < 0$, $\alpha_2 > 0$ and $K > 0$, we obtain[77]:

$$\mathcal{C}_0 = \int_{\mathbb{R}} \mathrm{BS}\left(S^\star(x), K^\star(x), \sigma^\star, T, b^\star, r\right)\phi(x)\,\mathrm{d}x$$

where $S^\star(x) = \alpha_2 S_2(0)\, e^{\rho\sigma_2\sqrt{T}x}$, $K^\star(x) = K - \alpha_1 S_1(0)\, e^{\left(b_1 - \frac{1}{2}\sigma_1^2\right)T + \sigma_1\sqrt{T}x}$, $\sigma^\star = \sigma_2\sqrt{1-\rho^2}$ and $b^\star = b_2 - \frac{1}{2}\rho^2\sigma_2^2$.

Example 98 *We assume that* $S_1(0) = S_2(0) = 100$*,* $\sigma_1 = \sigma_2 = 20\%$*,* $b_1 = 10\%$*,* $b_2 = 0$ *and* $r = 5\%$*. We calculate the price of a basket option, whose maturity* T *is equal to one year. For the other characteristics* (α_1, α_2, K)*, we consider different set of parameters:* $(1, -1, 1)$*,* $(1, -1, 5)$*,* $(0.5, 0.5, 100)$*,* $(0.5, 0.5, 110)$ *and* $(0.1, 0.1, -5)$*.*

TABLE 9.14: Impact of the correlation on the basket option price

	α_1	1.0	1.0	0.5	0.5	0.1
	α_2	−1.0	−1.0	0.5	0.5	0.1
	K	1	5	100	110	−5
ρ	−0.90	20.41	18.23	5.39	0.66	24.78
	−0.75	19.81	17.62	6.06	1.35	24.78
	−0.50	18.76	16.55	6.97	2.31	24.78
	−0.25	17.61	15.37	7.73	3.12	24.78
	0.00	16.35	14.08	8.39	3.83	24.78
	0.25	14.94	12.61	8.99	4.46	24.78
	0.50	13.30	10.88	9.54	5.05	24.78
	0.75	11.29	8.66	10.05	5.59	24.78
	0.90	9.78	6.81	10.34	5.90	24.78

Using Gauss-Legendre quadratures, we obtain the prices of the basket option given in Table 9.14. We notice that the price can be an increasing, decreasing or independent function of the correlation parameter ρ.

[77] See Exercise 9.4.11 on page 602.

Remark 116 *We can extend the previous framework to other payoff functions. The PDE is the same, only the terminal condition changes:*

$$\mathcal{C}\left(T, S_1, S_2\right) = f\left(S_1\left(T\right), S_2\left(T\right)\right)$$

where $f\left(S_1\left(T\right), S_2\left(T\right)\right)$ is the payoff function.

Cega sensitivity The correlation risk studies the impact of the parameter ρ on the option price $\mathcal{C}_0$. For instance, Rapuch and Roncalli (2004) show that the price of the spread option, whose payoff is $\left(S_1\left(T\right) - S_2\left(T\right) - K\right)^+$, is a decreasing function of the correlation parameter ρ. They also extend this result to an arbitrary European payoff $f\left(S_1\left(T\right), S_2\left(T\right)\right)$. In particular, they demonstrate that, if the cross-derivative $\partial^2_{1,2} f$ is a negative (resp. positive) measure, then the option price is decreasing (resp. increasing) with respect to ρ. For instance, the payoff function of the call option on the maximum of two assets is defined as $f\left(S_1, S_2\right) = \left(\max\left(S_1, S_2\right) - K\right)^+$. Since $\partial^2_{1,2} f\left(S_1, S_2\right) = -\mathbb{1}\left\{S_1 = S_2, S_1 > K\right\}$ is a negative measure, the option price decreases with respect to ρ. In the case of a Best-of call/call option, the payoff function is $f\left(S_1, S_2\right) = \max\left(\left(S_1 - K_1\right)^+, \left(S_2 - K_2\right)^+\right)$ and we have:

$$\partial^2_{1,2} f\left(S_1, S_2\right) = -\mathbb{1}\left\{S_2 - K_2 - S_1 + K_1 = 0, S_1 > K_1, S_2 > K_2\right\}$$

We have the same behavior than the Max option. For the Min option, we remark that $\min\left(S_1, S_2\right) = S_1 + S_2 - \max\left(S_1, S_2\right)$. So, the option price is an increasing function of ρ. Other results could be found in Table 9.15.

TABLE 9.15: Relationship between the basket option price and the correlation parameter ρ

Option type	Payoff	Increasing	Decreasing
Spread	$\left(S_2 - S_1 - K\right)^+$		✓
Basket	$\left(\alpha_1 S_1 + \alpha_2 S_2 - K\right)^+$	$\alpha_1\alpha_2 > 0$	$\alpha_1\alpha_2 < 0$
Max	$\left(\max\left(S_1, S_2\right) - K\right)^+$		✓
Min	$\left(\min\left(S_1, S_2\right) - K\right)^+$	✓	
Best-of call/call	$\max\left(\left(S_1 - K_1\right)^+, \left(S_2 - K_2\right)^+\right)$		✓
Best-of put/put	$\max\left(\left(K_1 - S_1\right)^+, \left(K_2 - S_2\right)^+\right)$		✓
Worst-of call/call	$\min\left(\left(S_1 - K_1\right)^+, \left(S_2 - K_2\right)^+\right)$	✓	
Worst-of put/put	$\min\left(\left(K_1 - S_1\right)^+, \left(K_2 - S_2\right)^+\right)$	✓	

The sensitivity of the option price with respect to the correlation parameter ρ is called the cega:

$$\boldsymbol{c} = \frac{\partial\,\mathcal{C}_0}{\partial\rho}$$

Generally, it is difficult to fix a particular value of ρ, because a correlation is not a stable parameter. Moreover, the value of ρ used for pricing the option must reflect the risk-neutral distribution. Then, it is not obvious that the '*risk-neutral correlation*' is equal to the '*historical correlation*'. Most of the time, we only have an idea about the correlation range $\rho \in \left[\rho^-, \rho^+\right]$. The previous analysis leads us to define the lower and upper bounds of the option price when the cega is either positive or negative. We have:

$$\mathcal{C}_0 \in \left\{\begin{array}{ll} \left[\mathcal{C}_0\left(\rho^-\right), \mathcal{C}_0\left(\rho^+\right)\right] & \text{if } \boldsymbol{c} \geq 0 \\ \left[\mathcal{C}_0\left(\rho^+\right), \mathcal{C}_0\left(\rho^-\right)\right] & \text{if } \boldsymbol{c} \leq 0 \end{array}\right.$$

We can define the conservative price by taking the maximum between $\mathcal{C}_0\left(\rho^-\right)$ and $\mathcal{C}_0\left(\rho^+\right)$.

Remark 117 *In the case where $\rho^- = -1$ and $\rho^+ = 1$, the bounds satisfy the one-dimensional PDE:*

$$\begin{cases} \frac{1}{2}\sigma_1^2 S^2 \partial_S^2 \boldsymbol{\mathcal{C}}(t,S) + b_1 S \partial_S \boldsymbol{\mathcal{C}}(t,S) + \partial_t \boldsymbol{\mathcal{C}}(t,S) - r\boldsymbol{\mathcal{C}}(t,S) = 0 \\ \boldsymbol{\mathcal{C}}(T,S) = f(S, g(S)) \end{cases}$$

where:

$$g(S) = S_2(0)\left(\frac{S}{S_1(0)}\right)^{\pm\sigma_2/\sigma_1} \exp\left(\left(b_2 - \frac{1}{2}\sigma_2^2 \pm \left(\frac{1}{2}\sigma_1\sigma_2 - \frac{\sigma_2}{\sigma_1}b_1\right)\right)T\right)$$

The implied correlation Like the implied volatility, the implied correlation is the value we put into the Black-Scholes formula to get the true market price. At first sight, the concept of implied correlation seems to be straightforward. For instance, let us consider composite options, whose payoff is defined by $(S_1(T) - kS_2(T))^+$. It is a special case of the general payoff $(\alpha_1 S_1(T) + \alpha_2 S_2(T) - K)^+$ where $\alpha_1 = 1$, $\alpha_2 = k$ and $K = 0$. The parameters are those given in Example 98. The values $(k, \boldsymbol{\mathcal{C}}_0)$ taken by the relative strike k and the market price $\boldsymbol{\mathcal{C}}_0$ are respectively equal to $(0.10, 95.61)$, $(0.20, 86.10)$, $(0.30, 76.59)$, $(0.40, 67.08)$, $(0.50, 57.57)$, $(0.60, 48.06)$, $(0.70, 38.62)$, $(0.80, 29.46)$, $(0.90, 21.12)$, $(1.00, 14.32)$, $(1.10, 9.45)$ and $(1.20, 6.30)$. Using these 12 market prices, we deduce the correlation smile with respect to k in Figure 9.45. We now consider the option, whose payoff is $\left(\frac{1}{2}S_1(T) + \frac{1}{2}S_2(T) - 100\right)^+$. Which correlation should be used? There is no obvious answer. Indeed, we notice that a correlation smile is always associated to a given payoff. This is why it is generally not possible to use a correlation smile deduced from one payoff function to price the option with another payoff function. Contrary to volatility, the concept of implied correlation makes sense, but not the concept of correlation smile.

Riding on the smiles Until now, we have assumed that the volatilities of the two assets are given. In practice, the two volatilities are unknown and must be deduced from the volatility smiles $\Sigma_1(K_1, T)$ and $\Sigma_2(K_2, T)$ of the two assets. The difficulty is then to find the corresponding strikes K_1 and K_2. In the case of the general payoff $(\alpha_1 S_1(T) + \alpha_2 S_2(T) - K)^+$, we have:

$$\begin{cases} (\alpha_1 = 1, \alpha_2 = 0, K \geq 0) \Rightarrow K_1 = K \\ (\alpha_1 = -1, \alpha_2 = 0, K \leq 0) \Rightarrow K_1 = -K \end{cases}$$

and:

$$\begin{cases} (\alpha_1 = 0, \alpha_2 = 1, K \geq 0) \Rightarrow K_2 = K \\ (\alpha_1 = 0, \alpha_2 = -1, K \leq 0) \Rightarrow K_2 = -K \end{cases}$$

The payoff of the spread option can be written as follows:

$$\begin{aligned} (S_1(T) - S_2(T) - K)^+ &= ((S_1(T) - K_1) + (K_2 - S_2(T)))^+ \\ &\leq \underbrace{(S_1(T) - K_1)^+}_{\text{Call}} + \underbrace{(K_2 - S_2(T))^+}_{\text{Put}} \end{aligned}$$

where $K_1 = K_2 + K$. Therefore, the price of the spread option can be bounded above by a call price on S_1 plus a put price on S_2. However, the implicit strikes can take different values. Let us assume that $S_1(0) = S_2(0) = 100$ and $K = 4$. Below, we give five pairs

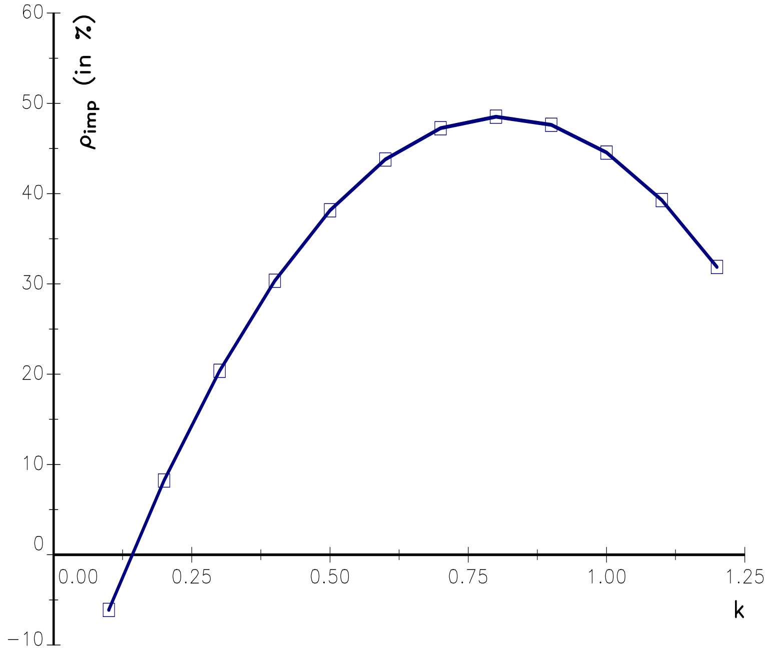

FIGURE 9.45: Correlation smile

(K_1, K_2) and the associated implied volatilities $(\Sigma_1(K_1, T), \Sigma_2(K_2, T))$:

Pair	#1	#2	#3	#4	#5
K_1	104	103	102	101	100
K_2	100	99	98	97	96
$\Sigma_1(K_1, T)$	16%	17%	18%	19%	20%
$\Sigma_2(K_2, T)$	20%	22%	24%	26%	28%
$\mathcal{C}_0$	10.77	11.37	11.99	12.61	13.24

We also compute the price of the spread option[78] and report it in the last row of the above table. We notice that the price varies from 10.77 to 13.24, even if we use the same correlation parameter. We face here an issue, because this simple example shows that two-dimensional option pricing is not just an extension of one-dimensional option pricing, and the concept of implied volatility becomes blurred.

9.3.2.2 The multi-asset case

How to define a conservative price? In the multivariate case, the PDE becomes:

$$\begin{aligned}\frac{1}{2}\sum_{i=1}^{n}\sigma_i^2 S_i^2 \partial^2_{S_i}\mathcal{C} + \sum_{i<j}^{n}\rho_{i,j}\sigma_i\sigma_j S_i S_j \partial^2_{S_i,S_j}\mathcal{C} + & \\ \sum_{i=1}^{n} b_i S_i \partial_i \mathcal{C} + \partial_t \mathcal{C} - r\mathcal{C} &= 0\end{aligned}$$

with the terminal value:

$$\mathcal{C}(T, S_1, \ldots, S_n) = f(S_1(T), \ldots, S_n(T))$$

[78] The parameters are $b_1 = 10\%$, $b_2 = 0\%$, $r = 5\%$, $\rho = 50\%$ and $T = 1$.

Here, $\rho_{i,j}$ is the correlation between the Brownian motions of S_i and S_j. Most of the time, the trader uses the same value ρ for all asset correlations $\rho_{i,j}$.

Rapuch and Roncalli (2004) show that the price is increasing (resp. decreasing) with respect to ρ if $\sum_{i<j}^{n} \sigma_i \sigma_j \partial^2_{S_i,S_j} f$ is a positive (resp. negative) measure. Let us consider the payoff function $f(S_1, S_{2,} S_3) = (S_1 + S_2 - S_3 - K)^+$, we have:

$$\sum_{i<j}^{n} \sigma_i \sigma_j \partial^2_{S_i,S_j} f = (\sigma_1\sigma_2 - \sigma_1\sigma_3 - \sigma_2\sigma_3) \cdot \mathbb{1}\{S_1 + S_2 - S_3 - K = 0\}$$

Hence, if $\sigma_1\sigma_2 - \sigma_1\sigma_3 - \sigma_2\sigma_3 > 0$, the price increases with respect to ρ, and if $\sigma_1\sigma_2 - \sigma_1\sigma_3 - \sigma_2\sigma_3 < 0$, the price decreases with respect to ρ. As a result, it is more difficult to define conservative prices for multi-asset options.

Issues with constant correlation matrices We consider a basket of n stocks. The basket volatility is given by:

$$\sigma_B = \sqrt{\sum_{i=1}^{n} w_i^2 \sigma_i^2 + 2 \sum_{i>j}^{n} \rho_{i,j} w_i w_j \sigma_i \sigma_j}$$

where w_i is the weight of asset i in the basket, σ_i the volatility of asset i and $\rho_{i,j}$ the correlation between asset i and asset j. The implied correlation ρ_{imp} of the basket is defined as the root of the following equation:

$$\sigma_B^2 - \sum_{i=1}^{n} w_i^2 \sigma_i^2 - 2\rho_{\mathrm{imp}} \sum_{i>j}^{n} w_i w_j \sigma_i \sigma_j = 0$$

Skintzi and Refenes (2003) deduce that:

$$\rho_{\mathrm{imp}} = \frac{\sigma_B^2 - \sum_{i=1}^{n} w_i^2 \sigma_i^2}{2 \sum_{i>j}^{n} w_i w_j \sigma_i \sigma_j}$$

Another expression of the implied correlation is[79]:

$$\rho_{\mathrm{imp}} = \frac{\sigma_B^2 - \sum_{i=1}^{n} w_i^2 \sigma_i^2}{\left(\sum_{i=1}^{n} w_i \sigma_i\right)^2 - \sum_{i=1}^{n} w_i^2 \sigma_i^2}$$

The concept of implied correlation has been very popular before the Global Financial Crisis. It was at the heart of a strategy known as volatility dispersion trading, which consists in selling variance swaps on an index and buying variance swaps on index components.

The previous analysis assumes a constant correlation matrix $\mathbb{C}_n(\rho)$ for modeling the dependance between asset returns. Over time, it has become the standard for pricing basket

[79] Indeed, we have:

$$\sigma_{\max} = \sqrt{\sum_{i=1}^{n} w_i^2 \sigma_i^2 + 2 \sum_{i>j} w_i w_j \sigma_i \sigma_j} = \sum_{i=1}^{n} w_i \sigma_i$$

implying that:

$$2 \sum_{i>j}^{n} w_i w_j \sigma_i \sigma_j = \left(\sum_{i=1}^{n} w_i \sigma_i\right)^2 - \sum_{i=1}^{n} w_i^2 \sigma_i^2$$

options with several assets. However, this approach implies a specific factor model. It is equivalent to assume that the underlying assets depend on a common risk factor with the same sensitivity. With such assumption, it is extremely difficult to estimate the conservative price of basket options with barriers, best-of/worst-of options, etc. To illustrate this problem, we consider the following payoff:

$$(S_1(T) - S_2(T) + S_3(T) - S_4(T) - K)_+ \cdot \mathbb{1}\{S_5(T) > L\}$$

We calculate the option price of maturity 3 months using the Black-Scholes model. We assume that $S_i(0) = 100$ and $\Sigma_i = 20\%$ for the five underlying assets, the strike K is equal to 5, the barrier L is equal to 105, and the interest rate r is set to 5%. In Figure 9.46, we report the option price when the correlation matrix is $\mathbb{C}_5(\rho)$. Since the option price decreases with respect to ρ, it can be bounded above by 2.20. If we simulate correlation matrices with uniform singular values, we notice that the maximum price of 2.20 is not a conservative price. For instance, if we consider the correlation matrix below, we obtain an option price of 3.99:

$$\mathbb{C} = \begin{pmatrix} 1.0000 & 0.2397 & 0.7435 & -0.1207 & 0.0563 \\ 0.2397 & 1.0000 & -0.0476 & -0.0260 & -0.1958 \\ 0.7435 & -0.0476 & 1.0000 & 0.2597 & 0.1153 \\ -0.1207 & -0.0260 & 0.2597 & 1.0000 & -0.7568 \\ 0.0563 & -0.1958 & 0.1153 & -0.7568 & 1.0000 \end{pmatrix}$$

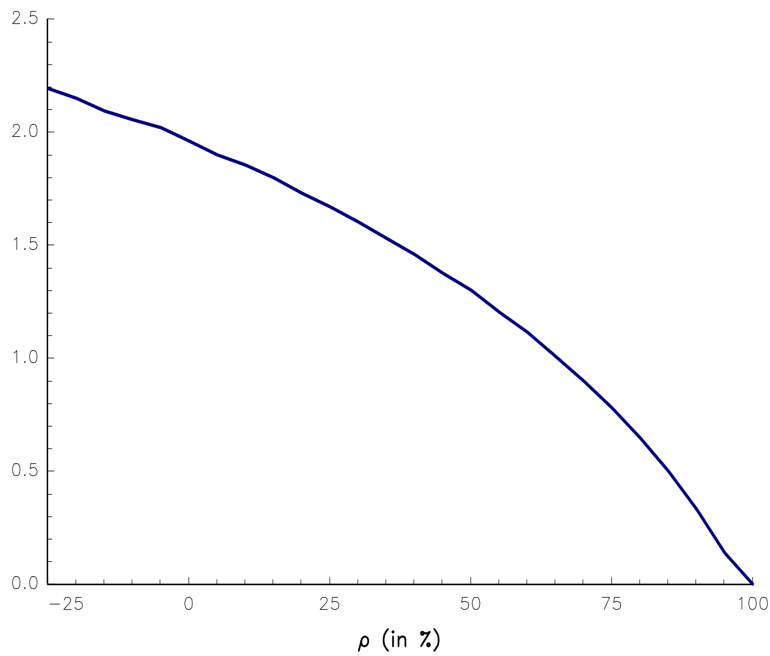

FIGURE 9.46: Price of the basket option with respect to the constant correlation

9.3.2.3 The copula method

Using Sklar's theorem, it comes that the multivariate risk-neutral distribution has the following canonical representation:

$$\mathbb{Q}(S_1(t), \ldots, S_n(t)) = \mathbf{C}^{\mathbb{Q}}(\mathbb{Q}_1(S_1(t)), \ldots, \mathbb{Q}_n(S_n(t)))$$

$\mathbf{C}^{\mathbb{Q}}$ is called the risk-neutral copula (Cherubini and Luciano, 2002). The copula approach has been extensively used in order to derive the bounds of basket options. For instance, Rapuch and Roncalli (2004) extend the results presented in Section 9.3.2.1 on page 583 to the copula approach. In particular, they show that if the payoff function f is supermodular[80], then the option price increases with respect to the concordance order. More explicitly, we have:

$$\mathbf{C}_1 \prec \mathbf{C}_2 \Rightarrow \boldsymbol{\mathcal{C}}_0 \left(S_1, S_2; \mathbf{C}_1\right) \leq \boldsymbol{\mathcal{C}}_0 \left(S_1, S_2; \mathbf{C}_2\right)$$

Therefore, the previous results hold if we replace the Black-Scholes model with the Normal copula model. Thus, the spread option is a decreasing function of the Normal copula parameter ρ even if we use a local or stochastic volatility model in place of the Black-Scholes model. In a similar way, one can find lower and upper bounds of multi-asset option prices by considering lower and upper Fréchet copulas. As shown by Tankov (2011), these bounds can be improved significantly when partial information is available such as the prices of digital basket options.

In practice, the Normal copula model is extensively used for pricing multi-asset European-style option for two reasons:

1. The first one is that multi-asset option prices must be '*compatible*' with single-asset option prices. This means that it would be inadequate to price single-asset options with a complex model, e.g. the SABR model, and in the same time to price multi-asset options with the multivariate Black-Scholes model. Indeed, this decoupling approach creates arbitrage opportunities at the level of the bank itself.

2. The Normal copula model is a natural extension of the multivariate Black-Scholes model since the dependence function is the same.

Nevertheless, we face an issue because the pricing of the payoff $f\left(S_1\left(T\right), \ldots, S_n\left(T\right)\right)$ requires knowing the joint distribution of the random vector $\left(S_1\left(T\right), \ldots, S_n\left(T\right)\right)$, whose an analytical expression does not generally exist[81]. This is why multi-asset options are priced using the Monte Carlo method. However, the analytical distribution of the marginals are generally unknown. Therefore, we have to implement the method of empirical quantile functions described on page 806:

1. for each random variable $S_i\left(T\right)$, simulate m_1 random variates $S_{i,m}^{\star}$ and estimate the empirical distribution $\hat{\mathbf{F}}_i$;

2. simulate a random vector $\left(u_{1,j}, \ldots, u_{n,j}\right)$ from the copula function $\mathbf{C}\left(u_1, \ldots, u_n\right)$;

3. simulate the random vector $\left(S_{1,j}, \ldots, S_{n,j}\right)$ by inverting the empirical distributions $\hat{\mathbf{F}}_i$:

$$S_{i,j} \leftarrow \hat{\mathbf{F}}_i^{-1}\left(u_{i,j}\right)$$

or equivalently:

$$S_{i,j} \leftarrow \inf\left\{x \left| \frac{1}{m_1} \sum\nolimits_{m=1}^{m_1} \mathbb{1}\left\{x \leq S_{i,m}^{\star}\right\} \geq u_i \right.\right\}$$

[80] The function f is supermodular if and only if:

$$\Delta^{(2)} f := f\left(x_1 + \varepsilon_1, x_2 + \varepsilon_2\right) - f\left(x_1 + \varepsilon_1, x_2\right) - f\left(x_1, x_2 + \varepsilon_2\right) + f\left(x_1, x_2\right) \geq 0$$

for all $\left(x_1, x_2\right) \in \mathbb{R}^2$ and $\left(\varepsilon_1, \varepsilon_2\right) \in \mathbb{R}_+^2$.

[81] An exception concerns the SABR model for which we have found an expression of the probability distribution thanks to the Breeden-Litzenberger representation.

4. repeat steps 2 and 3 m_2 times;

5. the MC estimate of the option price is equal to:

$$\hat{\mathcal{C}}_0 = e^{-rT} \left(\frac{1}{m_2} \sum_{j=1}^{m_2} f\left(S_{1,j}, \ldots, S_{n,j}\right) \right)$$

It follows that the first step is used for estimating the distribution of $S_i(T)$. For this step, we use m_1 simulations of the single-asset option model. However, this step generates independent random variables. Therefore, the steps 2 and 3 are used in order to create the right dependence between $(S_1(T), \ldots, S_n(T))$.

Example 99 *We consider the two-asset option with the following payoff:*

$$f\left(F_1(T), F_2(T)\right) = 100 \cdot \left(\max\left(\frac{F_1(T)}{F_1(0)} - 1, \frac{F_2(T)}{F_2(0)} - 1 \right) - K \right)^+$$

where $F_1(t)$ and $F_2(t)$ are two forward rates. We assume that $F_1(0) = 5\%$ and $F_2(0) = 6\%$. The maturity of the option is equal to one year, whereas the strike of the option is set to 2%. Using the SABR model, we have calibrated the volatility smiles and we have obtained the following estimates:

	α	β	ν	ρ
F_1	8.944%	1.00	0.322	−22.901%
F_2	12.404%	1.00	0.280	16.974%

In Figure 9.47, we have reported the price of the two-asset option with respect to the dependence parameter ρ. For the Black-Scholes model, we use the ATM implied volatilities[82] and the parameter ρ represents the implied correlation. For the SABR model, we use the Normal copula model, and ρ is the copula parameter. We notice that the Black-Scholes model overestimates the option price compared to the SABR model. We also verified that the option price is a decreasing function with respect to ρ.

9.3.3 Liquidity risk

Liquidity risk can be incorporated in the theory of option pricing, but it requires solving a stochastic optimal control problem (Çetin *et al.*, 2004, 2006; Jarrow and Protter, 2007; Çetin *et al.*, 2010). In practice, these approaches are not used by professionals, but some theoretical results help to understand the impact of liquidity risk on option pricing. However, there is no satisfactory solution, and '*cooking recipes*' differ from one bank to another one, one trading desk to another one, one trader to another one. But the issue here is not to solve this problem, but to understand the model risk from a risk management perspective.

It is obvious that liquidity risk impacts trading costs, in particular the price of the replication strategy because of bid-ask spreads. Here, we don't want to focus on '*normal*' liquidity risk, but on '*trading*' liquidity risk. Option theory assumes that we can replicate the option, meaning that we can sell or buy the underlying asset at any time. For liquid assets, this assumption is almost verified even if we can face high bid-ask spread. For less liquid assets, this assumption is not verified. Let us consider one of the most famous examples, which concerns call options on Sharpe ratio. Starting from 2004, some banks proposed

[82] They are equal to 9% for F_1 and 12.5% for F_2.

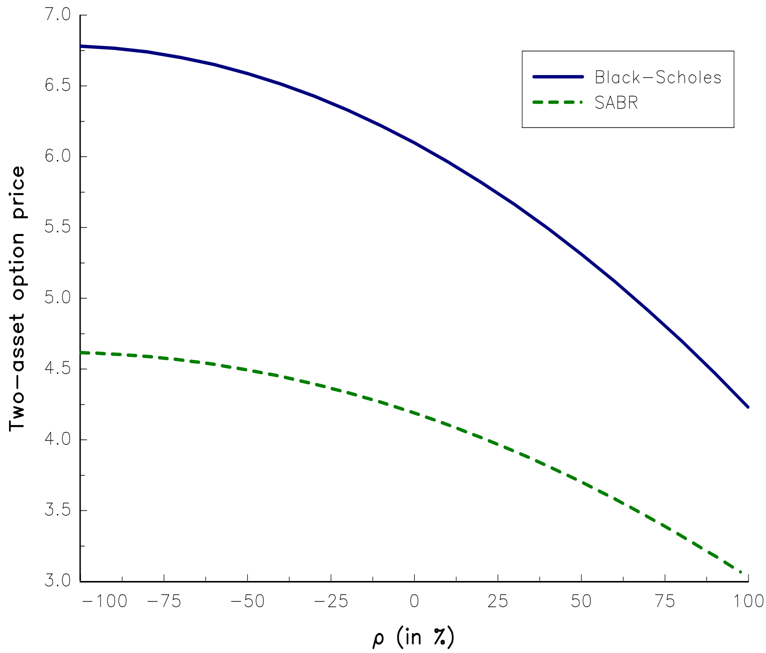

FIGURE 9.47: Comparison of the option price obtained with Black-Scholes and copula-SABR models

to investors a payoff of the form $(\mathrm{SR}(0;T) - K)^+$ where $\mathrm{SR}(0;T)$ is the Sharpe ratio of the underlying asset during the option period. This payoff is relatively easy to replicate. However, most of call options on Sharpe ratio have been written on mutual funds and hedge funds. The difficulty comes from the liquidity of these underlying assets. For instance, the trader does not know exactly the price of the asset when he executes his order because of the notice period[83]. This can be a big issue when the fund offers weekly or monthly liquidity. The second problem comes from the fact that the fund manager can impose lock-up period and gates. For instance, a gate limits the amount of withdrawals. During the 2008/2009 hedge fund crisis, many traders faced gate provisions and were unable to adjust their delta. This crisis marketed the end of call options on Sharpe ratio.

The previous example is an extreme case of the impact of liquidity on option trading. However, this type of problems is not unusual even with liquid markets, because liquidity is time-varying and may impact delta hedging at the worst possible time. Let us consider the replication of a call option. If the price of the underlying asset decreases sharply, the delta is reduced and the option trader has to sell asset shares. Because of their trend-following aspect, option traders generally buy assets when the market goes up and sell assets when the market goes down. However, we know that liquidity is asymmetric between these two market regimes. Therefore, it is more difficult to adjust the delta exposure when the market goes down, because of the lack of liquidity. This means that some payoffs are more sensitive to others.

[83]A subscription/redemption notice period requires that the investor informs the fund manager a certain period in advance before buying/selling fund shares.

9.4 Exercises

9.4.1 Option pricing and martingale measure

We consider the Black-Scholes model. The price process $S(t)$ follows a Geometric Brownian motion:

$$\mathrm{d}S(t) = \mu S(t)\ \mathrm{d}t + \sigma S(t)\ \mathrm{d}W(t)$$

and the risk-free asset $B(t)$ satisfies:

$$\mathrm{d}B(t) = rB(t)\ \mathrm{d}t$$

We consider a portfolio $(\phi(t), \psi(t))$ invested in the stock S and the risk-free bond B. We note $V(t)$ the value of this portfolio.

1. Show that:
$$\mathrm{d}V(t) = rV(t)\ \mathrm{d}t + \phi(t)\left(\mathrm{d}S(t) - rS(t)\ \mathrm{d}t\right)$$

2. We note $\tilde{V}(t) = e^{-rt}V(t)$ and $\tilde{S}(t) = e^{-rt}S(t)$. Show that:
$$\mathrm{d}\tilde{V}(t) = \phi(t)\ \mathrm{d}\tilde{S}(t)$$

3. Show that $\tilde{V}(t)$ is a martingale under the risk measure $\mathbb{Q}$. Deduce that:
$$V(t) = e^{-r(T-t)}\mathbb{E}^{\mathbb{Q}}\left[\left.V(T)\right|\mathcal{F}_t\right]$$

4. Define the corresponding martingale measure.

5. Calculate the price of the binary option $\mathbb{1}\{S(T) \geq K\}$.

9.4.2 The Vasicek model

Vasicek (1977) assumes that the instantaneous interest rate follows an Ornstein-Uhlenbeck process:

$$\begin{cases} \mathrm{d}r(t) = a(b - r(t))\ \mathrm{d}t + \sigma\,\mathrm{d}W(t) \\ r(t_0) = r_0 \end{cases}$$

and the risk price of the Wiener process is constant:

$$\lambda(t) = \lambda$$

We consider the pricing of a zero-coupon bond, whose maturity is equal to T.

1. Write the partial differential equation of the zero-coupon bond $B(t, r)$ when the interest rate $r(t)$ is equal to r.

2. Using the solution of the Ornstein-Uhlenbeck process given on page 1075, show that the random variable Z defined by:
$$Z = \int_0^T r(t)\ \mathrm{d}t$$
is Gaussian.

3. Calculate the first two moments.

4. Deduce the price of the zero-coupon bond.

9.4.3 The Black model

In the model of Black (1976), we assume that the price $F(t)$ of a forward or futures contract evolves as follows:

$$\mathrm{d}F(t) = \sigma F(t)\,\mathrm{d}W(t)$$

1. Write the PDE equation associated to the call option payoff:
$$\boldsymbol{\mathcal{C}}(T) = \max\left(F(T) - K, 0\right)$$
when the interest rate is equal to r.

2. Using the Feynman-Kac representation theorem, deduce the current price of the call option.

3. We assume that the stock price $S(t)$ follows a geometric Brownian motion:
$$\mathrm{d}S(t) = \mu S(t)\,\mathrm{d}t + \sigma S(t)\,\mathrm{d}W(t)$$
Show that the Black formula can be used to price an European option, whose underlying asset is the futures contract of the stock.

4. What does the Black formula become if we assume that the interest rate $r(t)$ is stochastic and is independent of the forward price $F(t)$?

5. What is the problem if we consider that the interest rate $r(t)$ and the forward price $F(t)$ are not independent?

6. We reiterate that the price of the zero-coupon bond is given by:
$$B(t,T) = \mathbb{E}^{\mathbb{Q}}\left[\left. e^{-\int_t^T r(s)\,\mathrm{d}s}\right| \mathcal{F}_t\right]$$
The instantaneous forward rate $f(t,T)$ is defined as follows:
$$f(t,T) = -\frac{\partial \ln B(t,T)}{\partial T}$$
We consider that the numéraire is the bond price $B(t,T)$ and we note $\mathbb{Q}^{\star}$ the associated forward probability measure.

   (a) Show that:
   $$\frac{\partial B(t,T)}{\partial T} = -B(t,T) \cdot \mathbb{E}^{\mathbb{Q}^{\star}}\left[\left. f(T,T)\right| \mathcal{F}_t\right]$$

   (b) Deduce that $f(t,T)$ is an $\mathcal{F}_t$-martingale under the forward probability measure $\mathbb{Q}^{\star}$.

   (c) Find the price of the call option, whose payoff is equal to:
   $$\boldsymbol{\mathcal{C}}(T) = \max\left(f(T,T) - K, 0\right)$$

9.4.4 Change of numéraire and Girsanov theorem

Part one

Let $X(t)$ and $Y(t)$ be two $\mathcal{F}_t$-adapted processes.

1. Calculate the stochastic differentials $\mathrm{d}(X(t)Y(t))$ and $\mathrm{d}(1/Y(t))$.

2. We note $Z(t)$ the ratio of $X(t)$ and $Y(t)$. Show that:
$$\frac{\mathrm{d}Z(t)}{Z(t)} = \frac{\mathrm{d}X(t)}{X(t)} - \frac{\mathrm{d}Y(t)}{Y(t)} + \frac{\langle \mathrm{d}Y(t), \mathrm{d}Y(t)\rangle}{Y^2(t)} - \frac{\langle \mathrm{d}X(t), \mathrm{d}Y(t)\rangle}{X(t)Y(t)}$$

Part two

Let $S(t)$ be the price of an asset. Under the probability measure $\mathbb{Q}$, $S(t)$ has the following dynamics:

$$\mathrm{d}S(t) = \mu_S(t) S(t)\,\mathrm{d}t + \sigma_S(t) S(t)\,\mathrm{d}W^{\mathbb{Q}}(t)$$

The corresponding numéraire is denoted by $M(t)$ and we have:

$$\mathrm{d}M(t) = \mu_M(t) M(t)\,\mathrm{d}t + \sigma_M(t) M(t)\,\mathrm{d}W^{\mathbb{Q}}(t)$$

We now consider another numéraire $N(t)$ whose dynamics is given by:

$$\mathrm{d}N(t) = \mu_N(t) N(t)\,\mathrm{d}t + \sigma_N(t) N(t)\,\mathrm{d}W^{\mathbb{Q}}(t)$$

and we note $\mathbb{Q}^\star$ the probability measure associated to $N(t)$. We assume that:

$$\mathrm{d}S(t) = \mu_S^\star(t) S(t)\,\mathrm{d}t + \sigma_S(t) S(t)\,\mathrm{d}W^{\mathbb{Q}^\star}(t)$$

1. Why can we assume that the diffusion coefficient of $S(t)$ is the same under the two probability measures $\mathbb{Q}$ and $\mathbb{Q}^\star$?

2. Find the process $g(t)$ such that:

$$\mathrm{d}W^{\mathbb{Q}^\star}(t) = \mathrm{d}W^{\mathbb{Q}}(t) - g(t)\,\mathrm{d}t$$

Let $Z(t)$ be the Radon-Nikodym derivative defined by:

$$Z(t) = \frac{\mathrm{d}\mathbb{Q}^\star}{\mathrm{d}\mathbb{Q}}$$

Show that:

$$\frac{\mathrm{d}Z(t)}{Z(t)} = g(t)\,\mathrm{d}W^{\mathbb{Q}}(t)$$

3. We recall that another expression of $Z(t)$ is:

$$Z(t) = \frac{N(t)/N(0)}{M(t)/M(0)}$$

Deduce that:

$$g(t) = \sigma_N(t) - \sigma_M(t)$$

Find the expression of $\mu_N(t)$.

4. Show that changing the numéraire is equivalent to change the drift:

$$\mu_S^\star(t) = \mu_S(t) + \sigma_S(t)(\sigma_N(t) - \sigma_M(t))$$

5. Deduce that:

$$\mu_S^\star(t)\,\mathrm{d}t - \left\langle \frac{\mathrm{d}S(t)}{S(t)}, \frac{\mathrm{d}N(t)}{N(t)} \right\rangle = \mu_S(t)\,\mathrm{d}t - \left\langle \frac{\mathrm{d}S(t)}{S(t)}, \frac{\mathrm{d}M(t)}{M(t)} \right\rangle$$

and:

$$\mu_S^\star(t)\,\mathrm{d}t = \mu_S(t)\,\mathrm{d}t + \left\langle \frac{\mathrm{d}S(t)}{S(t)}, \mathrm{d}\ln\frac{N(t)}{M(t)} \right\rangle$$

Part three

Under the risk-neutral probability measure $\mathbb{Q}$, we assume that the asset price and the numéraire are given by the following stochastic differential equations:

$$\mathrm{d}S(t) = r(t)\,S(t)\,\mathrm{d}t + \sigma_S(t)\,S(t)\,\mathrm{d}W_S^{\mathbb{Q}}(t)$$

and:

$$\mathrm{d}N(t) = r(t)\,N(t)\,\mathrm{d}t + \sigma_N(t)\,N(t)\,\mathrm{d}W_N^{\mathbb{Q}}(t)$$

where $N(0) = 1$, $W_S^{\mathbb{Q}}(t)$ and $W_N^{\mathbb{Q}}(t)$ are two Wiener processes and $\mathbb{E}\left[W_S^{\mathbb{Q}}(t)\,W_N^{\mathbb{Q}}(t)\right] = \rho t$. We note $\tilde{S}(t) = S(t)/N(t)$ the asset price expressed in the numéraire $N(t)$.

1. Find the stochastic differential equation of $\tilde{S}(t)$:

$$\tilde{S}(t) = \frac{S(t)}{N(t)}$$

2. Let $Q^{\star}$ be the martingale measure associated to the numéraire $N(t)$.

   (a) We assume that $\sigma_N(t) = 0$. Show that the discounted asset price is an $\mathcal{F}_t$-martingale under the risk-neutral probability measure.

   (b) We consider the case $W_S^{\mathbb{Q}}(t) = W_N^{\mathbb{Q}}(t)$. Using Girsanov theorem, show that:

$$\mathrm{d}\tilde{S}(t) = \tilde{\sigma}(t)\,\tilde{S}(t)\,\mathrm{d}W^{\mathbb{Q}^{\star}}(t)$$

   where $W^{\mathbb{Q}^{\star}}$ is a Brownian motion under the probability measure $Q^{\star}$ and $\tilde{\sigma}(t)$ is a function to be defined.

   (c) What does this result become in the general case?

9.4.5 The HJM model and the forward probability measure

We assume that the instantaneous forward rate $f(t, T_1)$ is given by the following stochastic differential equation:

$$\mathrm{d}f(t, T_1) = \alpha(t, T_1)\,\mathrm{d}t + \sigma(t, T_1)\,\mathrm{d}W^{\mathbb{Q}}(t)$$

where $\mathbb{Q}$ is the risk-neutral probability measure.

1. We consider the forward probability measure $\mathbb{Q}^{\star}(T_2)$ where $T_2 \geq T_1$. Define the corresponding numéraire $N(t)$ and show that the Radon-Nikodym derivative is equal to:

$$\frac{\mathrm{d}\mathbb{Q}^{\star}}{\mathrm{d}\mathbb{Q}} = e^{-\int_0^{T_2}(r(t)-f(0,t))\,\mathrm{d}t}$$

2. We recall that the dynamics of the instantaneous spot rate $r(t)$ is:

$$r(t) = r(0) + \int_0^t \left(\sigma(s,t)\int_s^t \sigma(s,u)\,\mathrm{d}u\right)\mathrm{d}s + \int_0^t \sigma(s,t)\,\mathrm{d}W^{\mathbb{Q}}(s)$$

   Show that:

$$\frac{\mathrm{d}\mathbb{Q}^{\star}}{\mathrm{d}\mathbb{Q}} = e^{\int_0^{T_2} a(t,T_2)\,\mathrm{d}t + \int_0^{T_2} b(t,T_2)\,\mathrm{d}W^{\mathbb{Q}}(t)}$$

where:

$$a(t,T_2) = -\int_t^{T_2} \left(\sigma(t,v)\int_t^v \sigma(t,u)\,\mathrm{d}u\right)\mathrm{d}v$$

and:

$$b(t,T_2) = -\int_t^{T_2} \sigma(t,v)\,\mathrm{d}v$$

3. Using the drift restriction in the HJM model, show that:

$$W^{\mathbb{Q}^\star(T_2)}(t) = W^{\mathbb{Q}}(t) - \int_0^t b(s,T_2)\,\mathrm{d}s$$

is a Brownian motion under the forward probability measure $\mathbb{Q}^\star(T_2)$.

4. Find the dynamics of $f(t,T_1)$ under the forward probability measure $\mathbb{Q}^\star(T_2)$.

5. Show that $f(t,T_1)$ is a martingale under the forward probability measure $\mathbb{Q}^\star(T_1)$.

6. We recall that the price of the zero-coupon bond satisfies the SDE:

$$\mathrm{d}B(t,T) = r(t)B(t,T)\,\mathrm{d}t + b(t,T)B(t,T)\,\mathrm{d}W^{\mathbb{Q}}(t)$$

   (a) Show that:
   $$\frac{B(t,T_2)}{B(t,T_1)} = \frac{B(s,T_2)}{B(s,T_1)}e^{X(s,t)}$$
   where $X(s,t)$ is a random variable to define.

   (b) Deduce that $B(t,T_2)/B(t,T_1)$ is a martingale under $\mathbb{Q}^\star(T_1)$.

9.4.6 Equivalent martingale measure in the Libor market model

Let $L_i(t) = L(t,T_i,T_{i+1})$ be the forward Libor rate when resetting and maturity dates are respectively equal to T_i and T_{i+1}. Under the forward probability measure $\mathbb{Q}^\star(T_{i+1})$, the dynamics of $L_i(t)$ is given by the following SDE:

$$\mathrm{d}L_i(t) = \gamma_i(t)L_i(t)\,\mathrm{d}W_i^{\mathbb{Q}^\star(T_{i+1})}(t)$$

1. Using the definition of the Libor rate, find the relationship between $B(t,T_{j+1})/B(t,T_j)$ and $L_j(t)$. Let $T_{k+1} > T_{i+1}$. Deduce an expression of the ratio:

$$\frac{B(t,T_{k+1})}{B(t,T_{i+1})}$$

in terms of Libor rates $L_j(t)$ $(j = i+1,\ldots,k)$.

2. We change the probability measure from $\mathbb{Q}^\star(T_{i+1})$ to $\mathbb{Q}^\star(T_{k+1})$. Define the numéraires $M(t)$ and $N(t)$ associated to $\mathbb{Q}^\star(T_{i+1})$ to $\mathbb{Q}^\star(T_{k+1})$. Deduce an expression of $Z(t)$:

$$Z(t) = \frac{\mathrm{d}\mathbb{Q}^\star(T_{k+1})}{\mathrm{d}\mathbb{Q}^\star(T_{i+1})}$$

in terms of Libor rates $L_j(t)$ $(j = i+1,\ldots,k)$.

3. Calculate $\mathrm{d}\ln Z(t)$.

4. Calculate the drift ζ defined by:

$$\zeta = \left\langle \frac{\mathrm{d}L_i(t)}{L_i(t)}, \mathrm{d}\ln Z(t) \right\rangle$$

5. Show that the dynamics of $L_i(t)$ under the forward probability measure $\mathbb{Q}^{\star}(T_{k+1})$ is given by:

$$\frac{\mathrm{d}L_i(t)}{L_i(t)} = \mu_{i,k}(t)\,\mathrm{d}t + \gamma_i(t)\,\mathrm{d}W_k^{\mathbb{Q}^{\star}(T_{k+1})}(t)$$

where $\mu_{i,k}(t)$ is a drift to determine.

6. What does the previous results become if $T_{k+1} < T_{i+1}$?

9.4.7 Displaced diffusion option pricing

Brigo and Mercurio (2002a) consider the diffusion process $X(t)$ given by:

$$\begin{cases} \mathrm{d}X(t) = \mu(t, X(t))\,\mathrm{d}t + \sigma(t, X(t))\,\mathrm{d}W^{\mathbb{Q}}(t) \\ X(0) = X_0 \end{cases}$$

They assume that the asset price $S(t)$ is an affine transformation of $X(t)$:

$$S(t) = \alpha(t) + \beta(t) \cdot X(t)$$

where $\beta(t) > 0$.

1. By applying Itô's lemma to $S(t)$, find the condition on $\alpha(t)$ and $\beta(t)$ in order to satisfy the martingale condition:

$$\mathbb{E}^{\mathbb{Q}}\left[e^{-bt} \cdot S(t) \mid \mathcal{F}_0\right] = S_0$$

where b is the cost-of-carry parameter.

2. We consider the CEV process:

$$\mathrm{d}X(t) = \mu(t) X(t)\,\mathrm{d}t + \sigma(t) X(t)^{\gamma}\,\mathrm{d}W^{\mathbb{Q}}(t)$$

where $\gamma \in [0, 1]$. Show that the solutions of $\alpha(t)$ and $\beta(t)$ are:

$$\begin{cases} \alpha(t) = \alpha_0 \cdot \exp(bt) \\ \beta(t) = \beta_0 \cdot \exp\left(\int_0^t (b - \mu(s))\,\mathrm{d}s\right) \end{cases}$$

3. Deduce the SDE of $S(t)$.

4. We consider the case $\gamma = 1$. Give the SDE of $X(t)$. Calculate the solutions of $X(t)$ and $S(t)$.

5. Give the price of the European call option, whose payoff is equal to $(S(T) - K)^{+}$.

6. We now assume that $\sigma(t) = \sigma$.

   (a) Using the formula of Lee and Wang (2012), give an approximation of the implied volatility $\Sigma(T, K)$.

   (b) Calculate the volatility skew:

$$\omega(T, K) = \frac{\partial\,\Sigma(T, K)}{\partial\,K}$$

   (c) Give the price of the binary call option in the case of the BS model.

   (d) Deduce the BCC price when we consider the SLN model.

   (e) Give an approximation of the BCC price based on the implied volatility skew.

9.4.8 Dupire local volatility model

We assume that:

$$\mathrm{d}S(t) = bS(t)\,\mathrm{d}t + \sigma(t, S(t))\,S(t)\,\mathrm{d}W^{\mathbb{Q}}(t)$$

1. Give the forward equation for pricing the call option $\boldsymbol{\mathcal{C}}(T, K)$. Deduce the expression of the local variance $\sigma^2(T, K)$.

2. Using the Black-Scholes formula, find the relationship between the local volatility $\sigma(T, K)$ and the implied volatility $\Sigma(T, K)$.

3. We consider the discounted payoff function:

$$\tilde{f}(T, S(T)) = e^{-r(T-t)}(S(T) - K)^+$$

   Using Itô's lemma, calculate the derivative of the call option with respect to the maturity:

$$\partial_T \boldsymbol{\mathcal{C}}(T, K) = \frac{\mathbb{E}\left[\mathrm{d}\tilde{f}(T, S(T)) \middle| \mathcal{F}_t\right]}{\mathrm{d}T}$$

4. Calculate $\partial_K \boldsymbol{\mathcal{C}}(T, K)$ and $\partial_K^2 \boldsymbol{\mathcal{C}}(T, K)$ using the discounted payoff function. Retrieve the forward equation[84] of Dupire (1994).

5. We introduce the log-moneyness x:

$$\begin{aligned} x &= \varphi(T, K) \\ &= \ln \frac{S_0}{K} + bT \end{aligned}$$

   and the functions $\tilde{\sigma}(T, x)$ and $\tilde{\Sigma}(T, x)$, which are defined by the relationships:

$$\Sigma(T, K) = \tilde{\Sigma}(T, \varphi(T, K))$$

   and:

$$\sigma(T, K) = \tilde{\sigma}(T, \varphi(T, K))$$

   (a) Calculate d_1, d_2 and $d_1 d_2$.

   (b) Write the derivatives $\partial_K \Sigma(T, K)$, $\partial_T \Sigma(T, K)$ and $\partial_K^2 \Sigma(T, K)$ using the variables T and x.

   (c) Deduce the relationship between $\tilde{\sigma}(T, x)$ and $\tilde{\Sigma}(T, x)$.

   (d) Show that:

$$\partial_x \tilde{\Sigma}(0, 0) = \frac{1}{2} \partial_x \tilde{\sigma}(0, 0)$$

9.4.9 The stochastic normal model

Let $F(t)$ be the forward rate. We assume that the dynamics of $F(t)$ is given by the SABR model:

$$\left\{ \begin{array}{l} \mathrm{d}F(t) = \alpha(t) F(t)^\beta \,\mathrm{d}W_1^{\mathbb{Q}}(t) \\ \mathrm{d}\alpha(t) = \nu\alpha(t)\,\mathrm{d}W_2^{\mathbb{Q}}(t) \end{array} \right.$$

where $\mathbb{E}\left[W_1^{\mathbb{Q}}(t)\, W_2^{\mathbb{Q}}(t)\right] = \rho\, t$. In what follows, we consider the special case $\beta = 0$.

[84] This approach has also been proposed by Derman *et al.* (1996).

1. How to transform the Black volatility $\Sigma_B(T,K)$ into the implied normal volatility $\Sigma_N(T,K)$?

2. Give the expression of the implied normal volatility[85] $\Sigma_N(T,K)$ for the general case $\beta \in [0,1]$.

3. Deduce the formula of $\Sigma_N(T,K)$ when $\beta = 0$.

4. What is the ATM normal volatility?

5. Calculate $\partial_K \Sigma_N(T,K)$.

6. Recall the price of the call option for the normal model, whose volatility is σ_N.

7. We now assume that σ_N is equal to the SABR normal volatility $\Sigma_N(T,K)$. Deduce the cumulative distribution function of $F(T)$.

8. By considering the following approximation[86]:

$$\sqrt{F_0 K} \ln \frac{F_0}{K} \simeq F_0 - K$$

calculate the probability density function of $F(T)$.

9. Show that:

$$F(t) = F_0 + \frac{\alpha}{\nu} \int_0^{\nu^2 t} \exp\left(-\frac{1}{2}s + W_2(s)\right) \mathrm{d}W_1(s)$$

where $W_1(t)$ and $W_2(t)$ have the same properties as $W_1^{\mathbb{Q}}(t)$ and $W_2^{\mathbb{Q}}(t)$.

10. We note:

$$X(t) = \int_0^t \exp\left(-\frac{1}{2}s + W_2(s)\right) \mathrm{d}W_1(s)$$

and:

$$M^a(t) = \exp\left(-\frac{1}{2}at + aW_2(t)\right)$$

Let us introduce the function $\Psi^{n,a}(t)$:

$$\Psi^{n,a}(t) = \mathbb{E}\left[X^n(t) M^a(t)\right]$$

where $n \in \mathbb{N}$ and $a \in \mathbb{R}_+$. Verify that $\Psi^{n,a}(t)$ satisfies the ordinary differential equation:

$$\frac{\mathrm{d}\Psi^{n,a}(t)}{\mathrm{d}t} = \frac{a(a-1)}{2}\Psi^{n,a}(t) + n\rho a \Psi^{n-1,a+1}(t) + \frac{n(n-1)}{2}\Psi^{n-2,a+2}(t)$$

where $\Psi^{n,a}(0) = 0$. What is the link between $\Psi^{n,a}(t)$ and the statistical moments of $F(t)$?

11. Calculate $\Psi^{0,a}(t)$, $\Psi^{1,a}(t)$, $\Psi^{2,a}(t)$, $\Psi^{3,0}(t)$ and $\Psi^{4,0}(t)$. Deduce the first four central moments of $F(t)$.

12. Calculate an approximation of the volatility, skewness and kurtosis of $F(t)$ when $t \simeq 0$.

[85] Hagan *et al.* (2002) calculate this expression in Appendix A.4 on page 102.
[86] Hagan *et al.* (2002), Equations (A67b) and (A68a), page 102.

13. We assume that $F_0 = 10\%$ and $T = 1$, and we consider the following smile:

K	7%	10%	13%
$\Sigma_B(T,K)$	30%	20%	30%

    (a) Calculate the equivalent normal volatility $\Sigma_N(T,K)$.
    (b) Calibrate the parameters of the stochastic normal model.
    (c) Draw the cumulative distribution function of $F(T)$. What is the problem?
    (d) Draw the probability density function of $F(T)$ when we consider the approximation $\sqrt{F_0 K}\ln\dfrac{F_0}{K} \simeq F_0 - K$.
    (e) Calculate the skewness and the kurtosis of $F(T)$. Comment on these results.

9.4.10 The quadratic Gaussian model

We consider the quadratic Gaussian model:

$$r(t) = \alpha(t) + \beta(t)^\top X(t) + X(t)^\top \Gamma(t) X(t)$$

where the state variables $X(t)$ follow an Ornstein-Uhlenbeck process:

$$\mathrm{d}X(t) = (a(t) + B(t)X(t))\,\mathrm{d}t + \Sigma(t)\,\mathrm{d}W^{\mathbb{Q}}(t)$$

1. Find the PDE associated to the zero-coupon bond $B(t,T)$.

2. We assume that the solution of $B(t,T)$ has the following form:

$$B(t,T) = \exp\left(-\hat{\alpha}(t,T) - \hat{\beta}(t,T)^\top X(t) - X(t)^\top \hat{\Gamma}(t,T) X(t)\right)$$

   where $\hat{\Gamma}(t,T)$ is a symmetric matrix. Show that $\hat{\alpha}(t,T)$, $\hat{\beta}(t,T)$ and $\hat{\Gamma}(t,T)$ satisfy a system of ODEs.

3. Find a condition that $\hat{\Gamma}(t,T)$ is a symmetric matrix. Why do we need this hypothesis?

4. Let $\mathbb{Q}^\star(T)$ be the forward probability measure. Recall the dynamics of $X(t)$ under $\mathbb{Q}^\star(T)$. Using the explicit solution, demonstrate that $X(t)$ is Gaussian:

$$X(t) \sim \mathcal{N}(m(0,t), V(0,t))$$

   Find the dynamics of $m(0,t)$ and $V(0,t)$. Compare these results with those obtained by El Karoui *et al.* (1992a).

5. Define the Libor rate $L(t,T_{i-1},T_i)$.

6. Demonstrate that the pricing formula of the caplet is equal to:

$$\text{Caplet} = B(0,t)\cdot\mathbb{E}^{\mathbb{Q}^\star(t)}\left[\max(0, g(X))\right]$$

   where $\mathbb{Q}^\star(t)$ is the forward probability measure and $g(x)$ is a function to define.

7. Show that:

$$\text{Caplet} = B(0,t)\int_{\mathcal{E}} h(x)\,\mathrm{d}x$$

   where $h(x) = g(x)\,\phi(x; m(0,t), V(0,t))$ and $\mathcal{E}$ is a set to define.

8. We consider the following function:

$$\mathcal{J}\left(a,b,c,m,V,x_1,x_2\right)=\int_{x_1}^{x_2}\frac{e^{-ax^2-bx-c}}{\sqrt{2\pi V}}e^{-\frac{1}{2V}(x-m)^2}\,\mathrm{d}x$$

   Find the analytical expression of $\mathcal{J}$.

9. Deduce the analytical expression of the caplet.

9.4.11 Pricing two-asset basket options

We assume that the risk-neutral dynamics of $S_1(t)$ and $S_2(t)$ are given by:

$$\left\{\begin{array}{l}\mathrm{d}S_1(t)=b_1S_1(t)\,\mathrm{d}t+\sigma_1S_1(t)\,\mathrm{d}W_1^{\mathbb{Q}}(t)\\ \mathrm{d}S_2(t)=b_2S_2(t)\,\mathrm{d}t+\sigma_2S_2(t)\,\mathrm{d}W_2^{\mathbb{Q}}(t)\end{array}\right.$$

where $W_1^{\mathbb{Q}}(t)$ and $W_2^{\mathbb{Q}}(t)$ are two correlated Brownian motions:

$$\mathbb{E}\left[W_1^{\mathbb{Q}}(t)\,W_2^{\mathbb{Q}}(t)\right]=\rho\,t$$

1. By considering the following payoff $(\alpha_1S_1(T)+\alpha_2S_2(T)-K)^+$, show that the price of the option can be expressed as a double integral.

2. We consider the computation of $I=\mathbb{E}\left[\left(Ae^{b+c\cdot\varepsilon}-D\right)^+\right]$ where $\varepsilon\sim\mathcal{N}(0,1)$, and A, b, c and D are four scalars.

   (a) Find the value of I when $A>0$ and $D>0$.

   (b) Deduce the value of I in the other cases.

3. We assume that $\alpha_1<0$, $\alpha_2>0$ and $K>0$. Using the Cholesky decomposition, reduce the computation of the double integral to a single integral.

4. Extend this result to the case $\alpha_1>0$, $\alpha_2<0$ and $K>0$.

5. Discuss the general case.